OPTIMAL DESIGN STRATEGIES FOR SURVIVABLE CARRIER ETHERNET NETWORKS

MOHAMMAD NURUJJAMAN

A THESIS
IN
THE DEPARTMENT
OF
COMPUTER SCIENCE & SOFTWARE ENGINEERING

PRESENTED IN PARTIAL FULFILLMENT OF THE REQUIREMENTS
FOR THE DEGREE OF DOCTOR OF PHILOSOPHY
CONCORDIA UNIVERSITY
MONTRÉAL, QUÉBEC, CANADA

APRIL 2013

CONCORDIA UNIVERSITY

Engineering and Computer Science

This is to certify that the thesis prepared

By:	**Mohammad Nurujjaman**
Entitled:	**Optimal Design Strategies for Survivable Carrier Ethernet Networks**

and submitted in partial fulfillment of the requirements for the degree of

Doctor of Philosophy (Computer Science)

complies with the regulations of this University and meets the accepted standards with respect to originality and quality.

Signed by the final examining committee:

Dr. Rabin Raut
______________________ Chair

Dr. Pin-Han Ho
______________________ External Examiner

Dr. Anjali Agarwal
______________________ External to Program

Dr. Lata Narayanan
______________________ Examiner

Dr. Thomas G. Fevens
______________________ Examiner

Dr. Chadi Assi
______________________ Thesis Supervisor

Approved by

____
Chair of Department or Graduate Program Director

__________ ______________________
Date Dean of Faculty

Abstract

Optimal Design Strategies for Survivable Carrier Ethernet Networks

Mohammad Nurujjaman, Ph.D.

Concordia University, 2013

Ethernet technologies have evolved through enormous standardization efforts over the past two decades to achieve carrier-grade functionalities, leading to carrier Ethernet. Carrier Ethernet is expected to dominate next generation backbone networks due to its low-cost and simplicity. Ethernet's ability to provide carrier-grade Layer-2 protection switching with SONET/SDH-like fast restoration time is achieved by a new protection switching protocol, Ethernet Ring Protection (ERP). In this thesis, we address two important design aspects of carrier Ethernet networks, namely, survivable design of ERP-based Ethernet transport networks together with energy efficient network design. For the former, we address the problem of optimal resource allocation while designing logical ERP for deployment and model the combinatorially complex problem of joint Ring Protection Link (RPL) placements and ring hierarchies selection as an optimization problem. We develop several Mixed Integer Linear Programming (MILP) model to solve the problem optimally considering both single link failure and concurrent dual link failure scenarios. We also present a traffic engineering based ERP design approach and develop corresponding MILP design models for configuring either single or multiple logical ERP instances over one underlying physical ring. For the latter, we propose two novel architectures of energy efficient Ethernet switches using passive optical correlators for optical bypassing as well as using energy efficient Ethernet (EEE) ports for traffic aggregation and forwarding. We develop an optimal frame scheduling model for EEE ports to ensure minimal energy consumption by using packet coalescing and efficient scheduling.

Acknowledgments

I would like to express my sincere gratitude to my thesis supervisor, Dr. Chadi Assi, who is very hard working, dedicated and extremely helpful to his students. It would have been impossible for me to accomplish this endeavor without his encouragement, constant support and guidance.

I collaborated with several scholars and researchers in the field of optimization and communication networks throughout my PhD. I'd also like to express my appreciation to Dr. Samir Sebbah, Dr. Hamed Alazemi, Dr. Ahmad Khalil and Dr. Mohammad F. Uddin for their active collaboration which yielded to authoring high-quality and well received journal and conference papers. Furthermore, I was granted a warm and friendly atmosphere in our research lab at Concordia University throughout my PhD. I am greatly thankful to all of my colleagues.

I also appreciate the funding support from the Fonds De Recherche du Québec- Nature et Technologies (FQRNT) and Natural Sciences and Engineering Research Council of Canada (NSERC).

My deepest appreciation goes to my loving wife. Aside from myself, no one has been more impacted than her by this dissertation. I would like to thank her for all her support, constant love and care. Finally, I am grateful to my parents. I could never achieve my ambitions without their encouragement, understanding, support and true love.

Contents

List of Figures

List of Tables

List of Acronyms

SONET	Synchronous optical networking
SDH	Synchronous Digital Hierarchy
CAPEX	Capital Expenditure
OPEX	Operational Expenditure
MEF	Metro Ethernet Forum
WDM	Wavelength Division Multiplexing
LAN	Local Area Network
VLAN	Virtual Local Area Network
EPL	Ethernet Private Line
EVPL	Ethernet Virtual Private Line
EP-LAN	Ethernet Private LAN
EVP-LAN	Ethernet Virtual Private LAN
EP-Tree	Ethernet Private Tree
EVP-Tree	Ethernet Virtual Private Tree
STP	Spanning Tree Protocol
MSTP	Multiple Spanning Tree Protocol
RSTP	Rapid Spanning Tree Protocol
MPLS	Multi Protocol Label Switching
GMPLS	Generalized MPLS
LP	Linear Programing

ILP	Integer Linear Programing
MILP	Mixed Integer Linear Programming
EEE	Energy Efficient Ethernet
ERP	Ethernet Ring Protection
RPL	Ring Protection Link
ESP	Ethernet Switched Paths
LSP	Label Switched Path
Eth-LSPs	Ethernet-LSPs
FDB	Filtering Database
ITU-T	ITU Telecommunication Standardization Sector
LPI	Low Power Idle
PBB-TE	Provider Backbone Bridge - Traffic Engineering
PPBB-TE	Photonic Provider Backbone Bridge - Traffic Engineering
MAC	Medium Access Control
NIC	Network Interface Card
NP	Nondeterministic Polynomial Time
QoS	Quality of Service
s-d	Source-Destination
SF	Sequential Fixing

Chapter 1

Introduction

1.1 Motivation

Synchronous optical networking/Synchronous Digital Hierarchy (SONET/SDH) circuit-switched time division multiplexing (TDM) equipments are dominating the installed infrastructures of today's backbone networks. Following the ITU-T's Global Standards Initiative (GSI), the current widely deployed circuit-switching SONET/SDH networks will evolve into Next Generation Networks (NGNs) whose data transfer is based on packets instead of circuits in order to converge and optimize their operation and meet the increasing demand for new multimedia services and mobility.

Ethernet can greatly reduce the complexity and cost associated with the large scale and broad scope of carriers' circuit-switching networks by being a cost-effective and less complex replacement for SONET/SDH. Recent studies show that retail enterprise Ethernet ports are projected to grow at a 37% compound annual growth rate between 2010 and 2015 [5] and that more than 75% of service providers have a strategy of using Ethernet instead of SONET/SDH for accessing and collecting customer traffic [6]. Given that the volume of Ethernet traffic is growing at unprecedented rates, Ethernet infrastructures and services become increasingly vital. Indeed, Ethernet has been a great success story as the packet-switching technology of choice in the vast majority of today's enterprise and local area networks (LANs). However, native Ethernet, as a technology of LAN, lacked some crucial features of carrier transport networks and thus required improvement especially in terms of failure recovery mechanism, scalability, traffic engineering, etc. Continuous efforts have been made by numerous working groups of IEEE and ITU-T to enhance native Ethernet to become a carrier-class technology of choice. These efforts are broadly focused into two different directions: (i) to introduce an efficient and faster failover technique for Ethernet networks and (ii) to evolve Ethernet frame headers in order to support carrier-class scalibility and traffic engineering capability.

The Ethernet frame forwarding requires "loop-free" network topology for maintaining proper forwarding plane and it relies on the Spanning Tree Protocol (STP) [7] to build a logical tree in mesh networks. Different variations of STP such as Multiple Spanning Tree Protocol (MSTP) [8], Rapid Spanning Tree Protocol (RSTP) [9] are also introduced to improve its performance. MSTP creates multiple logical trees in the same Ethernet network allowing multiple routes for traffic among a pair of source-destination and improves the efficiency of resource usage. In the event of a failure of a network element, the STP (or any of its variant protocol) needs to be re-executed to rebuild the logical trees in order to recover the affected traffic. This rebuilding process requires relatively larger convergence time, approximately in the order of seconds, compared to the counterpart technology of Ethernet, namely

SONET/SDH which provides 50-ms failover time. A new failure protection mechanism recently proposed, referred to as ITU-T recommendation G.8032 Ethernet Ring Protection (ERP) places Ethernet back into competition as a carrier-grade technology of choice. ERP guarantees sub 50-ms of failover time in a 1600 Km ring consisting of 12 nodes [3].

Toward the realization of carrier Ethernet networks, traditional Ethernet bridges/ switches must be gradually enhanced with advanced capabilities and forwarding models, while at the same time operating at ever increasing line rates [10]. During the last decades, Ethernet has been evolving through numerous standardization efforts such as IEEE 802.1Q, IEEE 802.1ad, IEEE 802.1ah. Latest carrier Ethernet technology called *Provider Backbone Bridge-Traffic Engineering (PBB-TE)*, which was recently ratified in IEEE standard 802.1Qay in June 2009 enhances carrier Ethernet networks with the support of traffic engineered point-to-point and point-to-multipoint connections called Ethernet Switched Paths (ESPs) by implementing frame forwarding based on service-VLAN identifier (S-VID) and destination MAC address. PBB-TE preserves the connectionless behavior of native Ethernet and adds a connection-oriented forwarding mode to current Ethernet networks by encoding an end-to-end connection identifier on the forwarding plane. PBB-TE enhances carrier Ethernet networks with traffic engineering, deterministic Quality of Service (QoS), and support for protection switching at Ethernet cost points. PBB-TE allows service providers to maximize network utilization and hence minimize the cost per bit carried and provides an ideal platform to emulate revenue generating voice services.

Similar to every other new technology, both ERP and carrier Ethernet introduce new challenges to the design of communication transport networks.

Novel protection architecture and operational principles are introduced by ERP. The Ring Protection Link (RPL) of ERP and the unique logical ownership of a link that is common between interconnected rings in multi-ring mesh networks play vital role in provisioning link capacity to protect network traffic in case of failures. Hence, the placement of RPLs and logical ownership of links need to be carefully determined to avoid unnecessary capacity redundancy in the network as well as to ensure efficient use of network resources through traffic engineering. One of the other growing concerns is the energy consumption in the routers/switches of telecommunication networks. The new standards of Ethernet allow it to be deployed in carrier-grade transport networks leveraging its ever increased line rate, e.g. 10 Gb/s, 100 Gb/s. Increased line rates also cause increased power consumption in switch ports. In order to address the growing concern, the IEEE ratified another new Ethernet standard, referred to as IEEE 802.3az Energy Efficient Ethernet (EEE). EEE enables the Ethernet switches to turn any particular port into "sleep" mode if there is no traffic to send and "wake" the port again ("active" mode) for sending available traffic. During sleep mode, a port can save as much as 90% of energy consumption than that in active mode. To ensure maximum energy saving, Ethernet frames should be efficiently scheduled to send from buffer to designated ports.

Given the recency of the newly emerging Ethernet standards, there has been very little work to date which studies the impact of RPL placements and the logical ownership of the links on overall capacity requirement to protect network services. Most of these studies follow the approach of exhaustive enumeration to investigate all possible network configuration scenarios and determine the best one. In addition to the ineffective solution approach, some of these studies failed to provide optimal solution due to ignoring a subtle flaw of their approaches. Additionally, to the best of our knowledge, there has been no previous work that addressed the scheduling of Ethernet frames in order to achieve optimal energy consumption with the motivation of greener transport networks. Hence, there is a need to study various aspects of network design using the promising new Ethernet standards such as ERP as well as explore and develop newer design strategies for building transport networks more energy efficient.

1.2 Objectives

The main objective of this thesis is to analyze and study the impact of recent carrier Ethernet technologies and standards on the design of telecommunication networks and in particular carrier grade networks. Towards the accomplishment of this objective, we divide the broader objective into three major tasks as follows.

- To analyze various aspects of network design with ERP in the context of single link failure scenarios. This includes the study of newly introduced architecture and operation of ERP and investigate the impact of RPL placements on overall capacity provisioning in both single and multi-ring transport networks. The study also includes analyzing the effect of unique logical ownership of the links that are common to multiple rings on capacity provisioning.

- To study the effect of concurrent dual link failures in ERP-based multi-ring mesh networks. Concurrent dual link failures may divide a mesh networks into multiple segments and thus interrupt network services. In addition to capacity provisioning, the placement of RPLs and the logical ownerships of the common links play important role on the number possible such instances of service disruptions. This study also includes developing a network design approach that fairly distribute network flows and ensures efficient use of network resources in ERP networks.

- To explore new approaches for reducing energy consumption in communication networks and develop energy efficient Ethernet switches. This includes individual study of carrier Ethernet standards such as IEEE 802.1Qay, IEEE 802.3az, etc. and the control plane of GMPLS. This study also includes developing optimal scheduling for Ethernet frames in the context of EEE and analyzing the feasibility of establishing energy efficient end-to-end connections in carrier Ethernet networks.

1.3 Contributions & Outline

This thesis is organized into six chapters, including this chapter, which are organized as follows:

- The fundamentals of recent Ethernet standards that are considered in this thesis are introduced in Chapter 2. It includes the principles of these new standards and the evolution of native Ethernet towards carrier-grade Ethernet. It also includes the detailed explanation of ERP architecture and its operational principles. This chapter also introduces various carrier Ethernet services and the connection-oriented forwarding mechanism of carrier Ethernet including VLAN-based switching. The summary of the previous works that are related to the contribution of this thesis are also included in this chapter.

- Chapter 4 presents a network design approach for ERP based mesh networks, to handle single link failures. While provisioning link capacity in ERP-based mesh networks, the placement of RPLs and the logical ownership of links that are common to multiple rings play important role. We show that solving the two problems sequentially would increase unnecessarily the capacity redundancy in the network. Thus, we jointly model the problem of RPL placements and determining the unique ownership of common links in both single and multi-ring Ethernet networks as a mixed integer linear program (MILP) and present a solution framework for ERP-based mesh network design. We develop multiple variations of this design approach with different objectives that network operators might be interested to. We present several numerical results and engineering insights analyzing the trade-offs between different achievable objectives of network design and the effects on overall capacity planning.

- Next, we investigate the design aspects of ERP-based mesh networks in the context of concurrent dual link failures which is presented in Chapter 5. The joint problem of RPL placements and the unique ownerships of the links play important role in providing necessary protection to network services from dual failures in addition to capacity provisioning. Concurrent dual link failures may divide the networks into multiple segments. We show that those segmentations can be categorized into two classes, physical and logical segmentations, based on the locations of the failed links. We also show that efficient placement of RPLs as well as efficient selection of the owners of the common links can significantly reduce the number of possible logical segmentations while physical segmentations are inevitable without changing the physical network topology. Thus, we develop a MILP model which jointly addresses the problem of both RPL placements and unique ownerships of the links with the objective of minimizing logical segmentations and capacity redundancy. We also present multiple variations of this model with different design objectives. We present the numerical results and analyze the trade-offs between capacity investment and improving network service availability against concurrent dual link failures.

- Finally in Chapter 6, we present a new carrier Ethernet network model which is promised to be energy efficient and leading to green transport network. We propose two novel architectures of Photonic PBB-TE (PPBB-TE) core and edge switches, which enhance the usability of PBB-TE networks by reducing power consumption in individual switches in conjunction with passive optical bypassing and EEE. The proposed PPBB-TE core nodes are designed to use passive optical correlators to forward incoming flows all-optically, while the PPBB-TE edge nodes detect flows and transmit them through optical or Ethernet ports. We also formulate the problem of energy-aware scheduling as an optimization problem whose objective is to minimize the overall energy consumption for transmitting Ethernet frames while satisfying their delay requirements.

- Chapter 6 concludes the thesis, summarizing the most significant findings of this thesis and outlines possible directions for future research.

Chapter 2

Metro Ethernet Fundamentals and Related Work

This chapter elaborates the road map of Ethernet evolution from a LAN technology towards transport networks' technology of choice. Both the limitations of native Ethernet and its enhancements to overcome these limitations are introduced. The logical network architecture and operational principles of ERP are also introduced. Finally, we overview recent related research to our work.

2.1 Native Ethernet & limitations

Ethernet has been enjoying a great success as the technology of choice for LAN technology for more than two decades. Ethernet was initially designed as a frame-based technology for Local Area Networks (LAN). Since then, Ethernet has been greatly known for its simplicity and low-cost equipments. Ethernet transmission rates have evolved to higher speeds from 10 Mb/s to 100 Gb/s upon the ratification of IEEE 802.3ba. Newer Ethernet standards (10 GbE, 100 GbE) also offer interoperability with other transport technologies such as

SONET/SDH, MPLS based layer-2 VPN, etc. Native Ethernet relies on MAC address based learning and flooding process for switching. Ethernet switches maintain a source address table (SAT) for frame forwarding. They also use logical tree topology defined by STP and its variants (RSTP, MSTP) to specify a unique path between any pair of nodes, which helps preventing unnecessary excessive traffic caused by forwarding loop. Despite higher speed and featuring interoperability with other transport technologies, native Ethernet lacks some essential features of transport networks such as scalability in larger networks, resilience and fast recovery from network failures, advance traffic engineering, the capability of operation, administration and maintenance, support for quality of service (QoS), etc.

2.2 Why Ethernet as Carrier?

Even though IP routers lead the new installations, current wide area networks are dominated by SONET, MPLS, and asynchronous transfer mode (ATM) technologies. However, most data traffic currently is generated from and terminated to Ethernet LANs. The success story of Ethernet as a LAN technology has lead to a number of industrial and academic initiatives aiming to bring the benefits of native Ethernet to carrier grade networks, while equipping Ethernet with missing transport features and make an appealing alternative to legacy transport technologies. Such initiative led to the innovation of carrier Ethernet which aspires to extend Ethernet beyond LANs. One of the main reasons to choose Ethernet over other competitive technologies such as SONET/SDH or MPLS is its ability to significantly reduce capital expenditure (CAPEX) and operation expenditure (OPEX) for network operators. The authors in [11] shows a comparable study of CAPEX which states that implementing Ethernet in transport networks could reduce the port-count to 40% and reduce CAPEX 20-80% compared to other non-Ethernet alternatives. Another economical study was performed by Metro Ethernet Forum (MEF) which also shows the benefit of Ethernet implementation through CAPEX and OPEX comparisons [12]. The study considered data collected from 36 service providers from both Europe and North America. It estimates the savings of 23% in CAPEX over a 3-year time in a medium-sized city by using Ethernet services over other legacy services.

2.3 Evolution of Carrier Ethernet

Carrier Ethernet is formally defined by MEF as "A ubiquitous, standardized, carrier-class Service and Network defined by five attributes that distinguish it from familiar LAN based Ethernet" [1]. From the end users' perspective, it is a service defined by five attributes whereas it is a set of certified Ethernet equipments that transports the offered services to customers from service providers' viewpoint. The five defined attributes are presented in Fig. 2.1 and listed as follows:

- Standardized Services
- Scalability
- Reliability
- Service Management
- Quality of Service

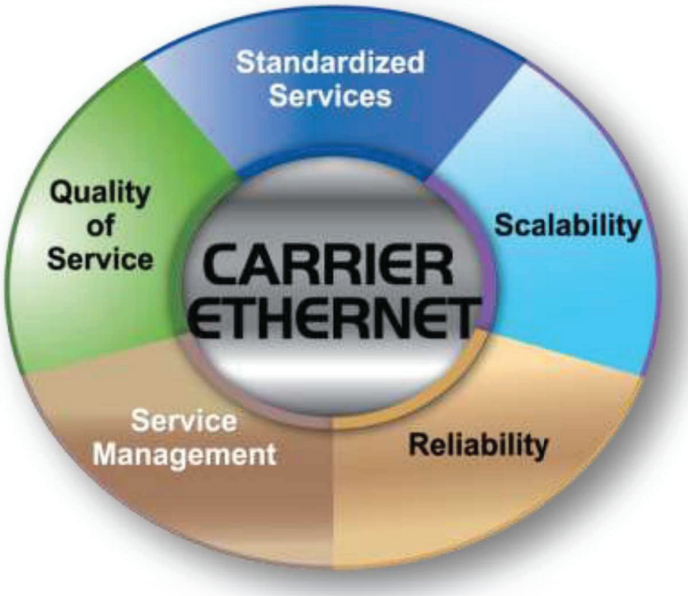

Figure 2.1: Five attributes of carrier Ethernet [source: [1]]

2.3.1 Standardized Services

Carrier Ethernet networks transport data through Ethernet Virtual Connection (EVC) according to the attributes of three defined services: E-Line (point-to-point), E-LAN (multipoint-to-multipoint), E-Tree (rooted-multipoint).

E-Line

E-Line is a point-to-point EVC, connecting two user network interfaces (UNIs) in carrier Ethernet networks. E-Line can be implemented in two different approaches as presented in Fig. 2.2 and described as follows:

- **Ethernet Private Line (EPL)** is the most popular Ethernet service due to its simplicity and high degree of transparency. It provides a point-to-point connection between two dedicated network interfaces (UNIs). It requires very little coordination of VLAN-IDs between the service providers and the customers. It is typically delivered over SONET/SDH and is an ideal replacement of existing TDM private lines.

- **Ethernet Virtual Private Line (EVPL)** provides the ability of service multiplexing at single physical interface (UNI). Multiple services can be offered through different EVCs using a single UNI. Different customers' frames are identified by VLAN-IDs and can be assigned to different EVCs. EVPL services require VLAN-ID coordination between the customer and the service provider. It is an ideal replacement of point-to-point Frame Relay connections or ATM layer-2 VPN services.

E-LAN

E-LAN provides multipoint-to-multipoint Ethernet virtual connections among multiple network interfaces (UNIs). Similar to E-Line, two types of E-LAN implementation are possible based on the multiplexing capability of the UNIs.

- **Ethernet Private LAN (EP-LAN)** offers full transparency to customer control protocols. Each UNI that is connected to EP-LAN service requires to be dedicated to that service only.
- **Ethernet Virtual Private LAN (EVP-LAN)** offers service multiplexing at each UNI and thus UNIs are allowed to offer more than one service through single physical interface. This type of service could be used to offer Internet access and corporate VLAN via single UNI.

Fig. 2.3 depicts the two types of implementation of E-LAN service type.

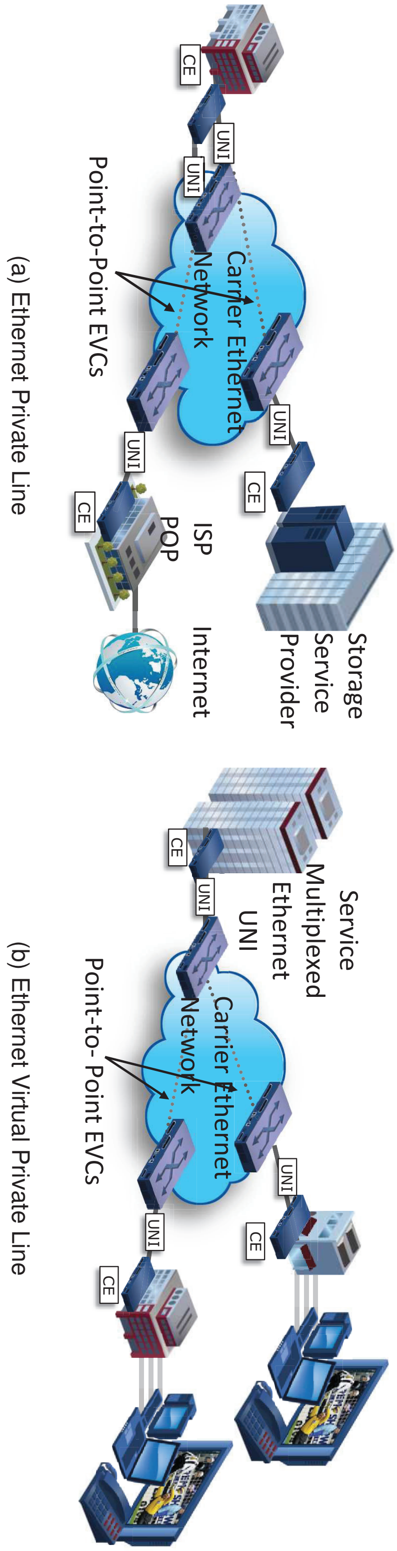

(a) Ethernet Private Line

(b) Ethernet Virtual Private Line

Figure 2.2: Ethernet Line (E-Line) [source: [1]]

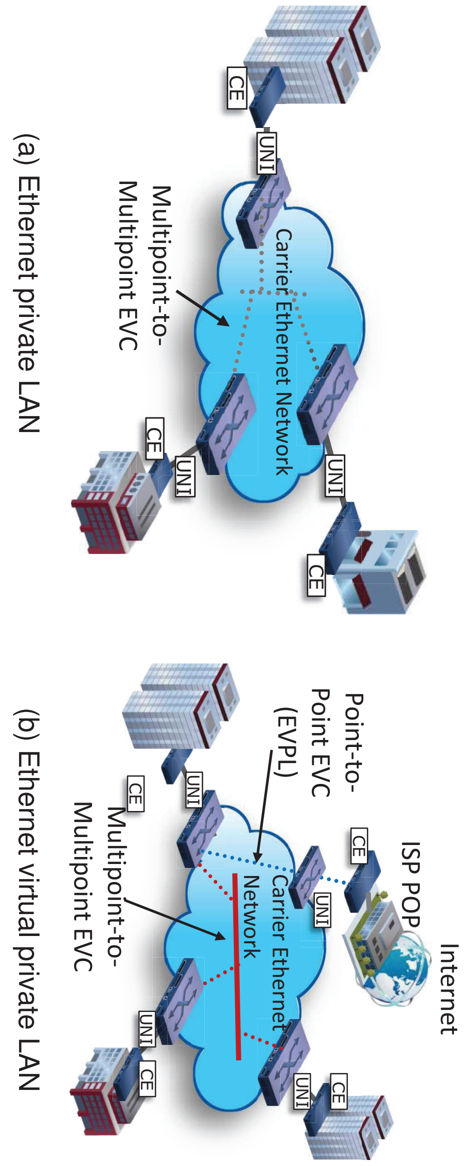

(a) Ethernet private LAN

(b) Ethernet virtual private LAN

Figure 2.3: Ethernet LAN (E-LAN) [source: [1]]

E-Tree

E-Tree service offers point-to-multipoint connectivity from root UNI to leaf UNIs and multipoint-to-point connectivity from leaf UNIs to root UNI. Leaf-to-leaf connectivity is prohibited. One or more UNI can be defined as a root and a root can communicate to other root. Similar to other service types, E-Tree can also be implemented with two different approaches:

- **Ethernet Private Tree (EP-Tree)** offers fully transparent EVCs from root to leaf UNIs and vice versa. It requires dedicated UNIs for a single tree and service multiplexing is not allowed with EP-Tree services.

- **Ethernet Virtual Private Tree (EVP-Tree)** offers multiple simultaneous services to be implemented at any single physical interface through service multiplexing. However, EVP-Tree requires more complex configuration than EP-Tree. It could be an ideal implementation to provide service for secure transmission of payroll information from branch offices to head office.

The implementations of E-Tree services are presented in Fig. 2.4.

2.3.2 Scalability

One of the major challenges of native Ethernet is to scale to meet the requirements of service provider offering in transport networks. Ethernet has evolved through numerous standardization efforts, to improve its scalability, which are mainly provided by different working groups of IEEE, IETF, ITU-T, and MEF. These standardization efforts have focused on leveraging the existing Ethernet protocol to make carrier Ethernet backward compatible with legacy Ethernet equipments. The objective is to enable carrier Ethernet to deliver

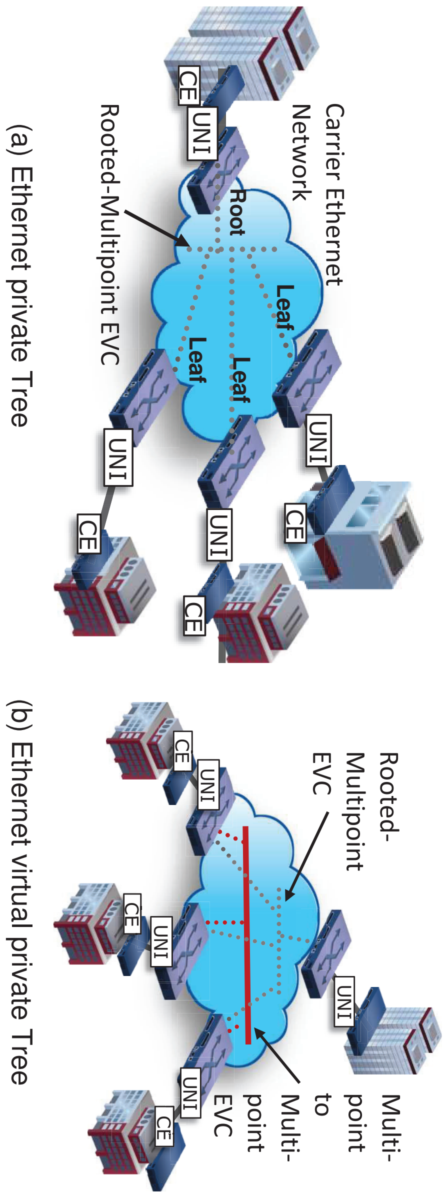
(a) Ethernet private Tree

(b) Ethernet virtual private Tree

Figure 2.4: Ethernet Tree (E-Tree) [source: [1]]

QoS supported traffic rather than best-effort traffic in large scale networks through architectural evolution such as enabling frame forwarding through connection-oriented tunnels instead of connection-less forwarding model, enabling centralized path configuration instead of distributed address learning, etc. Different milestones toward this evolution are elaborated as follows:

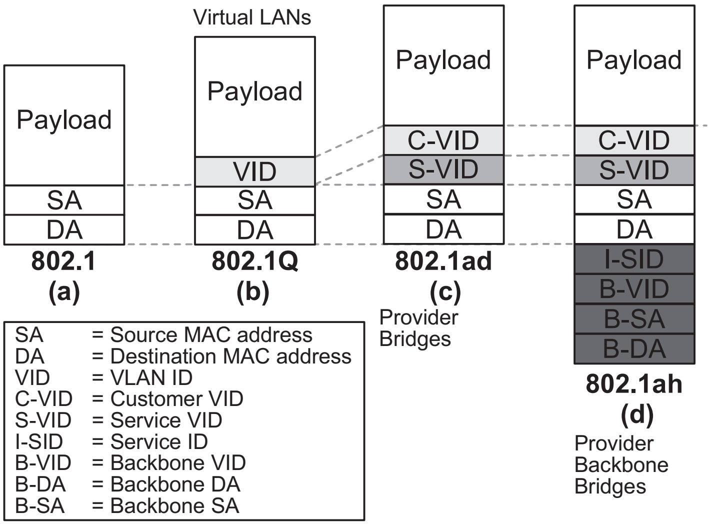

Figure 2.5: Architectural evolution of Ethernet [source: [2]]

IEEE 802.1Q: Virtual LAN (VLAN) switching

The concept of Virtual LAN was widely accepted by service providers to create multiple independent logical networks within a physical network and to differentiate customer networks. The forwarding of unicast, multicast and broadcast traffic is restricted by implementing VLANs. A unique 12-bit VLAN ID (VID) is assigned by the service provider within the Q-tag of each customer frame. Q-tags are added at the ingress nodes and removed at the egress nodes. VLAN facilitates easy administration of logical network groups, e.g. adding or removing members, and limits unnecessary traffic exchange from one logical group to another.

VLAN learning, a similar process to MAC learning, is maintained by VLAN switches to store and associate MAC addresses, VIDs, and port numbers in one or more *filtering databases* (FDBs). Two types of VLAN learning processes are defined by IEEE 802.1Q: independent VLAN learning (IVL) and shared VLAN learning (SVL). IVL maintains one FDB per VLAN, i.e., MAC learning within a VLAN space and thus frame forwarding is performed based on 60-bit combination of the MAC address and the VID. In contrary, SVL shares port information among the VLANs, hence maintains one FDB for all VLANs. The process of VLAN learning enables the service provider to differentiate traffic from different customers under the same provider. However, IEEE 802.1Q imposes limitation on the maximum number of supported customers by 4094 due to the 12-bit VID which is inadequate to support large number of customers in most of the recent networks.

IEEE 802.1ad: Provider Bridges (Q-IN-Q)

The IEEE standard 802.1ad, Provider Bridges, introduces stacking of VLAN IDs of two Q-tags, referred to as Q-IN-Q, instead of one VIS. The customer VLAN ID (C-VID) identifies the VLANs configured under a single customer and the service provider VLAN ID (S-VID) identifies the VLANs administered by any single service provider. By this approach of Q-tag stacking, both the customers and the service providers can maintain their own VLAN space of 4094 VLANs without requiring any coordination of VLAN IDs among them. However, in order to allow customers to access multiple distinct services through a single physical port, a provider edge bridge (PEB) is required where edge switches must operate on both C-VID and S-VID tags, resulting in potential SAT overflow. Moreover, S-VIDs are used for both service identification and frame forwarding in provider networks, causing S-VIDs overloaded. Hence, the scalability issue remained unresolved by IEEE 802.1ad.

IEEE 802.1ah: Provider Backbone Bridges (MAC-IN-MAC)

Provider Backbone Bridge (PBB) addresses the scaling issues of IEEE 802.1ad by introducing another hierarchical sub-layer, i.e., encapsulation of customer frames within a provider frame. PBB, also referred to as MAC-IN-MAC, employs the 16-bit MAC address of service provider's edge devices (B-SA & B-DA) and the service provider's VLAN-ID (B-VID). The outer MAC address is used to forward the Ethernet frames throughout the service provider network and removed at the egress node of that network. PBB significantly improves the scalability of Ethernet as well as increases the security by separating the customer and service provider MAC address space. It also improves the end-to-end performance by reducing the number of MAC addresses which need to be learned.

IEEE 802.1Qay: Provider Backbone Bridges-Traffic Engineering (PBB-TE)

Even though PBB provides a scalable and highly transparent provider infrastructure, service providers may still use best-effort approach while delivering carrier Ethernet services over numerous transport technologies such as SONET, MPLS, etc. However, this best-effort approach is not well-suited for time-sensitive applications. Provider Backbone Transport (PBT), also referred to as Provider Backbone Bridges-Traffic Engineering (PBB-TE), is a variation of PBB aimed to provide connection-oriented feature of TDM to connectionless Ethernet. PBT relies on MAC-IN-MAC forwarding scheme of PBB and also distributes the bridging table using the control plane. However, PBT does not allow some of the features of PBB such as broadcasting, MAC learning and spanning tree protocols. Rather, it provisions point-to-point and multipoint-to-multipoint Ethernet Switched Paths (ESPs), similar to MPLS tunnels, that are engineered to traverse throughout service provider networks.

The ESPs are identified by a range of reserved B-VIDs. These B-VIDs are not required to be globally unique and can be reused within another service provider network since these B-VIDs are used along with the MAC addresses (B-DA) of provider network's egress nodes. The outgoing port for a frame is determined by the combination of 60-bit B-VID and B-DA. Reserving only 16 B-VIDs out of available 4094 B-VIDs allow to establish a maximum of 16×2^{48} ESPs which are considered to be sufficient for transport networks [2].

A service provider must disable automatic MAC-address learning and flooding to enable PBT. It also must disable any variant of STP protocol, e.g. MSTP, RSTP and remove frames that are destined to an unknown destination. An ESP must be created in both directions to enable symmetrical connections. The PBT architecture allows path configuration from ingress to egress switches of the provider networks. Multiple ESPs can be established between any pair of source-destination ingress-egress nodes for traffic-engineering, load balancing or protection purpose.

2.3.3 Reliability

While the service-level reliability and carrier Ethernet components' resiliency have been defined, several other underlying transport technologies such as SONET/SDH have already offered high level of reliability and set carrier-grade resilience reference with sub-50 ms recovery times. Ethernet as a transport technology must meet this reference recovery time with a strong protection framework comprising faster failure restoration mechanism.

Metro Ethernet Forum (MEF) offers a large range of restoration times (5 s to less than 50 ms) for service-level protection in order to support a wide variety of applications and their requirements. To do so, four protection mechanisms have been defined by MEF: aggregate link and node protection (ALNP) to protect against link/node failure, end-to-end path protection (EEPP) to protect end-to-end primary paths with redundancy, RSTP for multipoint-to-multipoint E-LAN services, and link aggregation (LAG) to provide protection per link.

End-to-end path protection switching is proposed for PBT where each working path between edge nodes of provider networks are protected by provisioning a protection path in advance. Any failure along the path triggers the automatic replacement of working path B-VID at the ingress nodes to protection path B-VID in outgoing frames [2]. However, VLAN-level protections and restorations are provided by the family of STP protocols through topology reconfiguration. The restoration times associated with these variants of STP protocols vary between 1 s to 60 s [13] which certainly do not meet the carrier-grade requirements. The working groups of ITU-T introduces a recommendation, namely G.8032 Ethernet Ring Protection (ERP), focusing on VLAN-level protection switching which guarantees sub-50 ms recovery times. The architectures and operations of ERP are elaborated in more detail in Section 2.4.

2.3.4 Service Management

A comprehensive service management tool that provides the capability of Operations, Administrations, and Maintenance (OAM) is one of the prerequisites to deploy carrier Ethernet services in transport networks. Such a tool is required to provision services rapidly, diagnose fault and connection related problems at both intermediate and end points, and measure the performance attributes of delivered services. Several tools have been standardized based on three-layered approach focusing on the service layer, the connectivity layer, and the transport/data-link layer. Each layer is independent of other layers.

The service layer OAM, which provides the ability to manage end-to-end Ethernet services, is mainly defined by the IEEE standard 802.1ag Connectivity Fault Management (CFM) and ITU-T Y.1731. This OAM focuses on ensuring the compliance of offered Ethernet services with service level agreements (SLAs). CFM provides the ability to monitor the performance of service continuity by specifying numerous fault management functions such as continuity check (CC), link trace (LT), and loopback (LB). Some of the functions introduced by ITU Y.1731 are alarm indication signal (AIS), remote defect indicator (RDI), traceroute, etc. The measurement of typical SLA parameters such as frame loss, frame delay, delay-variations (jitter) are also enabled by the additional performance monitoring functions of ITU Y.1731. The IEEE standard 802.1ag and ITU Y.1731 also define the connection layer OAM which focuses on the connectivity between network elements. This OAM provides the capability to detect and troubleshoot any issue emerging between provider edge (PE) devices which ultimately facilitates to narrow-down the problem to a specific point in the infrastructure and fix the problem quickly.

The tr5ansport layer OAM is defined by the IEEE standard 802.3ah which provides the ability to manage a physical link between two Ethernet interfaces. It provides the link-level OAM functionality such as automatic discovery. The IEEE 802.3ah focuses on the access links of the native Ethernet access networks.

2.3.5 Quality of Service

Provider Backbone Transport (PBT) can provide deterministic transport of Ethernet services through a wide range of granular bandwidth and QoS options. Advanced level of SLA can be offered to meet the requirements of target applications by defining the service attributes associated with different Ethernet service types. The QoS requirements of carrier Ethernet are defined in MEF 10.1 within the specifications of bandwidth profile attribute. The bandwidth profile characterizes a connection based on five parameters: committed information rate (CIR), committed burst size (CBS), excessive information rate (EIR), excessive burst size (EBS), and color mode. The parameters are controlled and enforced at the UNIs by an algorithm, namely two-rate, three-color marker (trTCM) algorithm. Three colors (green, red and yellow) are used to mark customer frames according to the token bucket model. Green frames are guaranteed to deliver, yellow frames are delivered subject to available excess bandwidth and red frames are discarded. MEF 10.1 also defines some other performance measurement parameters for carrier Ethernet services such as frame delay, frame loss, jitter etc.

2.4 Ethernet Ring Protection (ERP)

While the evolution of Ethernet, as elaborated in previous section, has positioned carrier Ethernet to be the dominant technology of choice for transport networks, its ability to satisfy carrier-class requirements has been highly challenged by service providers in need of rapid service restoration following any network failure to guarantee high availability for carrier-grade network services. Ethernet's slow restoration time is attributed to its dependence on the

Spanning Tree Protocol (STP). In general, bridged Ethernet networks use STP or any of its variant protocol to ensure a loop-free topology. The STP protocol, originally standardized in the IEEE standard 802.1D, creates a spanning tree within a mesh network to specify a unique path for any source-destination pair and disable the links that are not part of the tree. The STP protocol requires extensive information exchange to build a tree and thus imposes larger convergence time (30 s to 50 s) to rebuild the tree upon the failure of any active link. An enhanced version of STP, namely Rapid Spanning Tree Protocol (RSTP) has been introduced (originally in the IEEE standard 802.1w and later incorporated in the IEEE standard 802.1D) to improve the convergence time. RSTP achieves faster spanning tree convergence after topology change by reducing the number of states of ports (from 5 to 3) and introducing more efficient exchange of bridge protocol data unit (BPDU). Later an extension to RSTP has been defined, referred to as Multiple Spanning Tree Protocol (MSTP), in the IEEE standard 802.1s which is later incorporated in the IEEE standard 802.1Q. Instead of disabling parallel links, MSTP rather exploits them to build multiple trees. MSTP is very useful especially when a network contains more than one VLAN. It provides the traffic engineering capability by configuring separate spanning tree for different VLANs or groups of VLANs. However, these developments of xSTP protocols still suffer from slow convergence (order of several seconds) and fall short of carrier-grade restoration time expectations. Indeed, reference has already been set for carrier-grade restoration time (50 ms) by some existing transport technologies. Ethernet therefore must meet this reference restoration time by adopting an efficient protection mechanism.

Resilient Packet Ring (RPR) has been defined in the IEEE standard 802.17 focusing on Metro Area Network (MAN) aiming to provide 50-ms restoration time. In addition to 50-ms protection switching time, RPR also includes a wide range of advantageous features. It supports data transfer among the user interfaces that are connected in a dual-ring configuration. RPR largely reduces the fiber requirements by using shared packet aware infrastructure while connecting large number of customers. It also offers a better management approach for excessive information rate (EIR) traffic under congestion scenarios. However, it introduces a new MAC header in order to achieve the objective of fast restoration time and thus becomes backward incompatible. RPR also requires a new set of complex protocols and algorithms which assumed to increase deployment cost leading to economically inviable.

International Telecommunication Union- Telecommunication Standardization Sector (ITU-T) working group has developed a new protection mechanism which enables the network providers to enjoy SONET/SDH-like sub 50-ms restoration time while leveraging the cost-effectiveness of Ethernet technology. This protection mechanism is introduced in the ITU-T recommendation G.8032 Ethernet Ring Protection (ERP). The objective of rapid restoration is achieved by exploiting standardized Ethernet OAM and Ring Automatic Protection Switching (R-APS) protocol. It operates on the principle of traditional Ethernet MAC and bridge functions and is thus completely backward compatible. Hence, the deployment of ERP is very simple, more often a simple software update on existing Ethernet switching equipments. ERP is developed as an alternative and to replace widely used xSTP protocols. ERP does not separate working and protection transport entities, however it reconfigures the transport entities during protection switching [3]. Hence, the link capacity should be carefully provisioned to allow protected service traffic and R-APS traffic to continue after protection switching.

2.4.1 Characteristics of ERP Architectures

ERP forms a logical ring topology to provide fast protection switching while maintaining a loop-free forwarding plane for Ethernet frames. The network elements of any given physical topology can be protected by either a logical ring or by a set of interconnected logical rings. Fig. 2.6 illustrates different components of ERP-based network architecture. A network protected by a single stand-alone logical ring consists of multiple components: Ethernet ring nodes, ring links, Ring Protection Link (RPL), RPL owner, and RPL node. Each Ethernet ring node uses at least two independent links connected to other adjacent ring nodes. A ring link uses a port, called ring port, to connect two adjacent Ethernet ring nodes. The minimum number of Ethernet ring nodes in an ERP is two. The G.8032 does not limit the maximum number of Ethernet ring nodes, however recommends the number of nodes to be in the range of 16 to 255 from an operational perspective. The other ERP components are elaborated later with their related functionalities. A mesh network can be designed as a composition of multiple logical Ethernet rings interconnected with each other, referred to as multi-ring/ladder network. In addition to the above mentioned components of a single ring, multi-ring ERP networks identify a special type of nodes, referred to as interconnection nodes that are used to interconnect multiple logical rings. The fundamentals of this protection switching architecture include: (i) the principle of loop avoidance, (ii) the utilization of learning, forwarding, and filtering database (FDB) mechanism, (iii) logical hierarchies among interconnected rings.

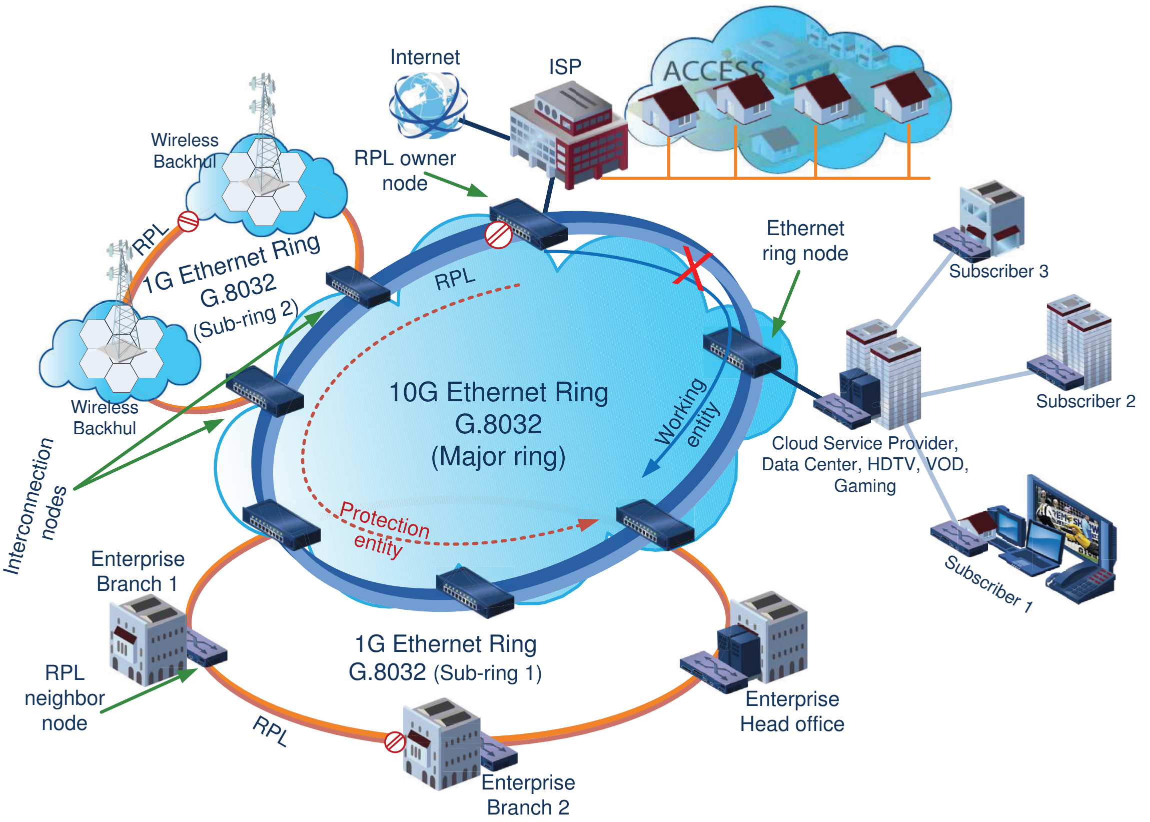

Figure 2.6: An example of ERP implementation

Loop avoidance

Loop avoidance is a very critical requirement for Ethernet networks. ERP must maintain a mechanism to prevent loops and ensure proper Ethernet operation and frame forwarding since it replaces the traditional Ethernet Spanning Tree Protocol (STP). Loop avoidance is achieved in ERP by blocking traffic at one of the ring links, referred to as the ring protection link (RPL). RPL is a logical link block placed to build a logical tree in the network; it is managed by one of its adjacent nodes called the RPL owner. The RPL owner is responsible for blocking transit traffic to its RPL port in normal operational state. The other adjacent node of the RPL is referred to as RPL node and may or may not block its port to the RPL. Under a failure condition, the RPL owner is responsible to unblock its end of RPL and allow the link to be used for traffic.

Filtering databases

Each Ethernet ring node maintains a filtering database (FDB) to store frame forwarding information learned by MAC learning process. Once a port block is relocated due to protection switching or reversion from protection state to normal state upon recovery, the information stored in FDB may become outdated. Hence, an “FDB Flush” operation should be performed by each ring nodes whenever a relocation of port blocking occurs. The FDB Flush operation clears all learned MAC addresses and their port associations. Each ring node reinitiates the MAC learning process to re-populate their FDBs after an FDB flush.

Logical hierarchy of interconnected rings

In a mesh network where multiple logical rings are interconnected, the interconnection nodes may have one or more links in between which are referred to as common links. However, these common links can belong to only one logical ring which will be responsible for triggering protection switching in case of failure of those links. The interconnected rings are categorized as *major rings* and *sub rings*. A major ring constitutes a closed ring while a sub-ring constitutes an arc or a segmented arc to allow other sub rings to be connected to the major ring. The major ring is always responsible for all of its links including the links that are shared with other sub-rings. If two sub-rings are interconnected and posses one or more common links between them, one of those sub-rings will be responsible for the common links and referred to as upper ring with respect to the other sub-ring. This characteristic leads to a logical hierarchy among the interconnected rings in ERP-based mesh networks.

2.4.2 Principles of ERP operations

The principles of Ethernet ring protection switching rely on the existence of Automatic protection Switching (APS) protocols in order to coordinate the actions around the ring nodes. ERP can operate in one of the two alternate modes: revertive or non-revertive. In revertive mode, the traffic is restored to the working entity once failure is recovered. A wait-to-restore (WTR) timer is adopted to avoid an erroneous switching operation caused by intermittent failure. The traffic channel reverts after the expiry of WTR timer. In non-revertive mode, traffic continues to use the protective entity and the RPL remains unblocked. Since the position of RPL and the resources of working entity are more likely to be optimally designed, the revertive operation is desired. However, this is performed at the cost of additional traffic disruption. Regardless of the operating modes, the ERP mainly operates based on two major functions: failure detection and protection switching.

Failure detection

A link failure is detected by the adjacent ring nodes of the failed links. A node failure is considered as failure of the two links attached to the failed node. The two nodes adjacent to the failed node detect such failure. The link status is monitored by an Ethernet continuity check (ETH-CC) function. Continuity check messages (CCMs) are periodically exchanged between maintenance end points (MEP) in every 3.3 ms to monitor link health. When an end point detects a failure, it signals the ERP control process to initiate protection switching.

Protection switching

Once a failure is detected, the failure detecting nodes block the ports of the failed links and start broadcasting the R-APS Signal Fail (SF) message periodically in the network. The SF messages are propagated along the ring and eventually reach the RPL owner and the RPL neighbor node. Upon receiving R-APS SF message, the RPL owner and the RPL neighbor node (if applicable) unblock their ends of RPL and the network state is changed from normal to protection state.

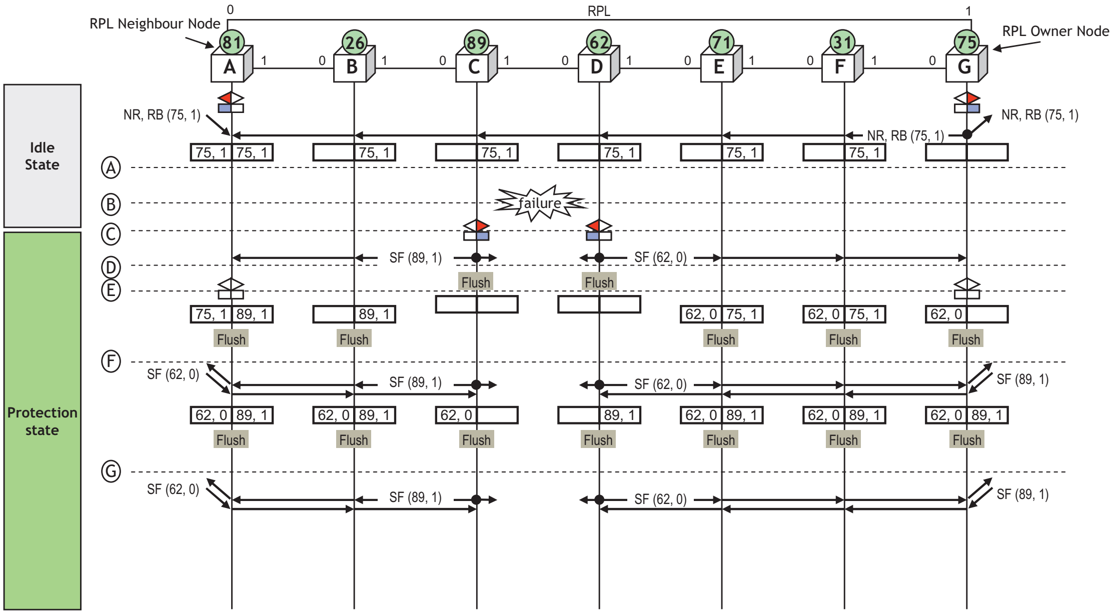

Figure 2.7: Failure scenarion in ERP [source: [3]]

Fig. 2.7 illustrates the series of actions taken by ERP control process once a failure is detected. The vertical dotted lines represent different states of the network at different reference point of time. In normal condition, the RPL is blocked by its owner node G. At reference point B, a failure occurs on the ring link between nodes C and D. Ethernet ring nodes C and D detect this failure at the reference point C; block the failed ring port and perform FDB flush after the hold-off time. The failure detecting nodes C and D start sending R-APS SF message periodically while the SF condition persists. At reference point E, all nodes receiving the SF message perform FDB flush. Both the RPL owner node G and the RPL neighbor node A receive the SF message. They unblock their ends of the RPL and perform FDB flush.

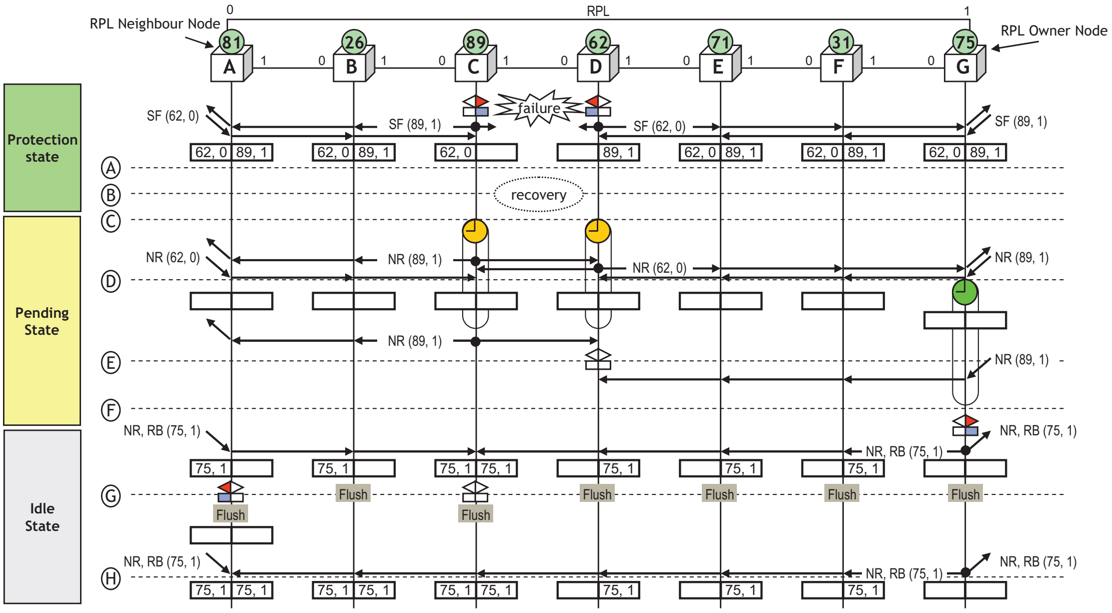

Figure 2.8: Failure receeovery process in ERP [source: [3]]

Fig. 2.8 illustrates the series of actions performed by the ERP control process once a failed link is recovered considering that the ring operates in revertive mode. At reference point B, the failed link between nodes C and D is recovered. At reference point C, the ring nodes C and D detect clearing SF condition and start a guard timer that prevents the nodes C and D from receiving any outdated R-APS messages. They also start sending R-APS NR messages periodically on both ring ports. The RPL owner node receives the NR message and starts the WTR timer at reference point D. Once the guard timer expires on nodes C and D, they start accepting R-APS messages. The node D receive R-APS NR message from node C and unblocks its previously-failed ring port.

When the WTR timer expires at reference point F, the RPL owner blocks its end of RPL, sends the R-APS (NR, RB) message and performs FDB Flush. Each node receiving the first R-APS (NR, RB) message flushes its FDB. When the ring node C receives an R-APS (NR, RB) message, it removes the block on the ring port of previously-failed link and stops sending R-APS NR message.

2.5 Related work

During the past decade, a large number of studies have been performed to improve the performance of xSTP protocols that are used in legacy Ethernet. The original STP protocol is modified and enhanced; the result in enhanced RSTP and then later MSTP. Several improvements of performance for RSTP [14–16] and traffic engineering approaches with MSTP [17–20] have been proposed for VLAN based Ethernet networks. A Shared Spanning Tree Protocol (SSTP) is introduced in [21] before the advent of MSTP, however, it uses very similar concept of MSTP. In spite of all theses efforts, xSTP protocols are yet unable to achieve carrier-grade rapid convergence, leading to the birth of ERP.

The advent of ERP introduces new challenges in network design. Some key features and unique operational principles of ERP such as placements of RPLs, determining logical hierarchy among interconnected rings, FDB flush operation, etc. need to be carefully addressed while implementing ERP to protect Ethernet transport networks. Given the recency of ERP protocol, very few studies in current literature address the network design issues of ERP implementation. However, the trend is growing. There has been some recent works that address the ERP performance issue caused by FDB flush operation. According to the ERP protocol, every event of failure or recovery from failure requires each Ethernet ring node to perform FDB flush operation. The FDB flush operation initiates a large amount of transient traffic that may affect the performance of ERP based networks.

The authors of [22] propose a simple and straight forward algorithm to manage FDBs in ERP networks even before the first recommendation of G.8032 is published. The study considers only single ring networks. It demonstrates the idea of providing protection in Ethernet ring networks without blocking any port and claims to increase the resource utilization as much as twice. An algorithm for efficient FDB flush operation is proposed in [23]. The authors introduce a priority based flush operation where the Ethernet ring ports are ordered according to the priority to perform the flush operation. The priority of the ports are determined based on the objective. The proposed algorithm can be implemented without modifying the original ERP standard and is promised to improve the protection switching time of the original standard. The authors in [24] propose a selective FDB advertisement approach to reduce the time to re-learn the MAC addresses in a ring node after FDB flush operation. The proposed approach leverage the R-APS subnet MAC address list (SAL) message type to multicast the MAC addresses that are not affected by any failure. The R-APS SAL messages are initiated by the failure detecting nodes, thus reducing the amount of transient traffic generated by the FDB flush operation. In [25], the authors introduce a new scheme, referred to as FDB flip, for fast FDB updates which utilizes the failure notification messages generated by the nodes adjacent to the failure (NAF). In this scheme, the authors propose to generate a so called flip-address list (FAL) which contains the MAC addresses associated with the failed link port. This list is then propagated along with the failure notification messages to other ring nodes. Other ring nodes then flip the port directions for only the MAC addresses that are in the list. This scheme does not require to generate excessive traffic to update FDBs and thus ensures the use of minimal link capacity for FDB flush operation. Besides these efforts to optimize resource utilization for FDB flush operation, another study discovers a potential inconsistency in newly learned MAC addresses after FDB flush operation [26]. The authors in [26] highlights that Ethernet data frames have lower priority than Ethernet control messages. hence, a data frame might be delayed at some intermediate nodes and delivered later to some other nodes while a protection switching occurred. The arrival of such delayed frames will cause erroneous MAC address entry in FDBs. To mitigate this issue, the authors propose three solution approaches: flush delay timer, purge trigger, and priority setting. They also develop a Markov-Chain model to estimate the mean protection switching time for the proposed solution schemes. All of the previous works focus on single ring ERP networks. [27] evaluates the performance of most of these previous schemes in multi-ring ERP networks.

The placements of RPLs and the selection of ring hierarchies are two key issues in designing ERP networks. Both play important roles in determining the capacity required to provide necessary protection. There has been some recent efforts that address these ERP design issues. The work in [28] is the first of this type which explicitly addresses the issue of RPL placement and ring hierarchy in mesh networks. However the authors exhaustively enumerate all possible scenarios of RPL positions combining all possible ring hierarchies and linearly search for the best configuration which requires minimum capacity to be invested to provide necessary protection. The authors assumed both guaranteed and best effort services where the best effort services are offered by exploiting the redundant capacity without any guarantee of restoration upon failure. Later, the authors in [29] propose an improved algorithm to find efficient RPL placement rather than the exhaustive enumeration approach. The proposed algorithm defines a variable Δ_ℓ which estimates the sum of so called "capacity gap" accumulated on link ℓ. The capacity gap is computed by the difference of the hop counts between the shortest path and the other alternate path. The proposed algorithm selects the link ℓ as RPL which has the smallest Δ_ℓ. The authors also develop an ILP model and evaluates the optimality of the solution achieved from the proposed algorithm with the solution of ILP and the exhaustive enumeration approach. However, this study ignores the other important design parameter, i.e., the selection of ring hierarchy. In [30], the authors develop an optimal design for ERP that maximizes the availability of Ethernet services. The authors also present a formal approach to analyze the availability of Ethernet services in multi-ring ERP mesh networks. However, due to the complexity of the designed model, the authors develop a heuristic algorithm which obtains a suboptimal solution for larger networks.

In addition to optimal resource provisioning, the placements of RPLs and the selection of ring hierarchy can also be determined to satisfy the goal of traffic engineering. [31] develops a load balancing scheme for ERP networks while determining the positions of RPLs. The authors exhaustively enumerate all possible RPL positions and linearly search for the best RPL placement to minimize the maximum link load. However, their study does not include the issue of logical ring hierarchies.

Besides these works, [32] focuses on failure detection and recovery process. In [32], the authors develop a faster failure detection process by maintaining an additional set of network state information which certainly enhance the ability of ERP networks to provide faster protection switching. All of these previous works consider single link failure scenarios while optimizing resource allocation or protection switching performance of ERP. To the best of our knowledge, there has not been any study which considers concurrent dual link failures while designing ERP-based mesh networks.

Chapter 3

Design of ERP: Single Failure

In this chapter, we focus on the optimal capacity planning for an ERP-based network by jointly selecting the Ring Protection Link (RPL) and the hierarchies among the interconnected rings. Unlike earlier work [28] where the authors performed exhaustively enumerate all possible RPL placements and ring hierarchies to search for the optimal solution, we formulate this combinatorial problem as a mixed integer linear program (MILP) and solve it effectively, which is to the best of our knowledge the first model in the literature that addresses the above mentioned design issues of ERP-based mesh networks.

The rest of this chapter is organized as follows; Section 3.1 provides a brief understanding of the operation principle of ERP. Section 3.2 highlights the insights of ERP design aspects and provides a motivative example. In Section 3.3, we reveal the limitations in the methodology of the prior work and propose some changes to overcome these limitations. The problem formulation and an ILP based design methodology is presented in Section 3.4. The numerical results are presented and analyzed in Section 3.5. Section 3.6 includes our concluding remark.

3.1 Ethernet Ring Protection: A Primer

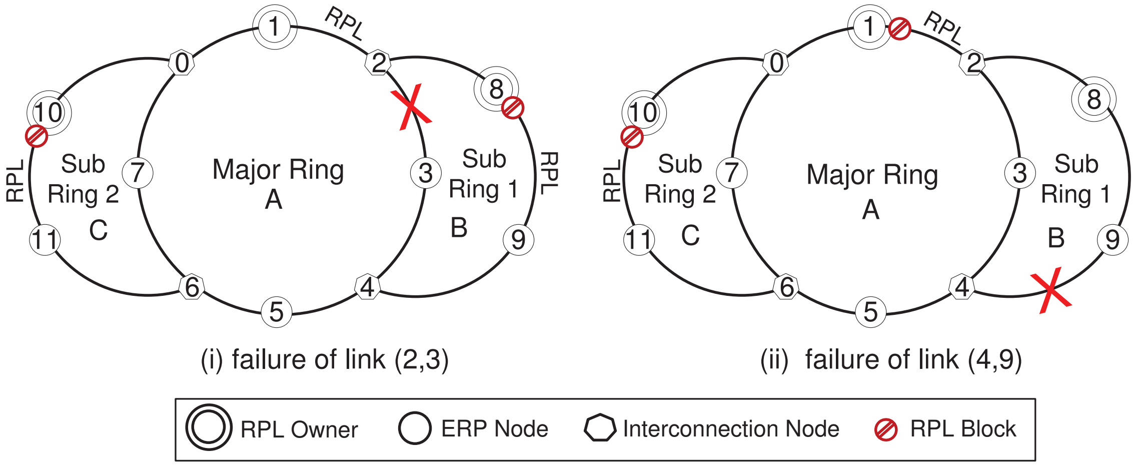

Figure 3.1: ERP Operations

A stand-alone single-ring ERP network consists of four components: Ethernet ring nodes, one Ring Protection Link (RPL), one RPL owner, and one RPL node. Each node in an ERP network has at least two ports to connect to its neighbors. A ring protection link is a unique feature for ERP and is introduced to prevent loops and ensure proper Ethernet operation and forwarding. This is a critical property of ERP since ERP replaces the traditional Ethernet Spanning Tree Protocol (STP). RPL is a logical link block placed to build a logical tree in the network; it is managed by one of its adjacent nodes called RPL owner. The RPL owner is responsible for blocking transit traffic to the RPL. The other adjacent node of the RPL is referred to as RPL node and may or may not block its port to the RPL. Fig. 3.1(i) shows a network instance where ring A forms a single stand-alone ERP instance. Link $1-2$ is the RPL and nodes 1 and 2 represent the RPL owner and the RPL node respectively. Service operators are allowed to select their placement of RPL in the network and can change its position as required by the command set defined in G.8032 Recommendation. ERP leverages the traditional Ethernet MAC source address learning to populate the filtering database (FDB) which is later used for Ethernet frame forwarding. A ring Automatic Protection Switching (R-APS) channel is rendered as an in-band multicast channel to exchange messages between ERP nodes. In addition to the stand-alone single-ring ERP components, a multi-ring ERP mesh topology requires a special type of nodes for connecting the rings and are referred to as interconnection nodes. The interconnection nodes may have multiple links in between which are referred to as shared links. The interconnected rings are categorized as *major rings* and *sub rings*. A major ring is formed by a stand-alone single ring whereas a sub ring can be formed as an arc or a segmented arc to allow other sub rings to be connected to the major ring. A multi-ring mesh network may be composed of one or more major rings and a set of sub rings. A sub ring can be connected to a major ring or other sub rings. Fig. 3.1(i) presents a multi-ring mesh network instance where major ring A is connected with two sub rings. Interconnection nodes {2, 4} and {0, 6} connect the major ring with sub ring 1 and 2 using shared links $\{2-3,\ 3-4\}$ and $\{0-7,\ 7-6\}$ respectively.

The links that are shared by multiple adjacent rings require a unique owner ring. The owner ring of the shared links is referred to as *upper ring* w.r.t. the other adjacent ring which is referred to as *lower ring*. This yields a hierarchy of interconnected rings in Ethernet mesh networks. In this particular scenario of Fig. 3.1(i), the major ring is formed by taking the ownership of all of the shared links ($0-7, 7-6, 2-3,\ and\ 3-4$). Thus, the major ring is the upper ring with respect to both sub rings 1 and 2. Each major and sub ring in a mesh network must have its own RPL. The upper rings are responsible for establishing a virtual R-APS channel through shared links so that the interconnection nodes of the lower rings can exchange control messages.

A link failure is detected by the two adjacent nodes connected to the failed link; upon detecting a failure, the nodes immediately block the ports of the failed link and initiate and periodically broadcast the R-APS Signal Fail (SF) message in the network. The RPL owner and the RPL node unblock the logical block on the RPL ports upon receiving R-APS SF signal and the network changes the state from idle-state (or working state) to protection (or recovery) state. Clearly, any link failure in ERP network causes topology changes which is resulted from the unblocking of RPL ports. Thus, immediately after failure, the ring nodes are required to clear their FDBs and re-initiate a MAC source learning process to mitigate the inconsistency between current network topology and the forwarding information [33]; as a result, a protection state tree is established for traffic forwarding. If the failure occurred on the RPL links, the ERP does not require to change the topology and thus an FDB flush is not required. In this case, a Do Not Flush (DNF) flag is set in R-APS SF messages to avoid unnecessary FDB flushes. In case of a failure on a shared link in a multi-ring mesh topology, the upper ring unblocks its RPL ports, and this topology changes does not require the lower rings to flush their FDBs. However, any failure, recovery, or topology changes in lower rings requires an FDB flush in upper rings. Fig. 3.1(i) depicts a failure scenario in one of the shared links $(2-3)$ and the upper ring (which is the major ring in this case) unblocks its RPL ports. In this scenario, the nodes in sub ring 1 do not require to flush their FDBs. Fig. 3.1(ii) presents a failure on link $(4-9)$ of sub ring 1 where sub ring 1 removes its RPL blocking which requires the FDB flush operation in the major ring.

3.2 ERP Design perspectives

The design aspect of Ethernet ring protection appears to be a unique challenge because of the unique operational principles of ERP. The positions of ring protection links and the unique ownership of the links which are shared by multiple rings may play an important role in determining the required capacity for carrying traffic and providing the necessary protection in Ethernet rings. A given physical network topology can be categorized as either a single logical ring or a mesh of multiple logical rings. The design objectives may vary in accordance with the given logical topologies. Next, we illustrate the design perspectives on both Ethernet rings.

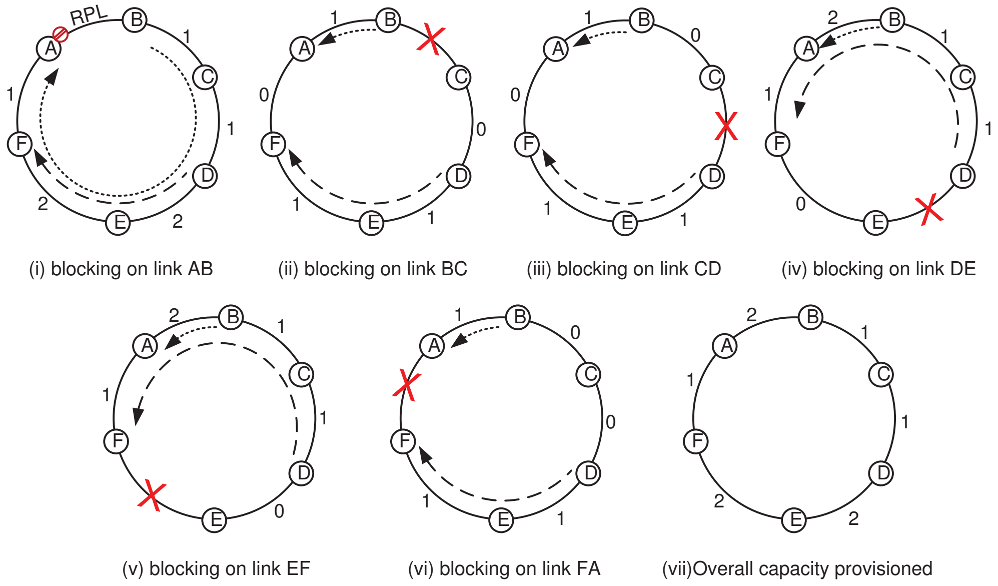

(i) blocking on link AB

(ii) blocking on link BC

(iii) blocking on link CD

(iv) blocking on link DE

(v) blocking on link EF

(vi) blocking on link FA

(vii)Overall capacity provisioned

Figure 3.2: Illustrative example: A single ring instance

3.2.1 Single stand-alone ring

Capacity provisioning in a single stand-alone ring topology may only rely on the placement of RPLs since no shared link exists in such network topology.

The objective of the network design should be to select an RPL placement in such a way that the overall capacity requirement is minimized for a given traffic instance. Clearly, there exist several possibilities for RPL placement in a ring and each such placement yields a different logical network topology. This topology clearly constructs a tree, and hence routing from any source to any destination is unique.

The required capacity on a link can be determined by two steps for a given traffic instance. First, we need to compute the load of that link for an assumed RPL position. Next, we need to compute the load of that link for every possible link failure scenario in the network. The maximum load among the above two computations would be the required capacity of that particular link for the particular RPL placement. The overall capacity requirement for the particular RPL placement of a ring is the sum of the required capacity of each link in the ring. Fig. 3.2 illustrates the steps of capacity provisioning in a single ring for two unit user demands between node pairs (B, A) and (D, F). Fig. 3.2(i) presents the routing of two given user demands with corresponding link loads in working state where link $A - B$ is selected as RPL. Figs. 3.2(ii) to 3.2(vi) show all possible link failure scenarios in the network and their corresponding link loads. Fig. 3.2(vii) depicts the capacity requirement of each link to carry the given user demands in working state and to provide necessary protection from link failure.

After a careful investigation of the provisioning process, we observe that the overall capacity requirement in a single ring network remains unchanged for a given set of traffic instance regardless of the RPL position. Next, we present a proof of our observation.

Let a network topology be denoted by $G(\mathcal{V}, \mathcal{L})$ where $\mathcal{V}$ is the set of vertices or nodes, and $\mathcal{L}$ is the set of links, indexed by v and ℓ, respectively. The state of a link is either blocked or unblocked to carry traffic. We follow similar notations to those used by the authors of [28]. Denote S to be a set of link state vectors which includes all possible K different link states, $S = \{S_k | k = 1, 2, ..., K\}$. S_k is a binary link state vector which represents the link states (blocked/unblocked) such that $S_k = \{S_{k,\ell} | S_{k,\ell} = 1$ for a blocked link, 0 otherwise$\}$. For example, the link state vectors of Figs. 3.2(i) and 3.2(ii) can be presented as $\{1, 0, 0, 0, 0, 0\}$ and $\{0, 1, 0, 0, 0, 0\}$ respectively where links $\{AB$, BC, CD, DE, EF, and $FA\}$ are represented by $\{\ell_1$, ℓ_2, ℓ_3, ℓ_4, ℓ_5, and $\ell_6\}$ respectively. Since each link state vector constructs a tree, it uniquely determines the routing as well as the corresponding link loads for a given traffic instance. The load on link ℓ is the total amount of traffic routed through the link for a certain link state vector S_k, and is denoted by λ_ℓ. To ensure reliable service, a link should reserve enough protection capacity by taking into account all possible failure scenarios in the network, i.e., all K different link state vectors in S. One can determine the capacity requirement C_ℓ for link ℓ by finding the maximum load on the link over the range of link states in S: $C_\ell \geq \lambda_\ell(S_k)$ for all $\{k \in 1, 2, ..., K\}$. Finally, any optimization of capacity provisioning should focus on the minimization of overall required capacity and can be presented as: $\min\limits_{S_k} \sum\limits_{\ell \in L} C_\ell$.

Remark: Given that a link state vector constructs a tree and the routing is unique in a tree, the capacity requirement for a set of link states is fixed for a given traffic instance.

Theorem 3.2.1. *The overall capacity requirement in a single ring network is independent of the RPL placement.*

Proof. we provide an indirect (by contradiction) proof of Theorem 3.2.1 in the case of a single ring ERP network.

Let us consider a ring with three links $\mathcal{L} = \{\ell_{i-1}, \ell_i, \ell_{i+1}\}$. Let us further assume that ℓ_i is the RPL and the required capacity provisioned is C_i. The theorem states that, $C_i = C_j$ where C_j is the overall capacity requirement if ℓ_j ($j = i + 1$ or $j = i - 1$) is chosen as RPL. For the sake of contradiction, let us assume that $C_i \neq C_j$, i.e., $C_i > C_j$ or $C_i < C_j$.

Now, if ℓ_i is considered as an RPL and thus blocking traffic, the corresponding link state vector is $\{0, 1, 0\}$. In order to compute the capacity provisioning, one should take into account all possible block states which are in this case $\{1, 0, 0\}$ and $\{0, 0, 1\}$. Then, the set of link state vectors is $S = \{\{1, 0, 0\}, \{0, 1, 0\}, \{0, 0, 1\}\}$.

Now, let us consider ℓ_{i+1} is the RPL and thus blocked. Hence, the corresponding link state vector is $\{0, 0, 1\}$. To compute the capacity requirement, we also take into account the blocking of ℓ_{i-1} and ℓ_i which yields the link state vectors $\{1, 0, 0\}$ and $\{0, 1, 0\}$ respectively. The resulting set of link state vectors then include $S' = \{\{1, 0, 0\}, \{0, 1, 0\}, \{0, 0, 1\}\}$.

By observation, it is evident that the two resulting set of link state vectors S and S' are congruence equivalent. Therefore, following the Remark, we can conclude that the corresponding capacity requirements $C_i = C_j$ which contradicts our previous assumption that is $C_i \neq C_j$. □

Note however that, the placement of RPL in a single ring may affect the capacity deployment in working state. Thus, the design objective in single ring ERP network may focus on minimizing the working capacity which facilitates for the service providers to opportunistically utilize the reserved capacity and temporarily assign the spare capacity to any low priority services [28]. Such optimization process is straight forward and trivial for a given traffic instance.

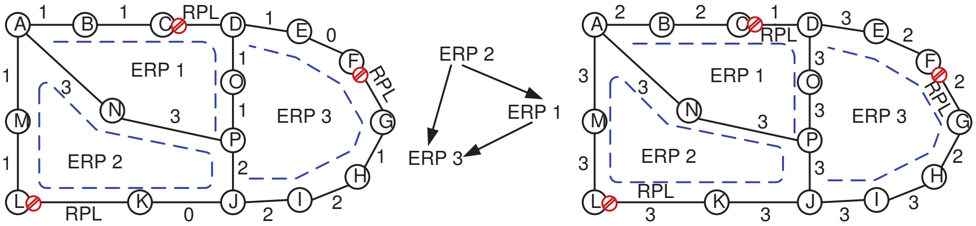

(i) Working state

(ii) Ring hierarchy

(iii) Capacity provisioning on each link

Figure 3.3: Illustrative example: Interconnected multi-ring instance 1

3.2.2 Mesh of interconnected multi-rings

The optimal capacity provisioning in multi-ring mesh networks gets considerably more complex because it entails, in addition to the RPL placement described for a single ring, determining the hierarchical interconnections among rings. Several hierarchies exist for a multi-ring mesh topology and each hierarchy requires a different set of RPL blocks to be investigated. The optimal capacity provisioning problem in a multi-ring ERP mesh network is hence to jointly determine the best ring hierarchy and RPL placement. This is a combinatorially complex problem given the large number of possible ring hierarchies and RPL placements. We present an illustrative example to estimate the variations in capacity provisioning due to the hierarchy changes.

Fig. 3.3(i) depicts a mesh network consisting of one main ring ERP_2 and two sub rings ERP_1 and ERP_3 which are sharing different links. Links AN and NP are shared between ERP_1 and ERP_2, links DO and OP are shared between ERP_1 and ERP_3, and link PJ is shared between ERP_2 and ERP_3. We assume that ERP_1 is the upper ring over ERP_3 and thus ERP_1 is the owner for links DO and OP. The ring hierarchy is represented by a directed graph in [28] where each node represents a ring and edges represent the interconnections between rings. The source and destination of an edge in the directed graph represent the upper-ring and sub-ring respectively. Fig. 3.3(ii) shows the directed hierarchy graph for the assumptions of main, upper and sub ring of the mesh network of Fig. 3.3(i). We further assume that RPLs of ERP_1, ERP_2, and ERP_3 are given and the optimal placement of the RPLs are out of scope of this example. We consider three unit demands between node pairs (A, H), (L, E), and (G, C). Fig. 3.3(i) shows the required capacity on each link (numbers presented next to each link) for the given demands in working state, yielding a total of 20 units. The protection capacity provisioning is performed by following all the steps as described for a single ring and taking into account the failure scenario on each link. Given space limitations and to avoid redundancy, all failure instances are not presented. However, Fig. 3.3(iii) summarizes the overall capacity requirement on each link to carry traffic in working state and to provide protection in case of a link failure which yields a total of 47 units. Next, we change the ring hierarchy as presented in Fig. 3.4(i) and observe its impact on capacity provisioning. For a fair comparison, we use the same network topology, the same RPL placement and user demands. Fig. 3.4(i) shows that ERP_1 is the main ring and ERP_3 is the upper ring w.r.t. the ring ERP_2. Fig. 3.4(ii) depicts the overall capacity requirement on each link for the given traffic instance, resulting in a total of 41 units, which is a reduction of 6 units over the previous solution.

The above illustrative example demonstrates the necessity of efficient network design to minimize the cost in terms of capacity requirement of the network. Both the placement of RPL and the selection of ring hierarchy should be jointly considered in the network design and planning phase which is the main focus of this work.

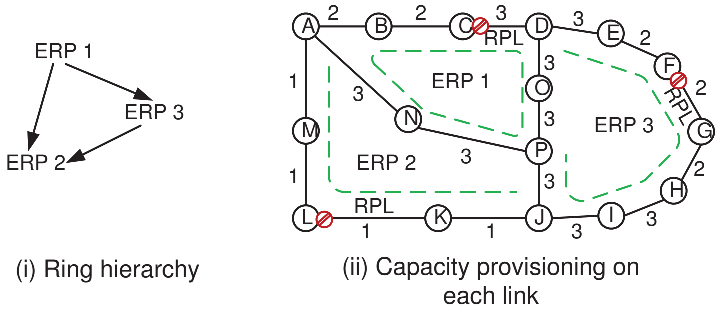

Figure 3.4: Illustrative example: Interconnected multi-ring instance 2

3.3 Limitations of related work and resolutions

Given the recent recommendation of ERP, very limited studies on ERP design exists in the available literature. To the best of our knowledge, [28] could be the only contribution which implicitly addresses the issue of RPL placement and ring hierarchy in mesh networks. However the authors performed an exhaustive search among all possible scenarios of RPL blocking in all possible ring hierarchies to find which one supports all user demands using the minimum capacity investment. The authors assumed both guaranteed and best effort services and they attempted to protect the guaranteed service traffic while maximizing the protection capacity which will be used by best effort traffic in working state operation. To derive a solution, the authors of [28] represented all possible link blocks, both RPL logical blocks and blocks due to link failures, by a set of link state vectors denoted by S as explained earlier. A set of link vectors exists for each possible ring hierarchy in the network. Assume that H is the total number of possible hierarchy designs, hence the set of all possible link state vectors under hierarchy h is denoted as $S^h = \{S_k^h | k = 1, 2, ..., K_h\}$ where K_h is the number of all possible link states for h. The load of link ℓ is the total traffic on the link for a given link state of S_k^h and is denoted by $\lambda_\ell(S_k^h)$. Then, the preferred hierarchy design is determined as $h^* = \arg\min_{h \in H} \left[\sum_{\ell \in L} \max_{k \in \{1,2,......,K\}} \{\lambda_\ell(S_k^h)\} \times W_\ell \right]$ [28]. Once, the hierarchy is selected, the preferred RPL position is obtained by $k^* = \arg \min_{k \in \{1,2,......,K\}} \left\{ \sum_{\ell \in L} \lambda_\ell(S_k^{h^*}) \right\}$ and the capacity provisioned on each link is computed as $C_l^* = \max_{k \in \{1,2,...,k\}} \{\lambda_\ell(S_k^{h^*})\}$ [28].

The design approach presented in [28] exhibits some subtle limitations that yields incorrect capacity provisioning which renders the obtained solution inefficient. In this section, we reveal these limitations and present the modifications of the existing exhaustive search approach to resolve the highlighted issues.

3.3.1 Overestimation of capacity provisioning

We first observe that all K_h possible link state vectors in the given hierarchy h are considered in determining the required link capacity, which results in overestimating the required overall capacity. This subtle problem of link capacity overestimation occurs because not all of the K_h possible link states represent a feasible failure scenario once the link state vector k^* of the preferred RPL placement is selected. Only a subset of link state vectors is required to represent all possible failure scenarios for a given RPL placement, as we illustrate next.

Fig. 3.5(a) shows a simple network with two rings A and B that are sharing link ℓ_2. Two hierarchies H_1 and H_2 are possible whose major rings are Ring A and Ring B respectively. H_1 and H_2 have 12 and 10 link state vectors; namely,

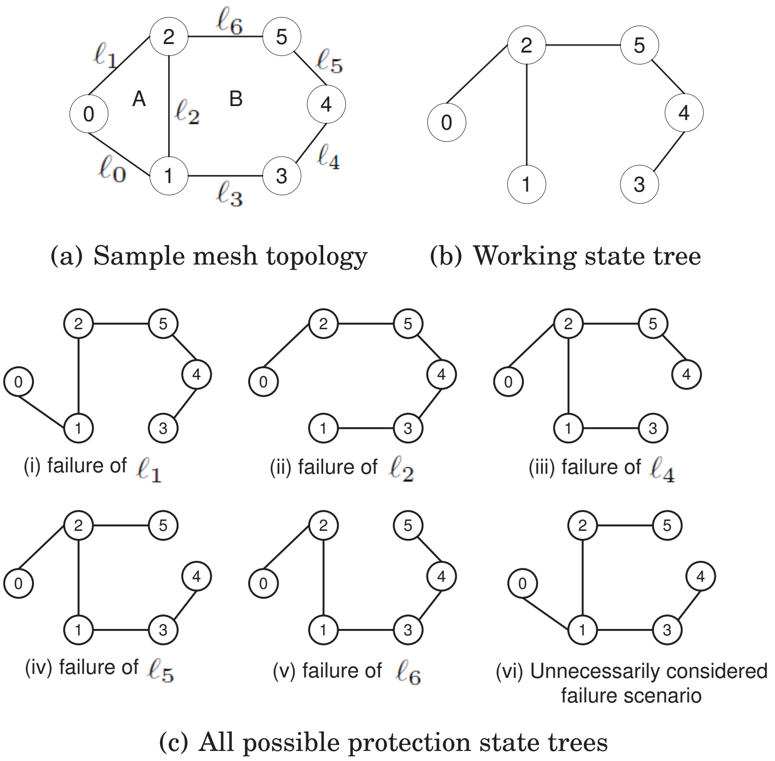

(a) Sample mesh topology (b) Working state tree

(i) failure of ℓ_1 (ii) failure of ℓ_2 (iii) failure of ℓ_4

(iv) failure of ℓ_5 (v) failure of ℓ_6 (vi) Unnecessarily considered failure scenario

(c) All possible protection state trees

Figure 3.5: Capacity provisioning steps

we have $S^{(1)} = \{S_k^1 | k = 1, 2, ..., 12\}$ and $S^{(2)} = \{S_k^2 | k = 1, 2, ..., 10\}$. For illustrative purposes, let us assume that H_2 provides better capacity provisioning and thus is the preferred hierarchy. We further assume that the preferred RPL placement for Rings A and B were found on links ℓ_0 and ℓ_3. Fig. 3.5(b) shows the working state tree of the network. Next, we consider all possible link failure scenarios for the given RPL placement on links ℓ_0 and ℓ_3; Fig. 3.5(c) represents the corresponding protection state trees of the network. Please note that, there are only six trees including the working-state tree and these trees are sufficient for the capacity provisioning for the given RPL placement. However 10 link state vectors exist in H_2 and the authors in [28] considered all of them in their capacity provisioning which, we observe, is not necessary given that multiple simultaneous failures occur less frequently. We present one example of such link state in Fig. 3.5(c)(vi). This figure shows two concurrent failures on links ℓ_1 and ℓ_5; the protection plans for these two failures share a common link (ℓ_2) on which additional capacity should be provisioned for the network to survive the failures of ℓ_1 and ℓ_5. Indeed, such scenarios are not considered in this work; the design method focuses only on provisioning capacity to survive against single failures. It is to be noted however that if the protection plans of two concurrent failures do not share any common links, surviving against concurrent failures is possible. Note that, for simplicity, we did not consider node failure scenarios in this example.

3.3.2 Infeasible configurations

Next we illustrate another subtle issue with the design method presented in [28]. Similar to STP, ERP must ensure both in working and protection state a loop-free topology for frame forwarding. The authors in [28] rely on the RPL placement by following the fundamental constraints of ITU-T G.8032 Recommendation to ensure loop-free topology. The rules defined by the recommendation are adequate for ensuring a logical loop-free tree for a single-ring ERP. However, in the case of a complex multi-ring mesh topology, e.g., ARPA2 network (Fig. 3.6), additional efforts must be exerted to avoid loops. Let us assume that for a certain traffic pattern, the preferred hierarchy in ARPA2 network is found as shown in Fig. 3.6 and the preferred RPL placement is as shown in the same figure. The RPL positions illustrated in the figure are legitimate placement obeying to the rules exercised by the authors in [28]. We observe the formation of a loop consisting of nodes $\{0, 1, 2, 3, 8, 9, 16, 17, 18, 19, 20, 14, 13, 12, 7\}$ in Fig. 3.6 even though one RPL is placed in each major and sub ring. In addition, a loop/cycle can be formed in the network upon a link failure even though the RPLs are placed to ensure loop-free topology in working state. For example, let us assume that RPL of ring D is placed on link $12-13$ instead of link $7-11$ in Fig. 3.6 which ensures that no loop exist in working state. However, in case of the failure of link $7-11$ or $10-11$, ring D unblocks its RPL link $12-13$ which again yields the same loop as mentioned earlier in failure state. This subtle issue is overlooked in [28]. A well designed ERP network should ensure a loop-free frame forwarding environment in both working and failure state.

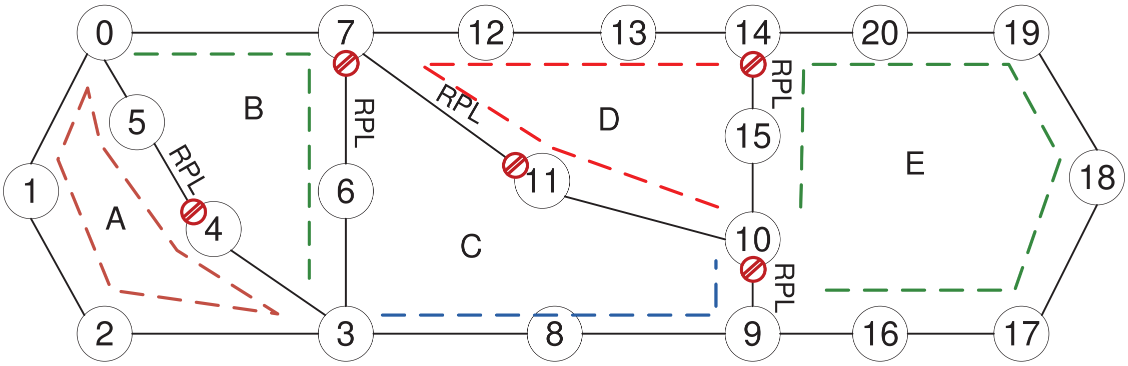

Figure 3.6: Loop existence in ARPA2

3.3.3 Solutions

We modify the exhaustive search approach by enforcing additional conditions to resolve the above mentioned issues. The modified approach is illustrated in Algorithm 3.1. The overestimation during capacity provisioning is resolved by building a set of feasible failure scenarios for each RPL configuration in S_k^h. The newly introduced set is a subset of S_k. For example, let us consider the link state vector S_1 of H_1 being a potential RPL solution. Then, we build the set of feasible failure scenario F_1^1 for S_1 such that $F_1^1 \subseteq S_k^{h_1}$. F_1^1 contains the link states that represent all possible single link failures for a given RPL configuration; only this subset will be used in the capacity provisioning process. Lines 7 to 17 in Algorithm 3.1 present the building process of F_1^1.

Now to remove cycles, we investigate all elements in S_k^z to verify the operability of the logical topologies that are produced by the link states. ERP networks are only operable in a loop-free topology and each set of configuration is verified by a procedure named *VERIFY-LOOP* as presented on lines 18 to 26 in Algorithm 3.1, which utilizes the Depth-first search (DFS) algorithm to ensure acyclic graph. DFS algorithm is usually used for traversing the trees or graphs with complexity $\Theta(|V + E|)$ where V and E are the number of vertices and edges respectively. We modify the classical DFS algorithm so that the algorithm returns true if a cycle is formed by the given topology and a cycle is identified if any visited node is attempted to be traversed again. We also impose an additional condition that the links that are shared by multiple rings cannot be the RPL of any of those rings. This additional condition ensures the network to remain loop-free in failure state. The time complexity of Algorithm 3.1 largely depends on the number of sharing instances and the number of link state vectors. It can be shown that the computational complexity of Algorithm 3.1 is $O(2^{\frac{R(R-1)}{2}} \times (E/R)^R \times (V \ \log \ V + E))$ where R is the number of rings. The details analysis is omitted due to the space constraints.

3.4 ILP-based solution methodology

In this section, we propose an Integer Linear Programming (ILP) model to jointly solve the ERP capacity planning and RPL placement in a hierarchical multi-ring mesh network. To the best of our knowledge, this is the first study to jointly address these two problems and propose an optimization approach

Algorithm 3.1 Modified exhaustive search

```
Input: Network topology, traffic matrix;
Identify the shared links in the network;
Build the set of all possible hierarchies $H$;
for all $h \in H$ do
    Create the set of all possible link states $S_h$;
end for
for all $h \in H$ do
    for all $s \in S_h$ do
        $RPL = s$;
        $bool : IsSharedRPL = $ VERIFY-RPL-SHARED-LINK$(RPL)$;
        if $IsSharedRPL = True$ then
            Remove the current $RPL$ from the set;
        else
            Build the set of feasible failure configurations scenario $f_{RPL}$ for $RPL$ such
            that $f_{RPL} \subseteq S_h$ ;
        end if
    end for
end for
for all $h \in H$ do
    for all $f_{RPL}^{curr} \in f_{RPL}$ do
        $bool : Isloop = $ VERIFY-LOOP$(f_{RPL}^{curr})$;
        if $Isloop = True$ then
            Remove the set of configuration $f_{RPL}$;
        else
            Continue;
        end if
    end for
    for all $f_{RPL}^{curr} \in f_{RPL}$ do
        for all link state $s_{curr} \in f_{RPL}^{curr}$ do
            Compute link load $\lambda_\ell$ on each link $\ell \in L$;
        end for
        Find max load $\lambda_\ell^{max}$ of link $\ell$ for $f_{RPL}^{curr}$;
        Assign capacity $C_\ell^{RPL}$ for link $\ell$ equivalent to $\lambda_\ell^{max}$;
    end for
end for
Find the set of configuration $f_{RPL}$ that require minimum capacity;
```

VERIFY-RPL-SHARED-LINK(RPL) Verify if any RPL is placed in shared link

```
Input: Set of RPL links;
Output: true or false;
bool result:= false;
for all $\ell \in RPL$ do
    if $\ell$ is shared/spanned by multiple rings then
        result = true;
        return result;
    end if
end for
return result;
```

VERIFY-LOOP Verify loop

```
Input: link state;
Output: true or false;
bool result:= false;
Run DFS algorithm to traverse all of the nodes of the network;
if any visited node is reached then
    result = true;
    return result;
end if
return result;
```

to find the optimal hierarchy of rings, RPL locations, and optimal capacity to survive any single link failure in the network.

We denote a network topology by $G(\mathcal{V}, \mathcal{L})$ where $\mathcal{V}$ is the set of vertices or nodes, and $\mathcal{L}$ is the set links, indexed by v and ℓ, respectively. Unless specified differently, we assume bidirectional links in the network, and asymmetric traffic modeled by a set of unit-capacity connections $\mathcal{C}$ (indexed by c). The set of outgoing and incoming links from/to any node v are defined by v^+ and v^- respectively. We assume that the set of all possible simple rings $\mathcal{R}$ (indexed by r) in the network are given. By simple rings we mean rings without straddling-ring links, e.g., in Fig. 3.1: $2-3-4-9-8$ is a simple ring, but $2-1-0-7-6-5-4-9-8$ is not because it has straddling-ring links $2-3-4$. Note however that ERP supports the logical rings with straddling links as long as the straddling links are protected by another logical ring. We define the following parameters, sets, and variables.

- Parameters and sets: α_r^ℓ equal to 1 if link ℓ belongs to ring r, 0 otherwise. $\mathcal{L}_r$ is the set of links spanned by ring $r \in \mathcal{R}$. S_c, D_c are the source and destination of connection c, respectively.

- Variables : We distinguish two classes of variables, including those used in ring hierarchy design and RPL placement and those used in capacity planning and optimization.

In the design of rings hierarchy and RPL placement we use the following variables: x_r : equal to 1 if ring r is activated/selected, 0 otherwise. Note that a ring is selected by our solution implies that the solution will provision capacity to protect the traversing connections of the selected ring. η_r^ℓ : equal to 1 if link ℓ is the RPL of ring r, 0 otherwise. They are used to select the RPL of each active ring. y_r^ℓ : equal to 1 if ring r is the main w.r.t. ℓ, 0 otherwise. They are used to select the main ring of a link, i.e., the ring which is responsible to unblock the RPL in case of its failure. These variables are useful, especially, in the case of links that are shared or common to multiple rings. In capacity planning, we distinguish between two configurations of capacity: capacity in working state and in failure or protection state. We use the following variables to differentiate between the two states:

w_ℓ^c : equal to 1 if connection c in normal or working state is routed through ℓ, 0 otherwise.

$w_\ell^{\ell',c}$: equal to 1 if link ℓ' is traversed by connection c in case of failure on link ℓ, 0 otherwise.

Similarly, we define two sets of constraints: the first (3.1) to (3.5) contain constraints to set up the hierarchy of rings, and define the optimal set of RPLs; the second set contains constraints to optimize the required capacity. The first set is as follows:

$$\eta_r^\ell \leq \alpha_r^\ell x_r \qquad \ell \in L, r \in R \tag{3.1}$$

$$y_r^\ell \leq \alpha_r^\ell x_r \qquad \ell \in L, r \in R \tag{3.2}$$

$$\sum_{\ell \in L} \alpha_r^\ell \eta_r^\ell = x_r \qquad r \in R \tag{3.3}$$

$$\sum_{r \in R} y_r^\ell \leq 1 \qquad \ell \in \mathcal{L} \tag{3.4}$$

$$y_r^\ell = y_r^{\ell'} \qquad \ell, \ell' \in \mathcal{L}_r \cap \mathcal{L}_{r'}, r, r' \in R \tag{3.5}$$

$$\eta_r^\ell = 0 \qquad \ell \in \mathcal{L}_r \;\; and \;\; \ell \in \mathcal{L}_{r'}, r \neq r', r, r' \in R \tag{3.6}$$

Constraint (3.1) states that link ℓ can be the RPL of ring r only if r is selected. Similarly, constraint (3.2) ensures that only a selected ring r can be the main w.r.t. ℓ. Constraint (3.3) states that a ring r, once it is selected, can have exactly one RPL. Constraint (3.4) limits a link to belong to at most one main ring and thus avoids unblocking of multiple RPLs in case of a failure on a shared link. This uniqueness is required to avoid forming a loop in ERP networks. Constraint (3.5) states that a set of links shared by any pair of rings r and r' must belong to the same main ring. For example, either ERP_1 or ERP_3 can be the main ring w.r.t. the two common links $D - O - P$ in Fig. 3.3 so that only one of them will unblock its RPL in case of a failure of any of the two common links.

Constraint (3.6) ensures that no RPL is placed on any link that is shared/spanned by multiple active rings. This is an additional constraint which is not part of the original standard ITU-T G.8032. The concept of RPL is introduced by G.8032 to ensure loop-free topology which is necessary for Ethernet forwarding. However, a loop can be formed when a RPL in unblocked in case of a link failure (i.e., in failure state) if the placement of RPL is not selected properly. We imposed this constraint to avoid forming loops especially in failure state. The capacity planning constraints are defined as follows :

- In working state :

$$\sum_{\ell \in v^+} w_\ell^c - \sum_{\ell \in v^-} w_\ell^c = \begin{cases} 1 & \text{if } v = S_c \\ -1 & \text{if } v = D_c \\ 0 & \text{Otherwise} \end{cases} \qquad c \in \mathcal{C} \tag{3.7}$$

$$w_\ell^c \leq 1 - \sum_{r \in R} \eta_r^\ell \qquad \ell \in L \tag{3.8}$$

$$w_\ell^c \leq \sum_{r \in R} y_r^\ell \qquad \ell \in L \tag{3.9}$$

Constraint (3.7) is the capacity flow conservation of each connection $c \in \mathcal{C}$ in working state. Constraint (3.8) states that a link ℓ can be used to carry traffic in working state only if it is not the RPL of any ring. Similarly, constraint (3.9) ensures that a connection c can use a link ℓ only if ℓ belongs to a main ring.

- In failure/protection state :

$$\sum_{\ell' \in v^+} w_\ell^{\ell',c} - \sum_{\ell' \in v^-} w_\ell^{\ell',c} = \begin{cases} 1 & \text{if } v = S_c \\ -1 & \text{if } v = D_c \\ 0 & \text{Otherwise} \end{cases} \qquad c \in \mathcal{C} \qquad (3.10)$$

$$w_\ell^{\ell',c} \leq 2 - y_r^\ell - \sum_{r':r' \in R - r} \eta_{r'}^{\ell'} \qquad r \in \mathcal{R}, \ell \in \mathcal{L}_r, \ell' \in L \qquad (3.11)$$

$$w_\ell^{\ell',c} = 0 \qquad \ell, \ell'(\ell' = \ell) \in \mathcal{L}, c \in \mathcal{C} \qquad (3.12)$$

Constraint (3.10) is capacity flow conservation in failure state. Constraint (3.11) states that the affected connections by a failure scenario ℓ cannot be restored through link ℓ', if ℓ' is the RPL of a ring other than the ring containing the failed link. Constraint (3.12) ensures that a link cannot protect itself.

Optimization objective $\min \sum_{\ell' \in L} \psi_{\ell'}$

$$\psi_{\ell'} \geq \max(\sum_{c \in C} w_{\ell'}^c, \max_{\ell} \sum_{c \in C} w_\ell^{\ell',c}) \qquad \ell, \ell' \in L \qquad (3.13)$$

Our objective is to find the minimum total capacity (sum over all links ℓ') in working and failure state of any link ℓ. The optimal capacity on each link ℓ', given by $\psi_{\ell'}$, is equal to the maximum capacity required on ℓ' between the working state and the failure state of any link ℓ.

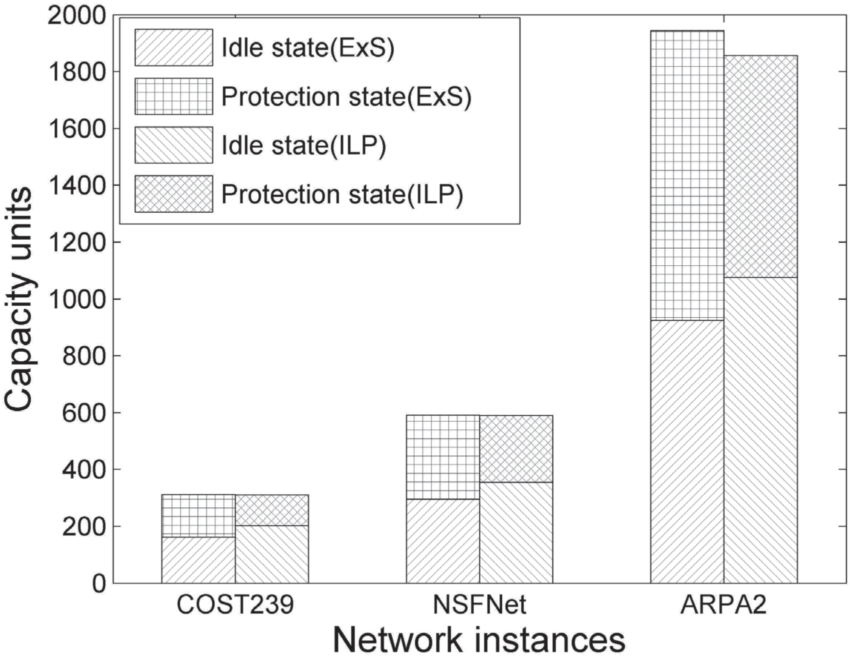

Figure 3.7: ILP vs ExS

3.5 Numerical Results

In this section we study the performance of the proposed ILP-based ERP design methodology and compare the numerical results with another approach [28] which relies on exhaustive enumeration to find the solution. We consider three network topologies, namely, the NSF, COST239, and ARPA2 [34] in our study and assume unit traffic demand between each pair of nodes. The results consist of both total working capacity required in working state operation and protection capacity required to protect from any single link failure in protection state.

Fig. 3.7 shows that the solutions achieved by ExS [28] require very slightly higher capacity than our ILP model in COST239 and NSF networks. However, in ARPA2 network, the capacity achieved by ExS is approximately 5% higher than that obtained by the model. Ideally, the ExS approach should find out the

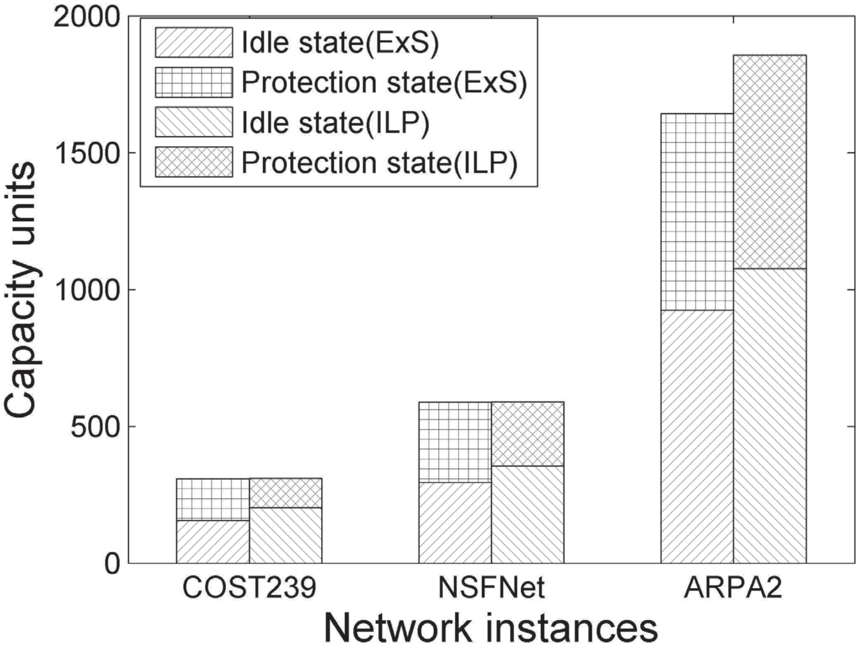

Figure 3.8: ILP vs ExS (excluding unnecessary configurations)

optimal solution and provide the exact capacity requirement as the proposed model. The difference in capacity requirement shown in Fig. 3.7 is due to the limitations (overestimation and invalid configurations) of ExS as explained in Sections 3.3.1 and 3.3.2 in greater details. Next we study the effect of the subtle issues that we found in ExS.

Fig. 3.8 depicts the performance comparison in terms of capacity units of ILP and the modified ExS. The ExS approach is modified to overcome its limitations by investigating every possible solution configurations, removing infeasible configurations from the solution space, and by rebuilding the set of failure scenarios for a given RPL configuration to eliminate overestimation. The details of the modification process are described in Section 3.3.3. Please note that the capacity estimation provided by ExS as shown in Fig. 3.8 is lower than ILP solutions in some cases (COST239, ARPA2) which are erroneous again. The proposed ILP avoids the configurations that might form a cycle/loop in the network not only in working state but also in protection state, i.e., the ILP guarantees the loop free network topology in both working and protection state by introducing constraint (3.6). The ExS and the modified ExS so far do not take into account this issue and thus the solutions obtained by these approaches include the configurations that do not form a loop in the network in working state but might form a loop in protection state. This is the reason behind the erroneous solutions with capacity requirement smaller than ILP are achieved by ExS. We further incorporate the additional constraint in ExS and present the results in Fig. 3.9, which illustrates that the ILP and the ExS obtain solutions which require exactly equal overall capacity in all three network instances.

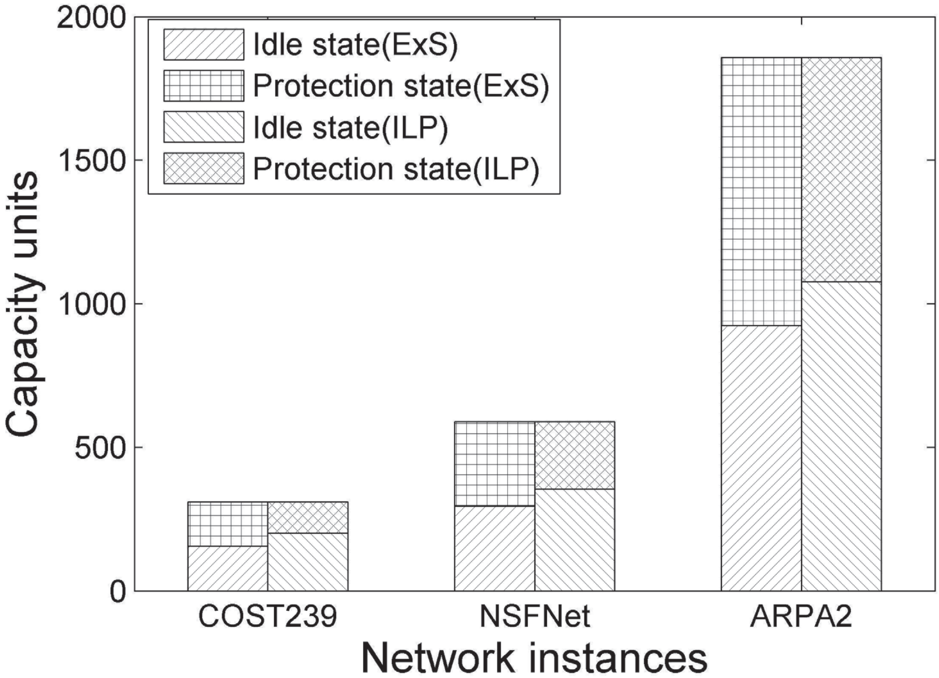

Figure 3.9: ILP vs ExS (including additional constraint)

Note however that, the correct optimal solutions of ExS are obtained by some modifications of the actual one proposed in [28] and thus comes at the expense of excessive running time. Table 3.1 provides some insights about the running time required by the proposed ILP and the ExS approach as well as the number of invalid configurations (link states) found in NSF and ARPA2 networks by ExS [28]. It is worth to mention that the running time of ExS becomes indeed a limiting factor as the size of the network increases. For example, for ARPA2, our model finds the solution in 519.9 s whereas ExS spends 2.8 days. This shows the substantial scalability of our model. 582 and 6144 infeasible configurations are identified so far in NSF and ARPA2 networks respectively. In addition, 876 and 948 configurations are detected that might introduce technically prohibitive cycles/loops in NSF and ARPA2 networks respectively.

Table 3.1: Comparison of ILP and ExS

	COST239		**NSF**		**ARPA2**	
	ILP	**ExS**	**ILP**	**ExS**	**ILP**	**ExS**
Running Time (s)	4.9	695.4	75.9	10183.3	519.9	240058 (3 days)
Total link states / *Invalid link states*	-	2383 / 0	-	14132 / 582	-	61920 / 6144
Total link states / *Cyclic link states*	-	2383 / 0	-	14132 / 876	-	61920 / 948

3.6 Chapter remark

In this chapter, we present an optimization model for jointly solving the problem of optimal ring hierarchy and capacity design in ERP-based multi-ring mesh networks. While the only prior work we are aware of resorted to exhaustive enumeration to obtain the solution and resulted in incorrect network capacity. We propose some modifications to the exhaustive enumeration approach. Though after modification, both the mathematical model and ExS approach provide optimal solution, the proposed model obtains the solutions in more efficient manner in terms of running time. The optimal solution is shown to deploy capacity in the network for achieving the protection from a single link failure.

Chapter 4

Design of ERP: Dual Failures

In this chapter, we study network design strategies to protect network services against concurrent dual failures using Ethernet Ring Protection (ERP). It is to be noted that ERP guarantees service recovery only against single failures in one ring. However, the ongoing growth in carrier networks increases the risk of dual concurrent failures, and designing networks to survive against dual failures becomes a growing and pressing concern for service providers. Protection switching against dual link failures have not been yet properly investigated and addressed by the ITU-T G.8032 recommendation, which specifies the operations of ERP. However, a dynamic recovery procedure is being discussed in the newer version of the recommendation G.8032v2 [3], but it has not yet been integrated into the recommendation. In a mesh network where multiple logical rings are interconnected, the protection switching may act unusually or unexpectedly in case of concurrent failures. The absence of a well-studied survivable plan in the recommendation to protect ERP-based mesh networks against such failures is one of its major limitations.

In ERP-based networks, where enough capacity is provisioned to carry traffic in working or protection state, demands that are affected by a single link failure are normally restored through the predetermined protection plan. However, multiple concurrent failures may still cause service outages with catastrophic consequences if the network is not designed to withstand these failures. Some dual failures will cause network segmentations (Physical and/or Logical) which may affect some services and cause outages (we refer to these as *category-1* outages). In addition, another type of service outages is observed in Section 4.1 and later detailed in Section 4.2 which is caused by inadequate capacity (we refer to these as *category-2* outages). In Section 4.1, we present a design strategy where the two categories of outages are addressed in a sequential two-step approach. We then extend our study to develop a joint design approach as presented in Section 4.2 which allocates resources in a more efficient manner comparing to former two-step approach.

4.1 Two-step approach

Due to its unique operational principles, Ethernet's protection scheme (ERP) requires particular attention when the network design method is extended to address dual failure restorability. For example, investing adequate additional capacity in ERP to provide 100% dual failure restorability cannot guarantee uninterrupted services upon dual link failures. Concurrent dual failures in a single stand-alone ring will cause unavoidable network partitioning (*Physical segmentation*) and there will be obvious service interruption if the source and destination nodes of the requested service are in different segments of the network. Nevertheless, some service outages due to network partitioning (*Logical segmentations*) in ERP multi-ring mesh networks can be avoided by efficient logical design of interconnected ring hierarchies.

In this section, we focus on minimizing the service outages caused by logical segmentations. We highlight a trade-off between the overall capacity investment and reducing service outages due to logical segmentations; this trade-off will be a subject for further investigation in this section. We develop a multi-objective Integer Linear Program (ILP) whose objective is to minimize the overall number of service outages caused by network segmentations due to dual link failures while minimizing the overall capacity investment in the network. Further, we consider those contending connections in our design which are restorable, but suffer from outages due to lack of capacity. We develop a routine to estimate the amount of additional capacity which needs to be deployed to eliminate contention for shared capacity. Finally, we present a comparative study about the impact of the design approaches on network-wide restorability.

4.1.1 Characterizing Service Outages in ERP

Outages due to partitioning and suggested remedies

As we mentioned earlier, any double link failure scenario in a single standalone ring will partition the network and will prevent some nodes in one segment to communicate with other nodes in the other segment. Such segmentations are referred to as physical segmentations, and there is no remedy for such a failure in a single ring topology. A physical segmentation will disrupt the service only when both the source and destination of a connection are in different segments of the network. Nonetheless, in ERP-based mesh networks, where multiple rings are interconnected with each other, service outages due to network partitioning resulting from some double link failures could be avoided by properly selecting the link RPLs as well as ring hierarchies, as will be illustrated in the sequel; such segmentations we refer to them as logical segmentations. A logical segmentation involves at least one failure on a link which is shared by interconnected rings. This work proposes a design strategy where the number of possible logical segmentations, in a network designed to withstand all single-link failures, can be reduced (hence the number of outages following double link failures) by efficiently selecting the owner of the shared links, i.e., by efficient design of logical hierarchy of interconnected rings and assignment of RPLs.

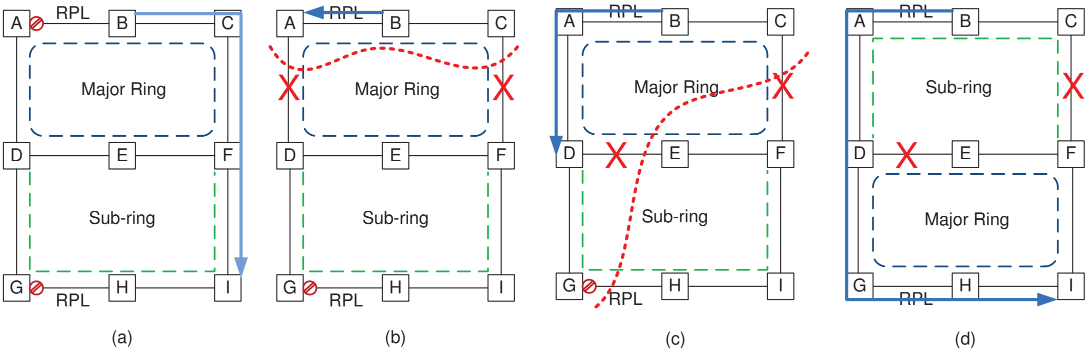

Figure 4.1: Physical and logical segmentation

To illustrate, we consider a simple network with two interconnected rings as shown in Fig. 4.1. The major ring includes nodes A, B, C, F, E, and D while the sub-ring includes nodes D, G, H, I, and F. The RPLs of the major and the sub-ring are placed on links $A-B$ and $G-H$ respectively. A service is requested from node B to node I which is routed through $B - C - F - I$ in normal (Idle) state as presented in Fig. 4.1(a). Fig. 4.1(b) depicts a double link failure situation where links $C-F$ and $A-D$ fail causing physical segmentation, which are not restorable without topology change or additional resources. Another double link failure scenario is presented in Fig 4.1(c) which includes double link failures on links $C-F$ and $D-E$. In this failure scenario, the network becomes

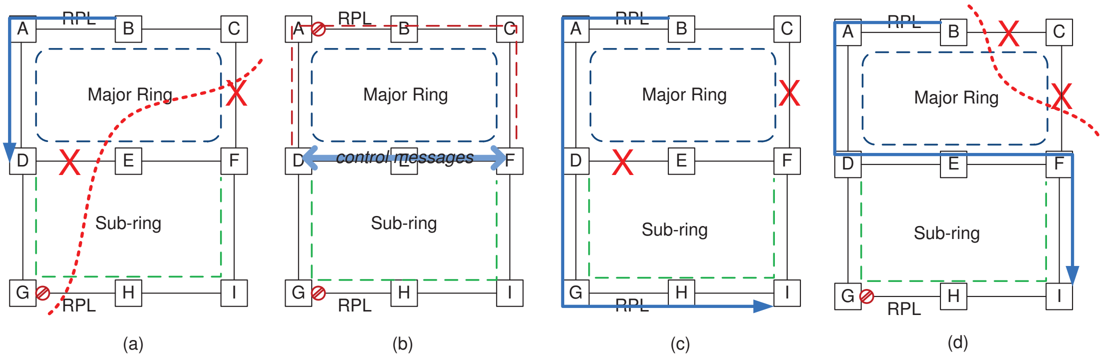

Figure 4.2: Dynamic procedure

logically segmented. This logical segmentation can be avoided by changing the logical hierarchy. Let us assume that the same network is designed as shown in Fig 4.1(d) where the major ring includes nodes D, E, F, I, H, and G and the sub-ring includes nodes D, A, B, C, and F. In case of a failure on link $C-F$, the RPL port of the sub-ring will be unblocked and the subsequent failure on link $D-E$ will unblock the RPL port of the major ring. Hence, the network segmentation caused by this double link failures (Fig 4.1(c)) will no longer cause any service outage.

The issue of network segmentation due to double link failures in interconnected ERP rings is somehow addressed by the ITU-T working group. A dynamic procedure has been suggested by the working group as a remedy against logical segmentations. In this procedure, interconnection nodes of two interconnected rings periodically exchange control messages to verify the connectivity between them by testing two tandem connections in the upper ring. Some additional management information is required to ensure proper functioning of the procedure. If any loss of connectivity is identified by the interconnection nodes, the block indication logic, based on the additional management information provided, performs the manual switch (MS) command to the sub-ring port which unblocks the RPL port of the sub-ring temporarily. Fig. 4.2(a) shows the identical double link failure situation of Fig. 4.1(c) where a logical segmentation has occurred. According to the suggested procedure, interconnection nodes D and F should periodically exchange control messages to verify the connectivity of two tandem connections $D-F$ and $D-A-B-C-F$ (Fig. 4.2(b)). Since the failure scenario of Fig. 4.2(a) yields a loss of connectivity between nodes D and F, the block indication logic that is implemented at nodes D and F performs the MS command to the sub-ring port and the sub-ring unblocks the RPL port on link $G-H$. Fig. 4.2(c) illustrates that the network is in MS mode and the particular logical segmentation is avoided.

The suggested procedure requires periodical exchange of control messages between all pairs of interconnected nodes to verify connectivity in order to overcome logical segmentation. In addition, the performance (e.g., restoration speed) of this procedure has not been studied and is not an integral part of the recommendation as of G.8032v2. The complex management associated with this procedure and the high overhead could result in poor network performance (e.g., slower restoration times), which makes it not appealing for service providers.

In contrast, here we present an effective network design (i.e., allocation of capacity and RPLs) which minimizes the number of logical segmentations (hence outages) in response to double link failures. Here, periodical exchange of additional control messages are not necessary; however, a service provider may still invoke the above reactive procedure to further improve the service availability. Given that the number of possible service outages is already minimized in the optimally designed ERP network through the design process, a significant reduction in the exchange of control messages is anticipated.

Note that there are situations where the service remains operational even though the network is segmented. Fig. 4.2(d) depicts this situation where the first failure ($C - F$) affects the requested service of Fig. 4.1(a) which is restored through $B - A - D - E - F - I$. A second failure on link $B - C$ segments the network, but the requested service remains operational. These situations which do not cause service interruption are not among the concerns of our design approach.

Service outages vs. network connectivity

Given the unique characteristics and operational principle of ERP, increasing network connectivity in ERP-based networks may not completely eliminate the outages caused by logical segmentation. We present an illustrative example of a 3-connected mesh network composed of multiple interconnected ERP rings as shown in Fig. 4.3. The major ring includes the nodes E, F, H, and G and is surrounded by four sub-rings. The RPL links are marked in the figure. A service is requested from node B to node D, which is routed through $B - F - H - D$ in idle (normal) state as presented in Fig. 4.3(a). Upon the first failure on link $F - H$, the major ring unblocks its RPL and the connection is restored through $B-F-E-G-H-D$. A second link failure on link $G-H$ causes a logical segmentation and the connection is disrupted (Fig. 4.3(b)). Clearly, logical segmentations exist in highly connected networks as well which, however, can be reduced by efficient design of the logical hierarchy.

Trade-off between capacity and outages

The authors of [35] presented a joint design approach for optimal capacity allocation in ERP-based mesh networks to withstand 100% restorability against single-link failures; they showed that the ring hierarchy selection and the RPL

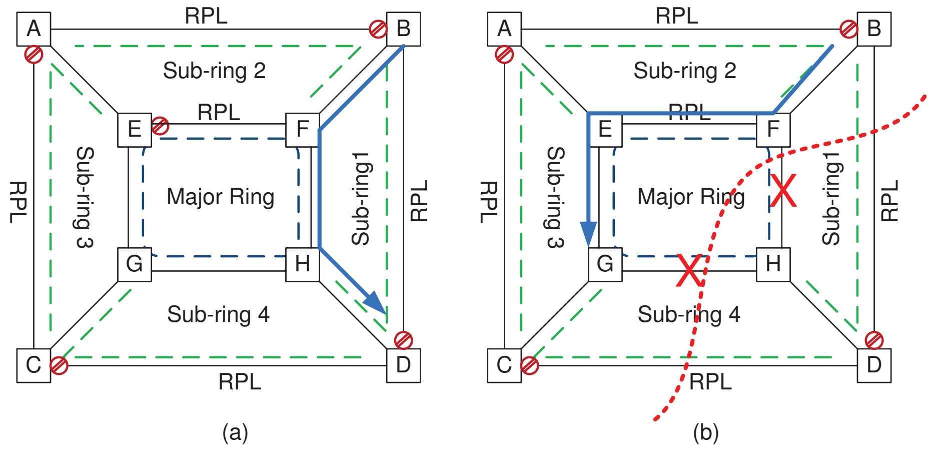

Figure 4.3: Segmentation in a 3-connected network

placement have significant impact on the capacity planning in ERP networks. Indeed as we will show here, the logical hierarchy of interconnected rings which is optimally designed to survive against all single-link failures may not be the same as the logical ring hierarchy that minimizes service outages caused by network segmentations (resulting from double link failures); these are two different design methods with different design objectives and hence design costs. To illustrate, we consider a small network with three interconnected rings R_1, R_2, and R_3 and one service request from node A to node I. Fig. 4.4(b) presents the outcome of the design approach presented in [35] which optimizes the capacity requirement with 100% restorability against single-link failures.

Fig. 4.4(a) shows the directed graph representation of the logical hierarchy of the rings which requires 9 unit of overall network capacity. In this figure, there are directed edges from R_1 to R_2 and R_3 which implies (in ERP terminology) that R_1 is a major ring and is responsible for the protection of the shared links with both R_2 and R_3 (see Fig. 4.4(b)). We then carefully

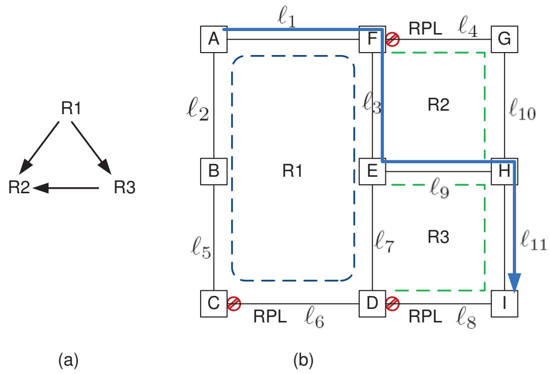

Figure 4.4: Minimized capacity investment against single-link failure

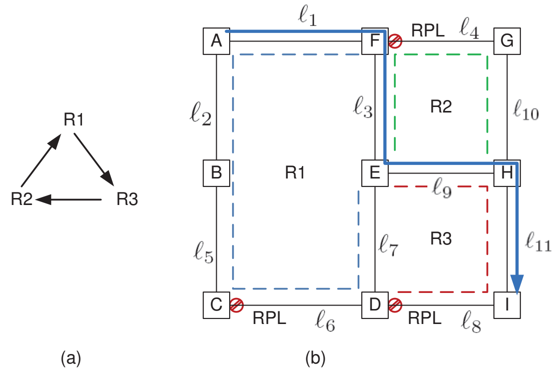

Figure 4.5: Reduced segmentation

examine all possible double link failures scenarios with the given ring hierarchy to identify the situations that cause service outages due to network segmentations. We observe 10 such instances of double link failures that involve the link pairs $\{\ell_1, \ell_2\}$, $\{\ell_1, \ell_5\}$, $\{\ell_1, \ell_6\}$, $\{\ell_1, \ell_7\}$, $\{\ell_3, \ell_2\}$, $\{\ell_3, \ell_5\}$, $\{\ell_3, \ell_6\}$, $\{\ell_3, \ell_7\}$, $\{\ell_9, \ell_8\}$, and $\{\ell_{11}, \ell_8\}$. However, the hierarchy of the given rings R_1, R_2, and R_3 can be designed in such a way that the number of service interruptions due to segmentation is reduced. Fig. 4.5(a) and Fig. 4.5(b) illustrate one of such ring hierarchies and logically designed rings respectively which observes 8 instances of service interruption due to failure of link pairs $\{\ell_1, \ell_2\}$, $\{\ell_1, \ell_5\}$, $\{\ell_1, \ell_6\}$, $\{\ell_1, \ell_7\}$, $\{\ell_3, \ell_4\}$, $\{\ell_3, \ell_{10}\}$, $\{\ell_9, \ell_8\}$, and $\{\ell_{11}, \ell_8\}$. Indeed, reduction of the number of potential service interruptions comes at the cost of increased capacity requirement. The latter design of the network requires 11 units of overall capacity to provide 100% restorability against single-link failures. Note that the example is illustrated with only one service request for simplicity.

Next, we continue our investigation with larger number of service requests to observe the trade-off between the capacity investment and the number of service interruptions. Table 4.1 presents the numerical results where unit demands between all pairs of nodes are considered. The best solution (includes hierarchy and RPL positions) requires 172 units of capacity which needs to be deployed to provide 100% restorability. However, 266 instances of possible service interruptions might be observed by this solution. In contrast, the alternative solution as presented in Table 4.1 could reduce the number of possible service interruptions to 188 (a 29.3% reduction) by changing the hierarchy and RPL positions of the preffered design at the cost of only 12 additional units (6.9%) of capacity. Hence, the obvious design question could be what will be the best design for the survivable ERP network? Clearly, the answer depends on the service requirements of the customers. Service providers may desire to reduce the number of potential segmentations for mission critical services and design the network with additional capacity investment. Next, we present our mathematical formulation that allows the service providers to explore tradeoffs between higher service availability and optimal capacity investment.

Table 4.1: Comparison of Alternative Solutions

	Hierarchy	**RPLs**	**Capacity**	**Possible outages**
Best solution	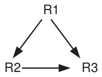	$\{\ell_1,\ \ell_{10},\ \ell_{11}\}$	172	266
Alternate solution	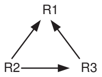	$\{\ell_6,\ \ell_{10},\ \ell_{11}\}$	184	188

4.1.2 Problem Formulation

In this section, we develop an optimization model with the objective of minimizing both capacity requirements and category-1 service outages. To do so, we reuse the set of parameters and variables that are defined in Section 3.4.

We also reuse the set of constraints consisting of 3.1 to 3.12.

The discussion, analysis, and examples in Section 4.1.1 has given us some insights about segmentations in ERP-based networks. The number of service outages that a given set of connections may experience due to segmentation depends on the routing of the connections in the working state; more precisely, the number of links that are used by the connection in working state. Denoteed by $\mathcal{L}_c^r$ is the set of links of ring r that are used by connection c in working state and $\bar{\mathcal{L}_c^r}$ the set of the rest of the links of ring r. Hence, the number of service outages due to segmentation for connection c in ring r (S_c^r) can be defined as S_c^r = $|\mathcal{L}_c^r| \times |\bar{\mathcal{L}_c^r}|$. Then, the total number of service outages due to segmentation for connection c can be found by accumulating over all rings: $\sum\limits_{r \in R} S_c^r$ or $\sum\limits_{r \in R} |\mathcal{L}_c^r| \times |\bar{\mathcal{L}_c^r}|$. The objective of the optimization problem, which is composed of two components, can be expressed as:

$$\min \left\{ \rho \times \sum_{\ell' \in L} \psi_{\ell'} + (1-\rho) \times \underline{\sum_{c \in \mathcal{C}} \sum_{r \in R} |\mathcal{L}_c^r| \times |\bar{\mathcal{L}_c^r}|} \right\}$$

where ρ is a weighing parameter that helps to strike good balance between two components. $|\mathcal{L}_c^r|$ can be expressed in terms of w_ℓ^c and y_r^ℓ as $|\mathcal{L}_c^r| = \sum\limits_{\ell \in r} w_\ell^c \times y_r^\ell$. However, this introduces nonlinearity to the model. We introduce an additional variable $o_{c,\ell}^r$ in order to maintain the linearity of the model, where $o_{c,\ell}^r$: equal to 1 if link ℓ of ring r is used by connection c in working state, 0 otherwise. Constraints (4.1-4.3) presents the linearized definition of $|\mathcal{L}_c^r|$.

$$o_{c,\ell}^r \leq w_\ell^c \qquad \ell \in \mathcal{L}_r, r \in \mathcal{R}, c \in \mathcal{C} \tag{4.1}$$

$$o_{c,\ell}^r \leq y_r^\ell \qquad \ell \in \mathcal{L}_r, r \in \mathcal{R}, c \in \mathcal{C} \tag{4.2}$$

$$o_{c,\ell}^r \geq w_\ell^c + y_r^\ell - 1 \qquad \ell \in \mathcal{L}_r, r \in \mathcal{R}, c \in \mathcal{C} \tag{4.3}$$

Then $|\mathcal{L}_c^r|$ can be found by $|\mathcal{L}_c^r| = \sum\limits_{\ell \in \mathcal{L}_r} o_{c,\ell}^r$ and constraint (4.4) defines $|\bar{\mathcal{L}}_c^r|$.

$$|\bar{\mathcal{L}}_c^r| = \sum_{\ell \in \mathcal{L}_r} y_r^\ell - \sum_{\ell \in \mathcal{L}_r} o_{c,\ell}^r \qquad r \in \mathcal{R}, c \in \mathcal{C} \tag{4.4}$$

Nevertheless, the underlined term in the objective $|\mathcal{L}_c^r| \times |\bar{\mathcal{L}}_c^r|$ which represents the number of outages that connection c may experience in ring r remains nonlinear. We apply an alternative approach which requires an additional variable $\gamma_{c,\ell}^r$ to avoid the nonlinearity, where $\gamma_{c,\ell}^r$ is an integer variable that represents the number of possible service outages for connection c given that link ℓ of ring r is used by c in working state. $\gamma_{c,\ell}^r$ is defined by $\gamma_{c,\ell}^r = o_{c,\ell}^r \times |\bar{\mathcal{L}}_c^r|$ and constraints (4.5) and (4.6) are used to linearize it.

$$\gamma_{c,\ell}^r \leq |\bar{\mathcal{L}}_c^r| + M(1 - o_{c,\ell}^r) \qquad \ell \in \mathcal{L}_r, r \in \mathcal{R}, c \in \mathcal{C} \tag{4.5}$$

$$\gamma_{c,\ell}^r \geq |\bar{\mathcal{L}}_c^r| - M(1 - o_{c,\ell}^r) \qquad \ell \in \mathcal{L}_r, r \in \mathcal{R}, c \in \mathcal{C} \tag{4.6}$$

where M is a large integer number.

Then, the revised **optimization objective** will be:

$$\min \left\{ \overbrace{\rho \times \sum_{\ell' \in \mathcal{L}} \psi_{\ell'}}^{capacity} + \overbrace{(1-\rho) \times \sum_{c \in \mathcal{C}} \sum_{r \in \mathcal{R}} \sum_{\ell \in \mathcal{L}_r} \gamma_{c,\ell}^r}^{service\ outages} \right\}$$

4.1.3 Numerical results I

In this section, we evaluate numerically our proposed design approach whose objective is presented in the previous section. We present a comparison between numerous variants of the model by varying the value of ρ. For example, selecting ρ = 1 allows us to focus only on minimizing the overall network capacity provisioning where the network is designed to withstand against single link failures only as presented in [35]. Alternatively, when $\rho = 0.5$, the model assigns balanced weights to the capacity as well as to minimizing the number of service outages that may result from double link failures. We consider three network topologies, namely, the COST239, NSFNET, and ARPA2 [34] in following study and assume three different traffic distributions (High load, medium load, and light load). In high traffic distribution, we consider unit demands between all possible source-destination pairs in the network whereas the medium and light traffic distributions are realized by randomly selecting 50% and 10% of the total demands that are considered in high traffic distribution respectively. Light, medium, and high traffic distributions are denoted by Instance 1, Instance 2, and Instance 3 respectively in the following figures which present the numerical results.

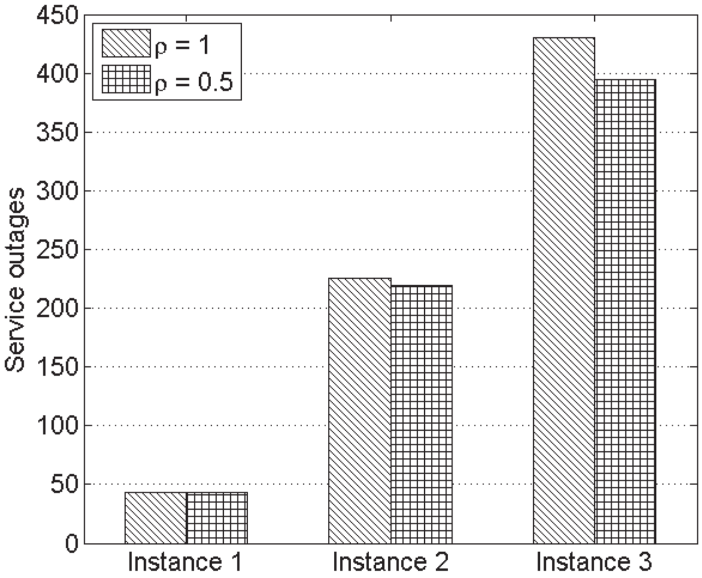

Figure 4.6: COST239 service outages

Fig. 4.6, Fig. 4.7, and Fig. 4.8 compare the numerical results in terms of the number of service outages caused by double link failures segmentations that are obtained by the proposed design approach for the COST239, NSFNET,

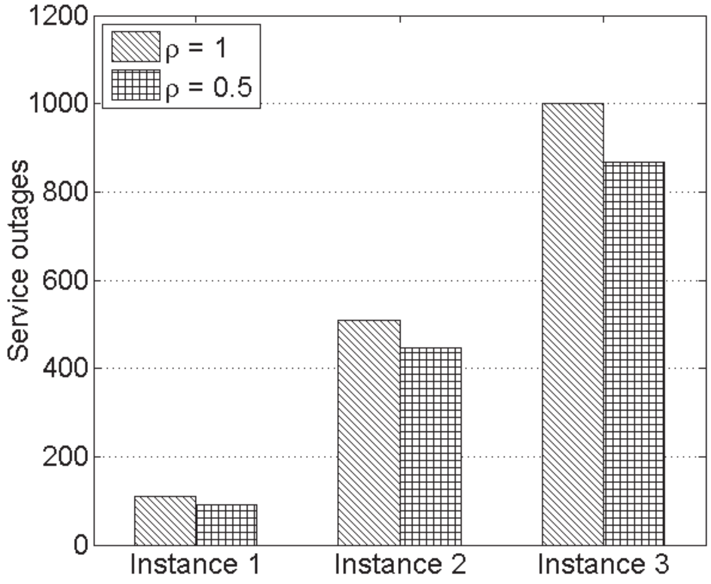

Figure 4.7: NSFNET service outages

and ARPA2 networks respectively. Each comparison consists of three traffic distributions: Instance 1 for light, Instance 2 for medium, and Instance 3 for high traffic scenarios.

The figures show that when $\rho = 0.5$, the number of outages resulting from double link failures is reduced and the reduction becomes substantial for traffic instance 3 (i.e., at high loads). For example, when $\rho = 0.5$, the design model achieves a reduction of 13.3% in the number of service outages for NSFNET network at the cost of only 6.9% increase in capacity deployment (Table 4.2) by comparison to the values when $\rho = 1$. Clearly, a higher value of ρ yields a more effective capacity allocation, which is obtained at the cost of having a network that is more vulnurable to service outages in the presence of double link failures and results lower service availability. Similar results are observed for COST239 and ARPA2 (Fig. 4.7 and Fig. 4.8) where the number of service outages is reduced by 8.1% and 3.3% respectively at the cost of 7.0% and 2.8% (Table 4.2) increase in capacity deployment for NSFNET and ARPA2 networks

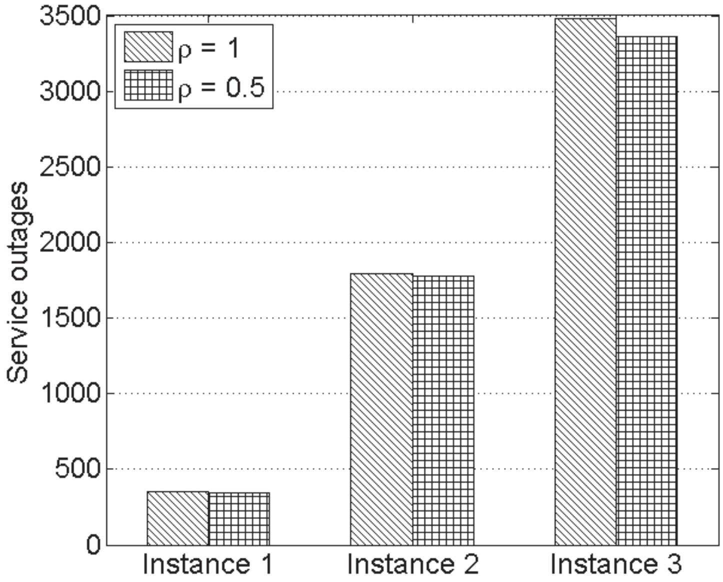

Figure 4.8: ARPA2 service outages

Table 4.2: Capacity trade-off between two approaches

	COST239		**NSFNET**		**ARPA2**	
	$\rho = 1$	$\rho = 0.5$	$\rho = 1$	$\rho = 0.5$	$\rho = 1$	$\rho = 0.5$
	(unit capacity)		**(unit capacity)**		**(unit capacity)**	
Instance 1	34	36	68	76	179	188
Instance 2	172	183	299	314	952	981
Instance 3	310	332	589	630	1856	1908

respectively.

4.1.4 Further Observations

By further dissecting the above numerical results, we observe that the reason some of the connections are vulnerable to a second failure is due to the lack of provisioned capacity. For example in traffic instance 3 of previous section, we identified that 22% - 32% of the total outages that may be caused by double link failures are due to insufficient capacity in the network, after restoring all connections affected by the first failure. In light of this observation, the service outages in ERP can further be characterized into three categories: (i) outages due to physical segmentations, (ii) outages due to logical segmentations, and (iii) outages due to lack of capacity. The first two categories have been addressed by the proposed ILP model on Section 4.1.2 which minimizes the number of outages caused by the logical segmentations while the physical segmentations are referred as unavoidable. Now, we address the third category of service outages and its possible remedy.

In an efficiently designed ERP mesh network, the spare capacity that is reserved for protection switching is shared as much as possible between existing connections. When a link fails, all of the connections that are traversing the link are disrupted. The network enters into a failure state and all of the affected connections are restored via alternate available paths. At this point, all of the connections in the network are operational; however some of these connections, more precisely the connections that share spare capacity with the affected connections of the first failure, are vulnerable to subsequent failure. Thus, one needs to identify these connections which are vulnerable in the presence of multiple concurrent failures and provision capacity in the network in a way to reduce the number of possible service outages caused by multiple failures.

We represent the network state (working/failure) by a binary link-state vector S_k [36], [28], such that $S_k = \{S_{k,\ell} = 0$ for blocked links; 1 otherwise. $\forall \ell \in \mathcal{L}\}$. A link ℓ can be referred to as blocked if either it is selected as an RPL in working state or it is affected by a failure. Then, the set of K different link state vectors corresponds to all possible single-link failure scenarios. Each S_k represents a tree of the network which uniquely determines the forwarding paths and corresponding link loads. The load of link ℓ is the number of connections passing through it and is denoted by $\lambda_\ell(S_k)$ which is interchangeably referred to as the required capacity of link ℓ. Let us denote the link capacity vector by $C_\ell^{\ell'}$ which is an integer set and specifies the number of connections that are traversing link ℓ' in working state and are provisioned to traverse link ℓ in case of failure on link ℓ'. Then $C_\ell^{\ell'} \geq \lambda_{\ell'}(S_k)$, $\forall \ell' \in \mathcal{L}$. Thus, the amount of capacity which needs to be reserved for protection switching on link ℓ is $C_\ell^* = \max\limits_{\forall \ell'} C_\ell^{\ell'}$. However, when a failure occurs and the protection switching is activated, some of the spare capacity on link ℓ may be used. In such event, C_ℓ^* should be updated according to the current network state. One may find that $\bar{C}_\ell \leq C_\ell^*$, where $\bar{C}_\ell$ is the amount of spare capacity still available on link ℓ after first failure occurred. $\bar{C}_\ell < C_\ell^*$ also represents that some connections may contend for the spare capacity on link ℓ upon next failure and may become vulnerable. Such connections are referred to as *Vulnerable Connections* while the rest of the connections which have $\bar{C}_\ell \geq C_\ell^*$ on all of the links of their working and restoration path are referred to as *Protected Connections*. To illustrate better the service outages due to lack of capacity, we present an example as follows.

Fig. 4.9(a) presents an ERP network with the logical hierarchy of two interconnected rings and the corresponding RPL positions. Two services (one unit each) are requested from node B to node F (c_1) and from node H to node F (c_2) which are routed through $B - C - F$ and $H - I - F$ respectively in working (Idle) state. Fig. 4.9(b) shows the capacity allocations (C_ℓ^*) on each link (presented besides each link). Let us assume that the first failure occurred on link $C - F$ and the affected connection c_1 is restored through alternate path $B - A - D - E - F$ (Fig. 4.9(c)). Now, we update the value of C_ℓ^* according to the

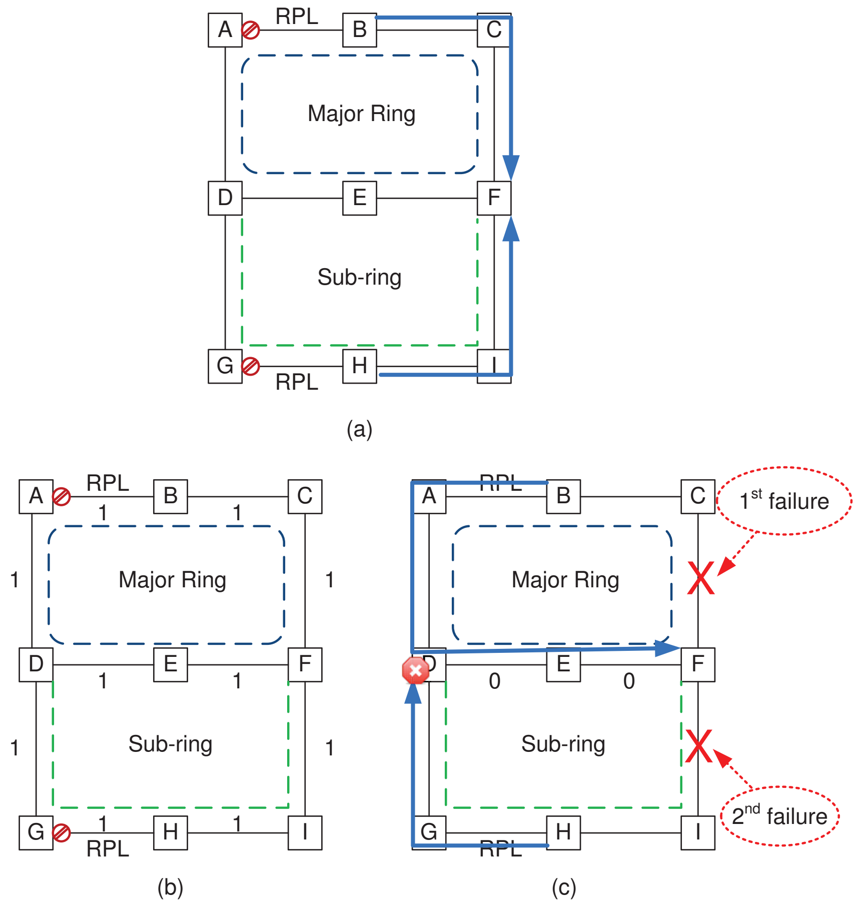

Figure 4.9: Service outages due to inadequate capacity

current network state and find that $C^*_{\ell_{DE}} = 1$ and $C^*_{\ell_{EF}} = 1$, however $\bar{C}_{\ell_{DE}} = 0$ and $\bar{C}_{\ell_{EF}} = 0$, i.e., no spare capacity is available on links $D - E$ and $E - F$ after link $C - F$ fails and the connection c_2 becomes vulnerable to next failure. Let us now assume that another failure occurs on link $F - I$ before the repair of link $C - F$. Then c_2 cannot be restored and it experiences service outage due to lack of capacity on links $D - E$ and $E - F$.

Suggested Remedy

Contention for capacity among vulnerable connections can be resolved by reserving more spare capacity on the links that are shared by these contending connections. We develop a procedure to estimate the amount of additional capacity requirement on contention links. The overall requirement of spare capacity in the network is recomputed in the subroutine such that all of the service outages due to lack of capacity are eliminated while the amount of spare capacity is minimized.

The developed routine operates on the optimal configuration found by the ILP model of Section 4.1.2, i.e., we assume the logical hierarchy of the interconnected rings and their corresponding RPLs are given to the routine. The function iterates over all single-link failure situations as described in the procedure *ESTIMATE-SPARE-CAPACITY*. The average running time of the routine is in the order of $O(\mathcal{LC} + \mathcal{L}^2)$ where $\mathcal{L}$ and $\mathcal{C}$ are the number of bidirectional links and the number of connections respectively. We denote the affected link by ℓ'. We identify the set of affected connections, restore them and update C^*_ℓ for each link $\ell \in \mathcal{L}$. Then we build the set of link state vectors S of K different link states. Each item S_k in the set S represents a double link failure scenario by blocking the first link ℓ' and any other link $\ell'' : \ell'' \in \mathcal{L}$ and $\ell'' \neq \ell'$.

We identify the set of vulnerable connections for each element S_k and compute the required additional capacity $C_{\ell,k}^{\ell',\ell''}$ on each contending link such that $C_{\ell,k}^{\ell',\ell''} = C_\ell^* - \bar{C}_\ell$. Then we evaluate the additional spare capacity which needs to be provisioned on link ℓ by $C_\ell^{\ell',\ell''} = \max_{\forall k} C_{\ell,k}^{\ell',\ell''}$ and update the value of C_ℓ^* by $C_\ell^* + C_\ell^{\ell',\ell''}$. Note that some of the elements S_k in S may represent physical or logical segmentations and hence, some of the connections may suffer service outages due to this. We ignore to restore such connections in the subroutine.

ESTIMATE-SPARE-CAPACITY 4.1 Capacity estimation

```
Input: Network topology, traffic matrix, logical design;
Output: Additional capacity per link to be provisioned;
for all failure on link $\ell' \in \mathcal{L}$ do
    Identify the set of affected connections $C_a$;
    Make necessary changes to the network topology (i.e., blocking failed link port,
    unblocking corresponding RPL);
    for all $c \in C_a$ do
        Restore the affected connection $c$;
    end for
    for all $\ell \in \mathcal{L}$ do
        Update $C_\ell^*$ and $\bar{C}_\ell$;
    end for
    Build the link state vector $S$ of $K$ items: each $S_k$ represents double ($\ell', \ell''$) failures;
    Compute $C_{\ell,k}^{\ell',\ell''}$ such as $C_{\ell,k}^{\ell',\ell''} = C_\ell^* - \bar{C}_\ell$;
    for all $\ell \in \mathcal{L}$ do
        Compute $C_\ell^{\ell',\ell''} = \max_{\forall k} C_{\ell,k}^{\ell',\ell''}$;
    end for
    return $C_\ell^{\ell',\ell''}$;
end for
```

Dual-failure restorability

Finally we extend our study to analyze the impact of our network design approaches on the level of network restorability. The double link failures restorability $R_2^{\ell',\ell''}$ of a given pair of links (ℓ', ℓ''), as defined in [36], is the fraction of the total failed connections traversing through links ℓ' and ℓ'' in working state that can be restored in the case of concurrent dual failures on links $\ell^{'}$ and $\ell^{''}$. Let us denote the number of non restorable connections in the case of failure on links $\ell^{'}$ and $\ell^{''}$ by $F_{\ell^{'},\ell^{''}}$ and the connections that traverse link $\ell^{'}$ and $\ell^{''}$ in working state by $W^c_{\ell^{'}}$ and $W^c_{\ell^{''}}$ respectively. Then, the restorability $R_2^{\ell^{'},\ell^{''}}$ can be defined as: $R_2^{\ell^{'},\ell^{''}}$ = 1 - $\frac{F_{\ell^{'},\ell^{''}}}{W^c_{\ell^{'}}+W^c_{\ell^{''}}}$. The network-wide restorability is denoted by R_2 which is defined as the average of over all ordered $(\ell^{'},\ell^{''})$ double link failures combinations [36]. Then R_2 = 1 - $\frac{\sum_{\forall(\ell^{'},\ell^{''}):\ell^{'}\neq\ell^{''}} F_{\ell^{'},\ell^{''}}}{\sum_{\forall(\ell^{'},\ell^{''}):\ell^{'}\neq\ell^{''}} (W^c_{\ell^{'}}+W^c_{\ell^{''}})}$. The above presented subroutine is used to compute the network-wide restorability as well and the numerical results are presented as follows.

Numerical Results II

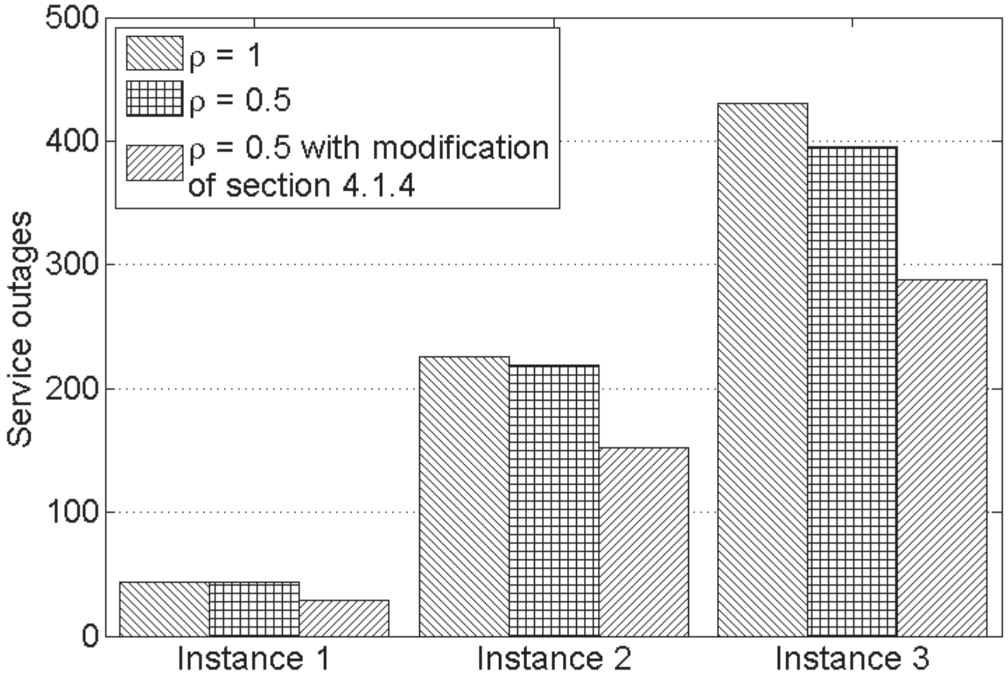

Figure 4.10: COST239 service outages

In this section, we analyze the additional capacity requirement estimated by the suggested remedy to eliminate the service outages due to the lack of capacity and the impact on the service outages. We compare the capacity-outages trade-off with the results that are presented in Section 3.5. The numerical results compare three design approaches: the first two approaches are different variants of the ILP model ($\rho = 1$ and $\rho = 0.5$ without modifications of Section 4.1.4) and the third approach ($\rho = 0.5$ with modifications of Section 4.1.4) estimates the additional capacity required to completely protect all restorable connections. We adopt the same traffic distributions as of numerical results presented in Section 4.1.3.

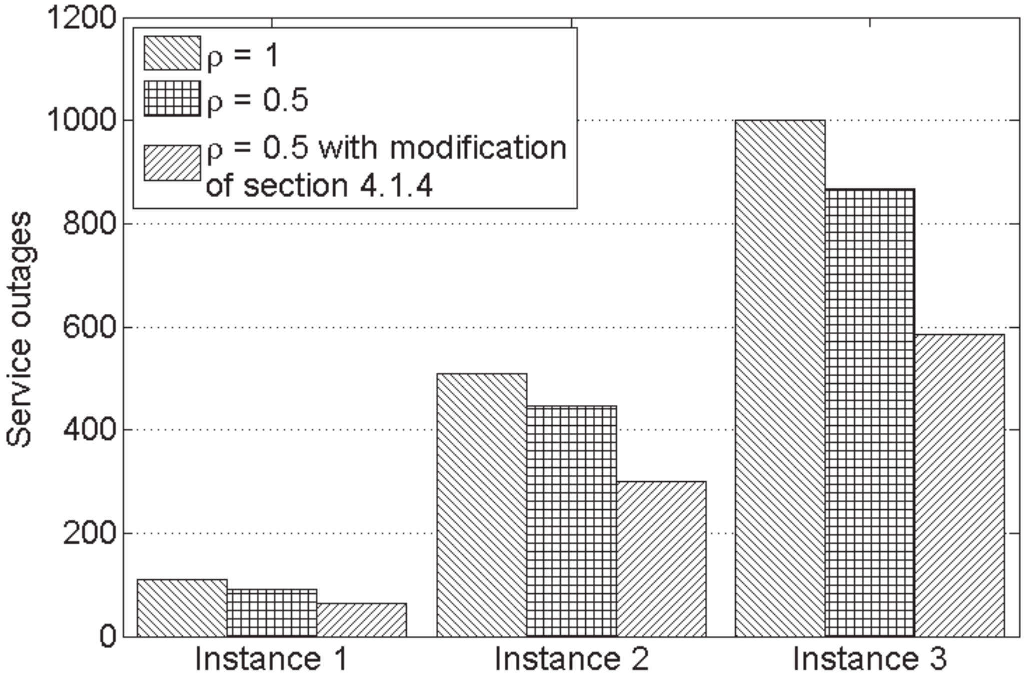

Figure 4.11: NSFNET service outages

Figs. 4.10, 4.11, and 4.12 present the number of service outages in three different network instances COST239, NSFNet, and ARPA2 respectively with different traffic distributions and Table 4.3 shows the corresponding capacity requirements. The figures show that our suggested remedy in the procedure

ESTIMATE-SPARE-CAPACITY can further reduce the number of service outages in the networks. For example, in COST239 with high traffic load (Instance 3), 15.6% of additional capacity (Table 4.3) yields a 27.1% reduction in service outages over the previous design method ($\rho = 0.5$). Similar results are observed for NSFNet and ARPA2 networks where the number of service outages are shown to be reduced by 32.7% and 21.9% in traffic instance 3 with additional 17.9% and 16.5% capacity investment respectively.

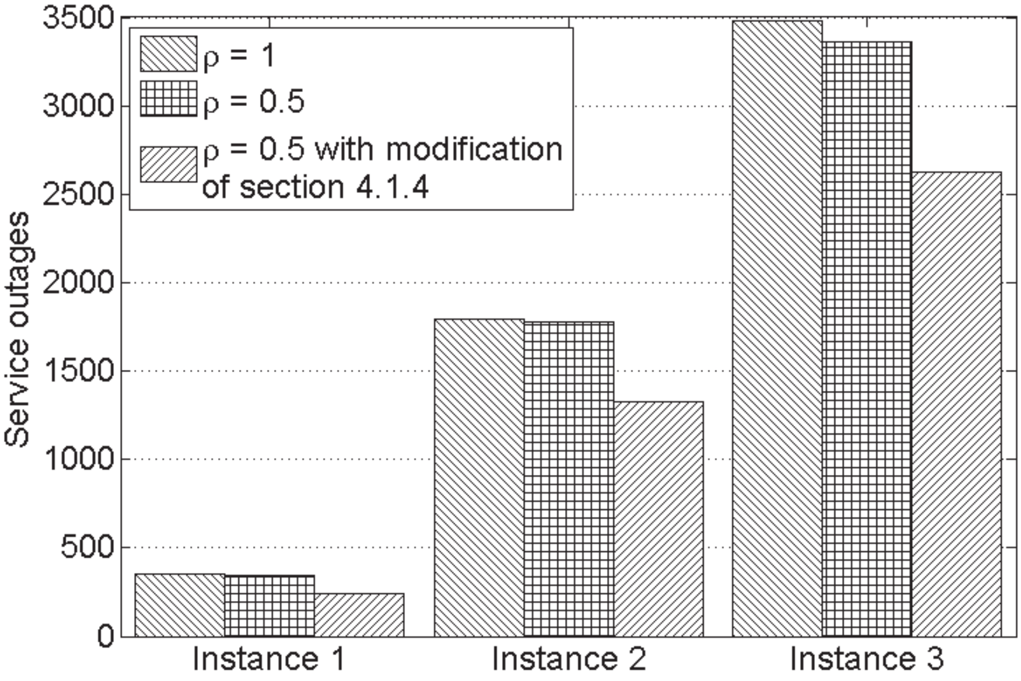

Figure 4.12: ARPA2 service outages

Fig. 4.13 presents the network-wide double link failures restorability (R_2) that can be achieved by the three design approaches in three network instances with high load (Instance 3). The figure shows that the network-wide restorability is improved by the third approach for all three network instances at the cost of additional capacity deployment. The first design approach ($\rho = 1$) which was intended to achieve 100% restorability against any single-link failure can achieve 81% restorability against double link failures (R_2) in NSFNet

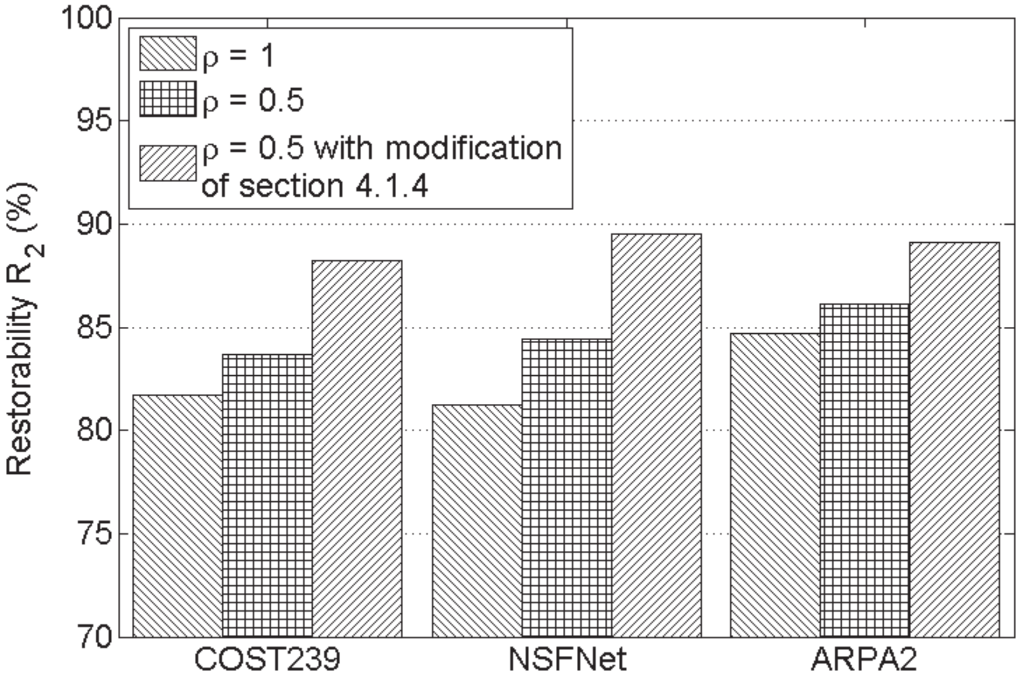

Figure 4.13: Comparison of network-wide restorability

network with high traffic load (Instance 3) and R_2 can be increased by 10% with additional capacity investment as estimated by the third approach. Similar trends are observed for COST239 and ARPA2 networks as well. A service provider may be interested to estimate the amount of capacity need to be deployed to achieve a targeted level of restorability.

4.2 Joint approach

Previous section addressed the problem of minimizing category-1 outages as part of the network design; it turns out that such service outages strongly depend on the particular RPL placement as well as the selection of the rings hierarchy. Our study reveals that the number of category-2 service outages which may occur under dual link failures is not negligible, as demonstrated in Table 4.4. Table 4.4 depicts some representative results on the outages per each category for COST239 network using the design approach of previous section. Clearly, a sizeable fraction of *category-2* outages may affect the network and cannot be ignored in the design. This section addresses the problem through a joint design approach where all outages resulting from concurrent dual link failures are minimized while capacity is optimally allocated on the links. We present a modified MILP formulation for the network design. The numerical results show that the two-step method cannot guarantee the optimality of the solution, whereas the proposed joint approach consistently yields to finding the optimal solution.

4.2.1 Category - 2 Outages

Given a network which is designed to survive against any single link failure, the provisioned capacity for its protection plan may be shared among demands which do not belong to the same risk groups. Upon a failure, all affected connections are restored through the reserved protection capacity; however, some connections may become vulnerable to a subsequent failure, especially those connections that share their protection plan with the connections affected by the first failure. These "vulnerable" connections are either completely unprotected for a second failure or may be in contention for resources with other connections which may be affected by a second failure. Thus, a second failure may yield network outages. Had enough capacity been provisioned, these outages may be mitigated. For example, let us assume that the network in Fig. 4.14 is designed to protect the two given connections (as shown) against any single link failure and the number on each link represents the allocated capacity. Note that, both connections are sharing protection resources on links $D-E$ and $E-F$ where only one (1) unit of capacity on each of the two links is

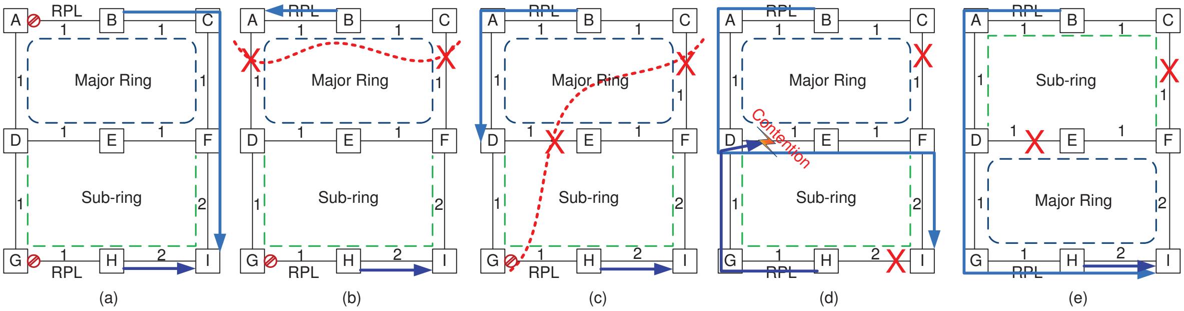

Figure 4.14: Category-1 and category-2 outages

needed to protect the given connections. However, in case of dual concurrent links failure scenario as presented in Fig. 4.14(d), where the two connections are affected together, both demands contend for the shared capacity. Assuming that the first failure occurs on link $C - F$, then connection $B - I$ is restored by using the shared resources causing the other connection ($H - I$) to become unprotected against a subsequent failure. If the subsequent failure occurs on link $H - I$, the connection ($H - I$) will suffer service outage.

4.2.2 Illustrative example

Given the sequential nature of the design method of previous section, the overall solution may not be globally optimal as demonstrated in following illustrative example. Fig. 4.15 depicts a mesh network composed of three rings R_1, R_2, and R_3 and three connection requests $C - H$, $B - G$, and $E - C$. Fig. 4.15(a) presents a capacity allocation solution (as well as RPL placement and hierarchy selection) obtained from the optimization model of previous section whose objective is to jointly minimize capacity and category-1 outages. The RPL placements are located and the logical ring hierarchies of the network are presented by the dotted lines. The solid lines represent the routing of the connection requests in working state and the numbers besides each link represents the capacity allocation on the links. The given solution requires in total 22 units of capacity to survive against any single link failure and there will be 29 possible instances of service outages (18 category-1 outages and 11 category-2 outages) due to dual-link failure scenarios. After exhaustively enumerating all possible dual-link failure scenarios, we found that two links ($D - I$, $I - H$) require additional capacity of 3 units on each link to eliminate category-2 service outages. For example, let us consider a dual link failure scenario where links $D-E$ and $A-F$ fail concurrently. Upon failure, the rings R_1 and R_3 unblock their RPLs and all three source-destination pairs remain connected. Connections $C - H$, $B - G$, and $E - C$ are intended to reroute through $C - D - I - H$, $B - C - D - I - H - G$, and $E - H - I - D - C$ respectively. However, links $D - I$ and $H - I$ do not have the required protection capacity to carry the rerouted demands. Indeed, three (3) units of additional capacity on each link $D - I$ and $H - I$ could provide the necessary protection against the given dual-link failure scenario. Hence, overall 28 (22+6) units of capacity are required by the two steps solution to eliminate category-2 outages and then, there will be 18 possible instances of category-1 outages. In contrary, Fig. 4.15(b) illustrates an alternate solution, which can be obtained by a joint solution approach. The solution presented in Fig. 4.15(b) shows different logical hierarchy of the rings as well as different RPL positions of the previous solution. This solution requires 27 units of overall capacity to eliminate category-2 outages while the category-1 outages remain 18 which is equal to the previous solution. The illustrative example clearly demonstrates the necessity to solve the two problems jointly to overcome the limitation of previous work.

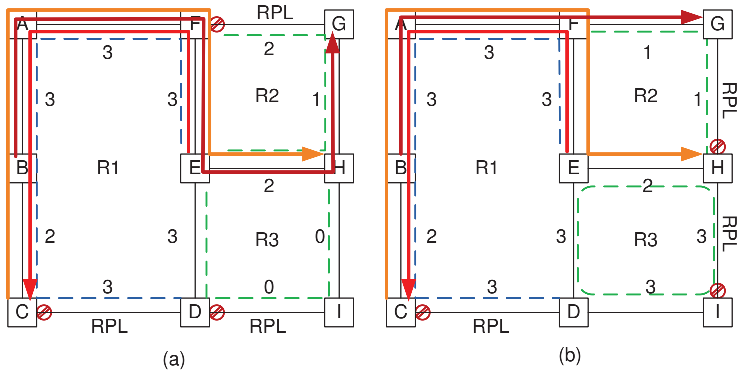

Figure 4.15: Illustrative example

4.2.3 Problem Formulation

Analysis

The previous section clearly highlights the need to jointly address category-1 and category-2 outages within the network design. As opposed to the sequential method, now we lay out our methodology for addressing this joint design problem. We demonstrate that both outage categories can be combinedly reduced by maximizing the number of connections that could be established, i.e., maximizing network flows, under any dual link failure scenarios. In this section, we present our analysis to show that maximizing network flows implies minimizing segmentations (category-1) and that a flow conservation constraint for protection switching, as illustrated next, ensures that enough capacity is allocated on each link to eliminate category-2 service outages.

We denote a network topology by a graph $\mathcal{G}(\mathcal{V}, \mathcal{L})$, where $\mathcal{V}$ is the set of vertices and $\mathcal{L}$ is the set of links, indexed by v and ℓ respectively. The set of all possible ring hierarchies and the RPL placements are denoted by $\mathcal{H}$ and $\mathcal{Z}$ and indexed by h and Z respectively. The set of the simple rings in $\mathcal{G}$ is denoted by $\mathcal{R}$ and is indexed by r. A simple ring is composed of a set of links that form a physical ring/cycle with no straddling links. For example, in Fig.

4.14(a), links $\{AB, BC, CF, FE, ED,$ and $DA\}$ forms a simple ring whereas links $\{AB, BC, CF, FI, IH, HG, GD,$ and $DA\}$ also form a physical ring but we do not refer to it as simple ring since there are two straddling links (DE, EF). The traffic demand set is denoted by $\mathcal{T}$. Each element of this set, t, defines a unit demand from source s_t to destination d_t where $s_t,\ d_t\ \in\ \mathcal{V}$. We denote $\mathcal{F}$ as the set of all possible dual failure scenarios where each element of this set, f, represents a dual failure of any links ℓ and ℓ', where $\ell,\ \ell'\ \in\ \mathcal{L}$.

Definition 1. *A **configuration** $c(\mathcal{G}, h, Z)$ is an ERP network $\mathcal{G}$ with a given logical hierarchy h among interconnected rings and the set of RPLs Z of the rings. The set of all possible configurations of a given ERP network is denoted by $\mathcal{C}$.*

Definition 2. *A feasible **flow** for a demand t in a configuration c experiencing an instance of dual-link failure f is denoted by $x^t_{f,c}$ such that:*
(a) For every vertex $j : j \in \mathcal{V} - \{s_t, d_t\}$, $\sum\limits_{i\in\mathcal{V}} x^t_{f,c}(i,j) = \sum\limits_{k\in\mathcal{V}} x^t_{f,c}(j,k)$ where $x^t_{f,c}(i,j)$ is the amount of flow on a link (i,j) between two adjacent nodes i and j.
(b) $\sum\limits_{i\in\mathcal{V}} x^t_{f,c}(s_t, i) = \sum\limits_{i\in\mathcal{V}} x^t_{f,c}(i, d_t) \geq 0$.
The amount of flow for a demand t in configuration c is $\sum\limits_{f\in\mathcal{F}} x^t_{f,c}$.

Definition 3. *A* segmentation *in a network affecting a demand t is a partition of $\mathcal{V}$ into at least two disjoint sets $\mathcal{V}'$ and $\mathcal{V}''$ such that $s_t \in \mathcal{V}'$ and $d_t \in \mathcal{V}''$ caused by an instance of concurrent dual-link failure f.*

Definition 4. *Let $\mathcal{P}(t,r)$ be a segment of a path used by a demand t which contains one or more edges of ring r and $\bar{\mathcal{P}}(t,r)$ be the other segment of r. Let $|\mathcal{P}(t,r)|$ and $|\bar{\mathcal{P}}(t,r)|$ be the number of links in these segments respectively. Then, the number of* service outages *that the demand t may possibly suffer from segmentations resulting from dual link failures in a given configuration c can be* *defined as* $o_c^t = \sum\limits_{r \in \mathcal{R}} \{|\mathcal{P}(t,r)| \times |\bar{\mathcal{P}}(t,r)|\}$.

Definition 5. *The* ***net flow*** *of a given configuration* c *is*

$$X(c) = \sum_{f \in \mathcal{F}} \sum_{t \in \mathcal{T}} x_{f,c}^t$$

and the ***net service outages*** *of a given configuration* c *is*

$$O(c) = \sum_{t \in \mathcal{T}} o_c^t$$

Lemma 1. *The number of service outages* o_c^t *that a demand* t *will possibly suffer from segmentations is known for a given ERP configuration* c *and is given by Definition 4.*

Proof. By definition, a given ERP configuration c always forms a logical tree and hence, the routing of any given demand t is unique. Once the routing is determined, $\mathcal{P}(t,r)$ and $\bar{\mathcal{P}}(t,r)$ are trivially found and thus the o_c^t can be determined. □

Lemma 2. *Let* o_c^t *and* $o_{c'}^t$ *be the number of service outages that demand* t *may suffer from segmentations resulting from dual link failures in configurations* c *and* c' *respectively. If* $o_c^t > o_{c'}^t$ *then* $\sum\limits_{f \in \mathcal{F}} x_{f,c}^t < \sum\limits_{f \in \mathcal{F}} x_{f,c'}^t$.

Proof. The set of all possible dual failure scenarios in a given network topology is defined by $\mathcal{F}$. The number of elements in $\mathcal{F}$, $|\mathcal{F}|$, depends on the number of links in the network and can be determined by $\frac{N(N-1)}{2}$ where N is the number of links. The number of service outages that a demand t may suffer in configuration c, o_c^t, can be determined by Definition 4, which depends on the number of links of each ring traversed by the demand t. Since, one of the links of each ring must be configured as the RPL and the demand t cannot be routed through the RPL, it is evident that $o_c^t < |\mathcal{F}|$. Hence, there exist some instances of dual failures which do not cause service outages for demand t in configuration c. Let $\mathcal{F}'_{c,t}$ and $\mathcal{F}''_{c,t}$ be the subsets of dual failures which cause and, respectively, do not cause service outages for demand t in configuration c, i.e., $\mathcal{F}'_{c,t}$, $\mathcal{F}''_{c,t} \subseteq \mathcal{F}$. Let $f'_{c,t}$ and $f''_{c,t}$ be the number of elements of these subsets respectively, i.e., $f'_{c,t} = |\mathcal{F}'_{c,t}|$ and $f''_{c,t} = |\mathcal{F}''_{c,t}|$.

Now, from Definition 2, the amount of flow for a demand t in configuration c can be expressed as

$$\sum_{f \in \mathcal{F}} x^t_{f,c} = \sum_{f \in \mathcal{F}'_{c,t}} x^t_{f,c} + \sum_{f \in \mathcal{F}''_{c,t}} x^t_{f,c}$$

If a dual failure scenario f causes service outage for demand t in configuration c, then there is no feasible flow for t in that particular dual failure scenario and thus $x^t_{f,c} = 0$. Hence, $\sum\limits_{f \in \mathcal{F}'_{c,t}} x^t_{f,c}$ does not contribute in determining the amount of flow for demand t. So,

$$\sum_{f \in \mathcal{F}} x^t_{f,c} = \sum_{f \in \mathcal{F}''_{c,t}} x^t_{f,c}$$

Similarly, since the dual failure instances of $\mathcal{F}''_{c,t}$ do not cause service outages for demand t in configuration c, $f''_{c,t}$ has no contribution in determining o^t_c. Hence, if $o^t_c > o^t_{c'}$ for any configurations c and c', we can say that $f'_{c,t} > f'_{c',t}$ and consequently $f''_{c,t} < f''_{c',t}$.

Since we assume unit demands, we conclude that if $o^t_c > o^t_{c'}$, $\sum\limits_{f \in \mathcal{F}''_{c,t}} x^t_{f,c} < \sum\limits_{f \in \mathcal{F}''_{c',t}} x^t_{f,c'}$. and thus,

$$\sum_{f \in \mathcal{F}} x^t_{f,c} < \sum_{f \in \mathcal{F}} x^t_{f,c'}$$

□

Lemma 3. *Let $X(c)$ be the net flow of configuration c. If $O(c) \leq O(c')$ then $X(c) \geq X(c')$.*

Proof. From Lemma 2, we can say that if $o^t_c \leq o^t_{c'}$ then $\sum\limits_{f \in \mathcal{F}} x^t_{f,c} \geq \sum\limits_{f \in \mathcal{F}} x^t_{f,c'}$ for any demand t in configuration c. Thus, accumulating over a given set of demands $\mathcal{T}$, we can state that if $\sum_{t\in\mathcal{T}} o_c^t \leq \sum_{t\in\mathcal{T}} o_{c'}^t$ then $\sum_{f\in\mathcal{F}}\sum_{t\in\mathcal{T}} x_{f,c}^t \geq \sum_{f\in\mathcal{F}}\sum_{t\in\mathcal{T}} x_{f,c'}^t$. However, from Definition 5, $\sum_{t\in\mathcal{T}} o_c^t$ is equivalent to $O(c)$ and $\sum_{f\in\mathcal{F}}\sum_{t\in\mathcal{T}} x_{f,c}^t$ is equivalent to $X(c)$. By replacing these equivalent terminologies, we can conclude that if $O(c) \leq O(c')$ then $X(c) \geq X(c')$. □

Theorem 1. *Let $O(c)$ be the number of service outages resulting from segmentations in a given configuration c such that $c = \arg\min_{c\in\mathcal{C}} O(c)$, then $X(c) \geq X(c') \quad \forall c' \in \mathcal{C} - \{c\}$.*

Proof. Let us assume that there is at least one configuration such that the net flow in that configuration is greater than $X(c)$, i.e., $\exists c' : X(c') > X(c)$. In such case, according to Lemma 3, the number of service outages resulting from segmentations in configuration c' must be smaller that $O(c)$, i.e., $O(c') < O(c)$. However, given that $O(c)$ is the minimum outages among any configuration in the network, we can conclude that $O(c') \not< O(c)$. Hence, our assumption is a contradiction, i.e., $\nexists c' : X(c') > X(c)$ and $X(c) \geq X(c') \quad \forall c' \in \mathcal{C} - \{c\}$. □

The above analysis clearly shows that in order to minimize outages resulting from dual concurrent failures, one could simply resort to maximizing network flows, given all possible dual link failures. This design will be elaborated in the next section.

ILP Formulation

We present our formulation for the joint optimal ERP design and capacity allocation problem. We consider Ethernet transport networks with bidirectional links where the capacity of each link is shared by the traffic in both directions. However, the network is presented by a graph $\mathcal{G}$ with directed arcs. The required capacity of a link is determined by the amount of traffic traversing through both of the corresponding arcs. A bidirectional link of the network is denoted by ℓ and the set of links is denoted by $\mathcal{L}$. The corresponding directed arcs of link ℓ are denoted by ℓ_{ij} and ℓ_{ji} where $i,\ j$ are two adjacent nodes and $i, j \in \mathcal{V}$ and the set of directed arcs is denoted by $\mathcal{E}$. The variables that are used to determine the ERP design and the capacity of the links are indexed by ℓ while the variables that are used to determine the routing of the demands are indexed by directed arcs ℓ_{ij} or ℓ_{ji}. We assume the set of simple rings $\mathcal{R}$ is given. Note that, our design method allows some rings of $\mathcal{R}$ to be pruned out. Some of the given simple rings may not need to be part of the logical ERP instance since none of their links are traversed by any of the demands in either working or protection state. A ring r is to be selected if and only if some demands absolutely require one or more of its links to be routed either in working or protection state. Capacity is provisioned only on the links of selected rings. According to the ITU-T recommendation G.8032, if more than one link are physically common to two rings, all of the common links must belong to only one of the logical rings. For example, in Fig. 4.14(a), links DE and EF are physically common to two simple rings. However, both of them must belong to either the upper ring or to the lower ring. It is restricted to design an ERP instance such that link DE belongs to one logical ring and link EF belongs to another logical ring. In this particular example, both links belong to the upper physical ring and form a logical “Major ring”. We further assume that the demands in $\mathcal{T}$ are unit-capacity demands. We define $\mathcal{F}$ as a set of failure scenarios ($\mathcal{F} = \{F(\ell, \ell') : \ell, \ell' \in \mathcal{L}\}$) such that each element of this set consists of a group of link(s) which for instance share the similar risk of failure or potentially could fail concurrently. The probability of concurrent failures on the links in the same group is considerably high because of common resource sharing (e.g., sharing fiber, common routers, etc.). We define the following parameters, sets, and variables that are used in the formulation.

- Parameters and sets: α_r^ℓ equal to 1 if link ℓ belongs to ring r, 0 otherwise. $\mathcal{L}_r$ is the set of links spanned by ring $r \in \mathcal{R}$. S_t, D_t are the source and destination of demand d, respectively.

- Variables: The variables are categorized into two classes based on their functions. One class (*class-1*) is used to design ring hierarchies and RPL placements whereas the other class (*class-2*) of variables is used in capacity planning and optimization.

Class-1 variables are similar to those are used in Section 3.4. We use the following variables as class-2

- $w_{\ell_{ij}}^t$ is used to determine the routing of the demands as well as the required capacity on the links in working state. $w_{\ell_{ij}}^t$: equal to 1 if demand t is routed through arc ℓ_{ij} in working state, 0 otherwise.

- $w_{\mathcal{F}(k)}^{\ell_{ij},t}$ is a set of variables that is used to determine the routing as well as capacity provisioning in protection state. $w_{\mathcal{F}(k)}^{\ell_{ij},t}$: equals to 1 if demand t is routed through arc ℓ_{ij} in case of k-th failure scenario of $\mathcal{F}$, 0 otherwise.

- ψ_ℓ^t determines the required capacity on link ℓ for demand t in working state.

- $\psi_{\mathcal{F}(k)}^{\ell,t}$ determines the required capacity on link ℓ for demand t in a failure scenario $\mathcal{F}(k)$.

- ψ_ℓ determines the capacity needed to be provisioned on link ℓ.

Similar to the variables, the constraints are categorized into two classes. We reuse the set of constraints 3.1 to 3.6 for the design of ERP architecture.

The capacity planning constraints are defined as follows :

- In working state :

$$\sum_{\forall j:\ell_{ij}\in\mathcal{E}} w^t_{\ell_{ij}} - \sum_{\forall j:\ell_{ji}\in\mathcal{E}} w^t_{\ell_{ji}} = \begin{cases} 1 & \text{if } i = S_t \\ -1 & \text{if } i = D_t \\ 0 & \text{Otherwise} \end{cases} \qquad t \in \mathcal{T} \tag{4.7}$$

$$w^t_{\ell_{ij}} \leq 1 - \sum_{r\in R} \eta^\ell_r \qquad t \in \mathcal{T}, \ell \in \mathcal{L} \tag{4.8}$$

$$w^t_{\ell_{ij}} \leq \sum_{r\in R} y^\ell_r \qquad t \in \mathcal{T}, \ell \in \mathcal{L} \tag{4.9}$$

Constraint (4.7) is the flow conservation of each demand $t \in \mathcal{T}$ in working state. Constraint (4.8) states that the arcs ℓ_{ij} and ℓ_{ji} can be used to carry traffic in working state only if their corresponding link ℓ is not the RPL of any ring. Similarly, constraint (4.9) ensures that a demand t can use the arcs ℓ_{ij} and ℓ_{ji} only if ℓ belongs to a ring. Similar to the constraints (4.8) and (4.9), two additional constraints are to be added for other directed arcs of ℓ.

- In failure/protection state :

$$\sum_{\forall j:\ell_{ij}\in\mathcal{E}} w_{\mathcal{F}(k)}^{\ell_{ij},t} - \sum_{\forall j:\ell_{ji}\in\mathcal{E}} w_{\mathcal{F}(k)}^{\ell_{ji},t} = \begin{cases} \le 1 & \textbf{if } i = S_t \\ \ge -1 & \textbf{if } i = D_t \\ = 0 & \textbf{Otherwise} \end{cases} \qquad t\in\mathcal{T}, \mathcal{F}(k)\in\mathcal{F} \tag{4.10}$$

$$w_{\mathcal{F}(k)}^{\ell_{ij},t} \le |\mathcal{F}(k)| + 1 - \sum_{\substack{\ell'\in\mathcal{F}(k)\\ \ell'\in\mathcal{L}_r}} y_r^{\ell'} - \sum_{r':r'\in\mathcal{R}-r} \eta_{r'}^{\ell} \qquad t\in\mathcal{T}, \ell\in\mathcal{L}, r\in\mathcal{R}, \mathcal{F}(k)\in\mathcal{F} \tag{4.11}$$

$$w_{\mathcal{F}(k)}^{\ell_{ij},t} \le \sum_{r\in\mathcal{R}} \alpha_r^{\ell} x_r \qquad t\in\mathcal{T}, \ell\in\mathcal{L} \tag{4.12}$$

$$w_{\mathcal{F}(k)}^{\ell_{ij},t} = 0 \qquad \ell\in\mathcal{F}(k), t\in\mathcal{T}, \mathcal{F}(k)\in\mathcal{F} \tag{4.13}$$

$$\psi_\ell^t \ge w_{\ell_{ij}}^t + w_{\ell_{ji}}^t \qquad \ell\in\mathcal{L}, \ell_{ij}, \ell_{ji}\in\mathcal{E}, t\in\mathcal{T} \tag{4.14}$$

$$\psi_{\mathcal{F}(k)}^{\ell,t} \ge w_{\mathcal{F}(k)}^{\ell_{ij},t} + w_{\mathcal{F}(k)}^{\ell_{ji},t} \qquad \ell\in\mathcal{L}, \ell_{ij}, \ell_{ji}\in\mathcal{E}, t\in\mathcal{T}, \mathcal{F}(k)\in\mathcal{F} \tag{4.15}$$

$$\psi_\ell \ge \max\Big(\sum_{t\in\mathcal{T}} \psi_\ell^t,\ \max_{\forall\mathcal{F}(k)} \sum_{t\in\mathcal{T}} \psi_{\mathcal{F}(k)}^{\ell,t}\Big) \qquad \ell\in\mathcal{L} \tag{4.16}$$

Constraint (4.10) is the flow conservation in the protection state for each demand $t \in \mathcal{T}$ and for each failure scenario in $\mathcal{F}$. Note that, we relax the conventional flow conservation approach in constraint (4.10). The conventional flow conservation ensures the flows to be routed from their sources to destinations. However, routing of all demands in ERP protection state might not be feasible, especially under dual-link failure scenarios that may cause physical/logical segmentations. The relaxation of the flow conservation in constraint (4.10) allows some demands not to be routed when there is no route available between source and destination due to the segmentations and this circumvents the infeasibility of the model. Constraint (4.11) states that, the affected demands by a failure scenario $\mathcal{F}(k)$ cannot be restored through arcs ℓ_{ij} and ℓ_{ji}, if their corresponding bidirectional link ℓ is the RPL of a ring other than the ring(s) containing the failed link(s). For instance, let us assume that link $A-B$ and $F-G$ fail concurrently in Fig. 4.15(b). The failed links belong to rings R_1 and R_2 respectively. Upon a failure, both rings R_1 and R_2 unblock their RPLs $C-D$ and $G-H$ respectively and the affected demands can be restored through the corresponding arcs of those RPLs. However, the RPL $H-I$ of ring R_3 will not be unblocked and thus, the affected demands cannot be restored through the link $H-I$. Constraint (4.12) affirms that a link ℓ is used to provide protection only if it belongs to a selected ring. Constraint (4.13) ensures that a link cannot protect itself. Similar to the constraints (4.11), (4.12) and (4.13), three additional constraints are to be added for other directed arcs of ℓ. Constraints (4.14) and (4.15) are used for determining the capacity of the links by transforming the traffic load of their corresponding arcs. Constraint (4.16) assures that enough capacity is reserved on each link to carry demands in both working and protection states.

The **objective** of the optimization problem is composed of two components. The first component is to minimize the overall network capacity, to be provisioned to withstand any single/dual link failures. The second component is to maximize the overall outgoing flows from all given sources under any single/dual-link failure scenarios. A parameter ρ is used as a "rewarding factor" for each successful restoration of the flows. The optimization solver may need to explore alternate protection routes to restore affected demands and may also require additional capacity to be provisioned. The rewarding factor ρ determines the amount to be rewarded over provisioned capacity for any successful restoration. In other words, ρ provides the flexibility to network designers to prioritize either increasing recoverable demands or reducing the amount of capacity to be provisioned. The objective function is expressed as:

$$\min \left\{ \sum_{\ell \in \mathcal{L}} \psi_\ell - \rho \times \sum_{t \in \mathcal{T}} \sum_{\forall \mathcal{F}(k)} \sum_{\forall j: \ell_{ij} \in \mathcal{E}, i = S_t} w_{\mathcal{F}(k)}^{\ell_{ij}, t} \right\}$$

4.2.4 Numerical results

In this section, we evaluate the performance of our joint design method in terms of minimal capacity requirement and total number of outages that the network will suffer from following any concurrent dual-link failures. We note here that the best design is indeed to provision minimal capacity in a network that will only suffer a minimal number of service outages following any dual failures. Most often though these are two contradicting objectives, as will be shortly illustrated. We start by first presenting an evaluation of one ERP design for optimal capacity allocation for protecting against only single link failures (*Previous work-1*) [35]. We also present results for the ERP design approach of previous section (*Previous work-2*). Both designs will be compared with the joint design presented earlier in this paper. The objective of this study is to illustrate the trade-offs between capacity provisioning and services outages (following concurrent dual failures) experienced in the network. We consider four traffic instances for this study (instances 1, 2, 3 and 4 consisting of 30, 50, 70 and 100 demands respectively, randomly selected) and we use the COST239 (11 nodes and 15 edges) for our evaluation and our results are averaged over multiple runs. Our proposed model (*Current work*) is evaluated with two different reward factors (ρ = 1 and 4). The numerical results are presented in Figure 4.16 which shows the overall allocated capacity (in terms of unit demands) and the number of outages that result from all possible dual-link failures. First, the figure shows that ignoring outages due to dual failures (Previous work-1) yields to truly minimal capacity allocation in the network; however, the price for this is the higher number of service outages caused by dual failures, which yields to a lower service availability provided by the network. Now considering minimizing category-1 outages (i.e., *Previous work-2*) as part of the design will surely increase the service availability (notice the reduction in the number of outages the network experiences) but indeed the operator must invest more capacity in the network. Our proposed method (current work) further reduces the service outages, in comparison with the other two methods, since it jointly considers both outage categories in the design. The figure shows the trade-off the reward factor plays; a high reward factor suggests that more emphasis should be put on achieving higher service availability (minimizing outages by maximizing the flow of traffic in the network under dual-link failure scenarios) and thus more capacity deployment in the network while a smaller value of ρ puts more emphasis on minimizing capacity and less so on service availability, therefore the higher number of outages

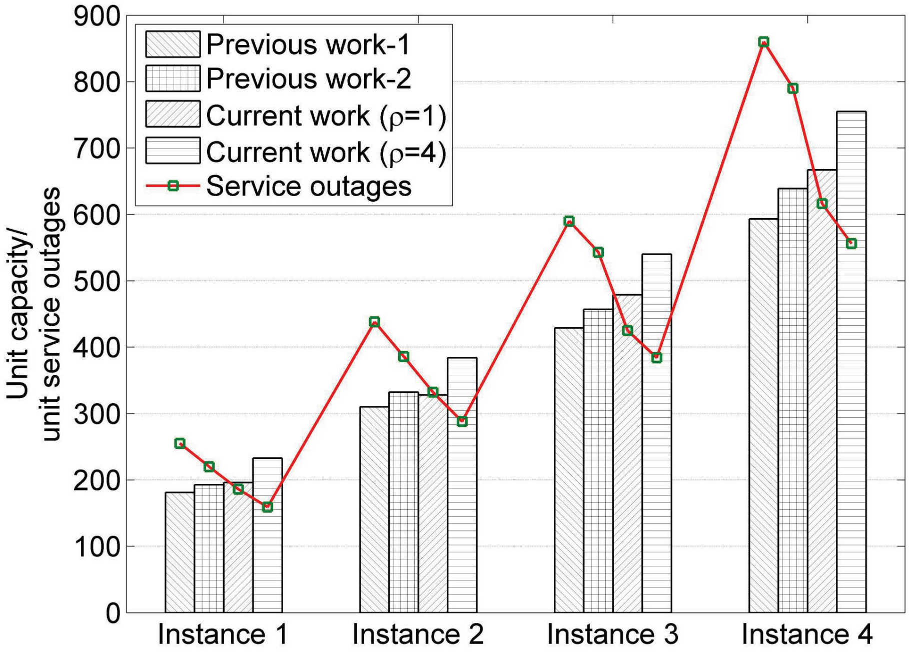

Figure 4.16: Performance Comparison with prior works using COST239 network

(the figure shows that outages are reduced by up to 37% over *Previous work-1* and by up to 29% over *Previous work-2* and that the additional investment in network is 25% and 15% respectively). This study indeed shows the strong relation between the allocated capacity and service availability; it also shows that our proposed model gives network operators a choice to put more emphasis on either one, by properly adjusting the reward factor.

Next, we present a comparative study of our proposed joint design approach with two other methods; namely, in the first one, the RPL placement and ring hierarchy among interconnected rings are selected randomly (*strategy-1*), but capacity is allocated to minimize dual link failure outages, and in the second (*strategy-2*), the two step method is used. Our proposed method is referred to as (*strategy-3*). We use four traffic instances for our evaluation, depicting light to heavy loads (30, 50, 70, and 100 unit demands respectively whose sources

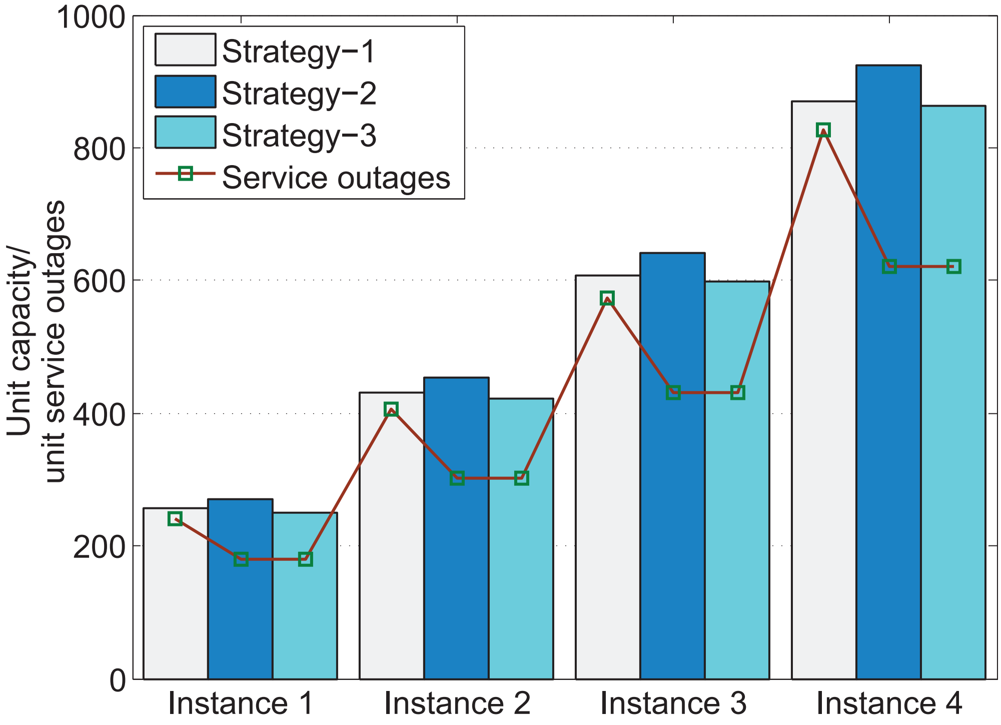

Figure 4.17: Comparison between different design strategies using Random network

and destinations are randomly generated); results are averaged over multiple runs. Two networks are considered in our evaluation, a random network with 9 nodes and 11 bidirectional edges (the topology presented in Fig. 4.15) and COST239. The metrics of comparison are the allocated capacity and the number outages following dual failures.

Fig. 4.17 and Fig. 4.18 present the numerical results from our evaluation using the two networks. For both figures, the results for *strategy 3* are obtained by assuming a reward factor (ρ) of 4. The figures show that the random strategy cannot guarantee the high service availability which may be required by network operators, this is mainly due to the random placement of RPLs and the selection of ring hierarchies (i.e., the design) that is done in a manner which is oblivious to outages caused by network segmentations. The figures show that this random design strategy results in network services which are

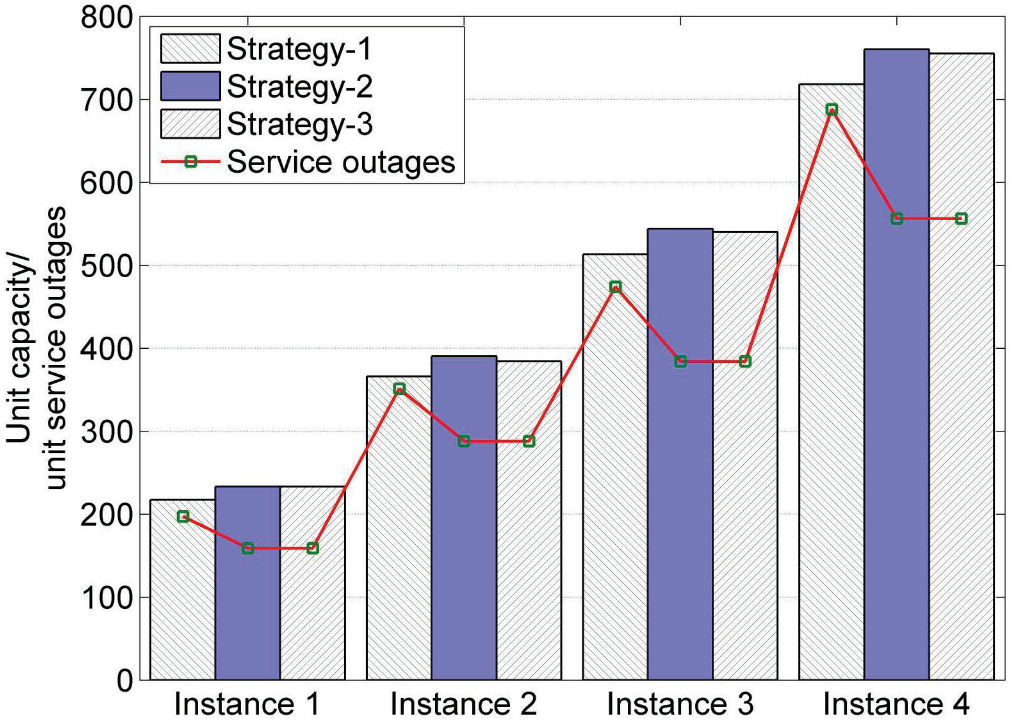

Figure 4.18: Comparison between different design strategies using COST239 network

more vulnerable to dual failures and the number of service outages, in comparison with the other two strategies, is around 25% higher for some traffic instances. In contrast, clearly, the other two design strategies achieve better service availability, as depicted in the figures, than the random one which implies the importance of properly selecting the RPL placement and hierarchy of rings. Further, both strategies 2 and 3 aim at minimizing the number of outages due to dual failures and hence achieve the same results; however, both design methods are fundamentally different. *Strategy 2* follows a sequential approach and aims at minimizing 1) capacity allocated and category 1 outages and then 2) allocate additional capacity to eliminate category 2 outages. On the other hand, *strategy 3* does the same but rather jointly, as explained earlier, while provisioning less capacity in the network (8% less than strategy 2 and 3% less than strategy 1 for the random network). Similar conclusions can

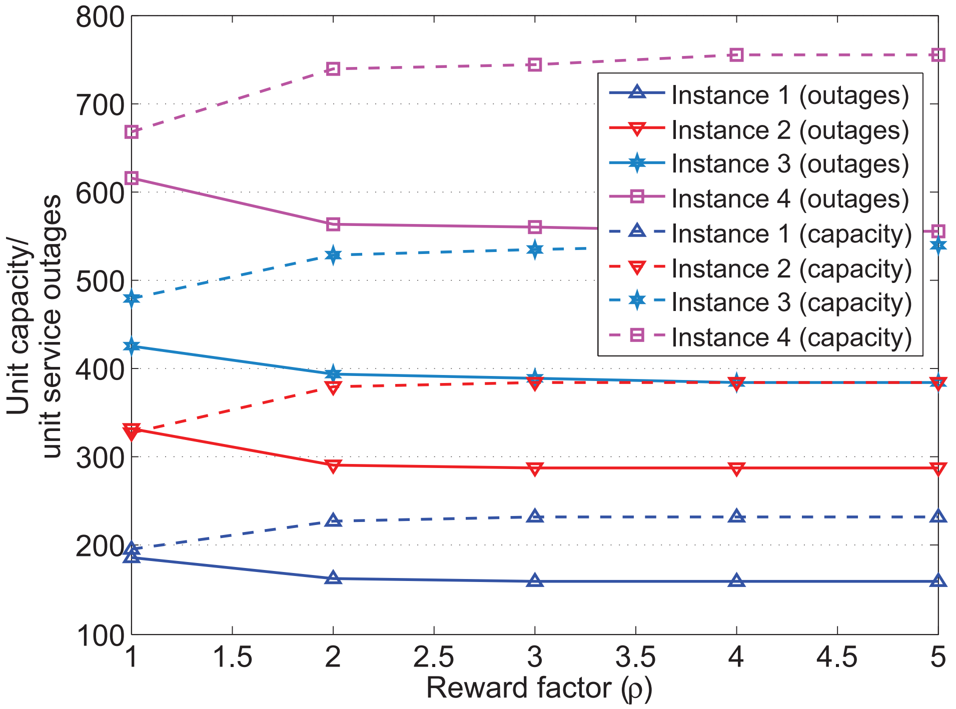

Figure 4.19: Comparison of capacity and service outages with varying reward factor (ρ) in COST239 network

be obtained from the COST239 network where the results are shown in Fig. 4.18.

Finally, we study the effect of varying the reward factor (ρ) on the performance of our proposed joint design method. We note that a higher value of ρ allows the model to favor maximizing the network flow subject to the set of all dual failures (i.e., increase service availability) and a smaller value steers the model to select designs which minimize the allocated capacity (recall, we mentioned earlier, these two are opposing factors), with lesser emphasis on outages. The results are presented in Fig. 4.19 for different traffic instances, using the COST239 network. As shown (for example, at higher loads), smaller ρ yields higher outages but smaller investment in capacity and higher values of ρ results in smaller number of outages and slight increase in allocated capacity; there is a threshold value of the reward factor, beyond which no service outages reduction can be seen. The threshold value of the reward factor varies according to the network topology and the traffic pattern. In most of our experiments, $\rho = 3$ is the threshold where service outages are minimized. Once this threshold value is reached, increasing the reward cannot reduce the service outages any further. Similar results are observed for the random network.

4.3 Chapter remark

In this chapter, we introduced and analyzed two categories of service outages that the demands may suffer in an ERP-based mesh network under any dual link failures. In Section 4.1, we developed an effective design approach for ERP mesh networks which addresses the issue of category-1 service outages and presented a routine to allocate additional capacity to eliminate category-2 service outages. Section 4.2 presented an improved design approach that jointly addresses both category of service outages. In Section 4.2, we presented a theoretical analysis and formal proof which shows that maximizing network flows subject to dual-link failures yields a network with high service availability and proposed an optimization model for solving this network design problem. The optimization model provides network engineers with the design flexibility to either minimize the provisioned capacity or minimize the service outages or find a balance between capacity investment and service outages resulting from dual link failures, by varying the value of a reward factor. Our results indicate that substantial reduction (up to 37%) in service outages is obtained over designs which are oblivious to dual link failures with little extra capacity investment. Further, both design approaches of Sections 4.1 and 4.2 are compared. Our results indicate that similar network service availability is achieved with less capacity deployment by later design model.

	COST239			**NSFNET**			**ARPA2**		
	Inst. 1	**Inst. 2**	**Inst. 3**	**Inst. 1**	**Inst. 2**	**Inst. 3**	**Inst. 1**	**Inst. 2**	**Inst. 3**
	(unit capacity)			**(unit capacity)**			**(unit capacity)**		
$\rho = 1$	34	172	310	68	299	589	179	952	1856
$\rho = 0.5$	36	183	332	76	314	630	188	981	1908
$\rho = 0.5$ *with modification of sec. 4.1.4*	45	218	384	94	393	743	246	1181	2224

Table 4.3: Capacity trade-off between three approaches

Table 4.4: Comparison of Category-1 and Category-2 service outages

COST239 network		
Number of demands	*Category-1 outages*	*Category-2 outages*
15	78	32
30	159	61
55	288	109

Chapter 5

Design of ERP: Traffic Engineering

Previous chapters of this thesis have focused on minimizing the overall network capacity requirement for a given set of traffic demand in ERP-based mesh networks. The optimal capacity allocation (OCA) problem is resolved by jointly selecting the ring hierarchy and determining the RPL placement using optimization models for both single and dual link failure scenarios. However, despite the importance of minimizing network cost through minimal capacity deployment, network operators usually confront a different optimization challenge. Typically, a network operator may already have an existing network deployed with finite link capacities and willing to implement ERP based protection mechanism. One of the most frequent design objectives is to maximize the revenue through allowing as much traffic as possible in the network by proper RPL placement and efficient selection of interconnected ring hierarchies. In addition, network operators are interested to exploit another advantageous feature of ERP which is the ability to implement multiple ERP instances over a single underlying physical network. Implementing multiple ERP instances could be beneficial for network operators in many different ways such as reducing end-to-end service latency, load balancing and so on which are discussed in more detail in Section 5.2. However, it may increase the complexity of network design. These network design issues and objectives are overlooked by the previous ERP designs.

In this chapter, we address the above mentioned design objectives by jointly determining the optimal RPL placement and selecting the ring hierarchies such that the network flow is maximized for a given set of sessions (s-d pairs). In the context of multiple ERP instances, it turns out that end-to-end service latency is reduced as well while maximizing network flows comparing to the one achieved by implementing single ERP instance. Section 5.1 presents the MILP formulation of ERP design which considers a single ERP instances will be implemented. The design strategy for multiple ERP instances is presented in Section 5.2.

5.1 Traffic engineering over single ERP instance

The network flow can be maximized in a number of ways. One way is to formulate the problem as a maximum multi-commodity flow (MMCF) problem [37] where the solution will maximize the flow, but may not fairly distribute the resources among the sessions. Here, some flows may starve for resources while some others (e.g. short hop flows) will be granted larger amount of bandwidth. Similarly, links of some parts of the network may become saturated keeping other parts underutilized. Another way to maximize network flows is known as *max-min* approach which promises to fairly allocate bandwidth among the sessions. Maximizing network flows has been extensively studied during the last decade for different types of transport networks (e.g., WDM, MPLS, wireless networks, etc.) [38, 39]. However, given the recency of the Ethernet standard, this design remains unexplored in the context of ERP networks. Due to the unique operational principles, the design of ERP networks require intense efforts. Nevertheless, previous works on flow maximization in the context of other transport networks do not basically include backup provisioning or design of a protection plan. In this work, we propose a novel design approach with an efficient selection of RPL placement and ring hierarchy for any given deployed network implementing ERP. The design objective is to maximize the network flows using the max-min approach and we develop an ILP model to achieve this design objective. Our ILP model jointly provisions backup/protection plan against any single link failure. To the best of our knowledge, this is the first work addressing traffic engineering in the context of ERP network design.

5.1.1 Problem Statement

Let $\mathcal{G}(\mathcal{V},\mathcal{L})$ be a bidirectional graph with positive finite capacity $c(\ell)$, $\forall \ell \in \mathcal{L}$ and K be the number of sessions indexed by $d_1, d_2, .., d_k$. Each of the sessions is specified by the triplet $d_i =< s_i, t_i, \gamma_i >$ where s_i, t_i denote the source and destination of session i respectively and γ_i denotes its demand. Given the capacity constraint on the links, satisfying all the incoming demands may not be always possible. We define a rate vector δ whose elements δ_i denote the rate assigned to the i-th session. A flow f^{s_i,t_i} is defined to be feasible if the network can allocate enough bandwidth in both the working and protection states to accommodate the allowable demand ($\delta_i \times \gamma_i$) of the session i. Note that the network is provisioned to survive against any single link failure in one ring. Therefore, the objective is to find the optimal RPL placements and

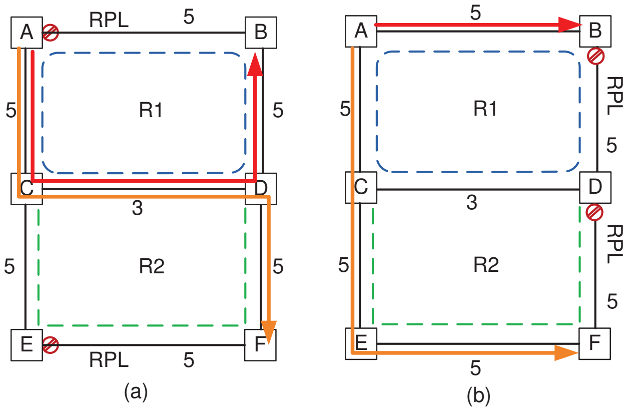

Figure 5.1: Variations of granted flow in different RPL placement

ring hierarchies to maximize the minimum allowed rate δ_i of each session.

5.1.2 Illustrative Example

We present two illustrative examples to show the effect of two major ERP design components (RPL, ring hierarchy) on overall network flows. The first example describes the impact of RPL placements whereas the second example focuses on the effect of ring hierarchy.

Fig 5.1 shows a mesh network composed of two logical rings R_1 and R_2. Two s-d pairs $A - B$ and $A - F$ are considered in this example each of which has a demand of 3 units. The capacity of the links are presented by the numbers placed beside each link. Fig. 5.1(a) shows an RPL placement on the links $A-B$ and $E - F$ for rings R_1 and R_2 respectively. The hierarchy of the two rings are shown by the dotted lines where R_1 is the major ring and R_2 is the sub-ring. The connections between the s-d pairs are presented by the solid directed lines. Note that, the capacity on link $C - D$ does not allow us to grant more than 50% of the demands for each δ_i, i.e., 1.5 unit demand for each session. Fig. 5.1(b) shows an alternate RPL placement with the same ring hierarchy where we can grant 83.3% of the requested demand, i.e., 2.5 unit demands for each

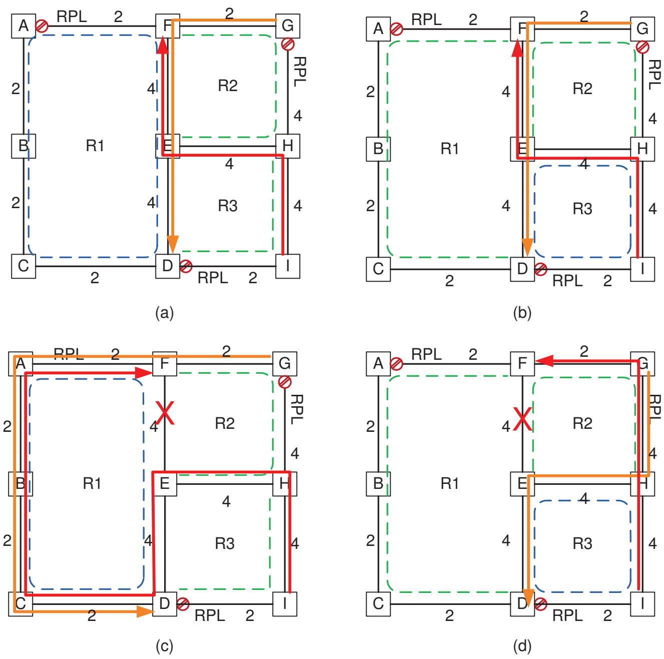

Figure 5.2: The impact of ring hierarchy on the amount of granted flow

session which increases the total amount of flow to 5 unit compared to 3 unit of previous placement.

Similarly in Fig. 5.2, we show (by varying ring hierarchy for a fixed set of RPL) that the selection of ring hierarchy affects the rate of the admissible flows. Fig. 5.2 shows a mesh network composed of three interconnected logical rings R_1, R_2, and R_3. We consider two sessions: $d_1 =< G, D, 3 >$ and $d_2 =< I, F, 3 >$. Fig. 5.2(a) and 5.2(b) show two different selections of ring hierarchies, but the RPL placements are fixed. In Fig. 5.2(a), R_1 is the major ring and R_2 is the upper ring w.r.t. the other sub-ring R_3 whereas in Fig. 5.2(b), R_3 is the major ring and R_2 is the upper ring w.r.t the other sub-ring R_1. Ring hierarchies and link capacities are presented by the dotted lines and the numbers beside each link respectively. The design of Fig. 5.2(a) limits the allowable rate for each session by 33.3% and the overall net flow to 2 units. Note that, the routing of the two sessions and the link capacities presented in

Fig. 5.2(a) show that the net flow/rate of each session can be further increased. However, the definition of the feasible flow states that a protection plan has to be provisioned for each admissible flow. Due to the lack of capacity on the links of the provisioned protection paths (one such instance is shown in Fig. 5.2(c)), the allowed rates δ_1 and δ_2 cannot be further increased for the ERP design of Fig. 5.2(a). An alternate ring hierarchy is shown in Fig.5.2(b) where 2 units of flow for each session can be provisioned (with 66.6% rate for each session) resulting in overall net flow of 4 units, while ensuring the survivability against any single link failure. Fig. 5.2(d) mimics the same failure scenario of Fig. 5.2(c) for the latter ERP design and shows that the capacity requirements on the links traversed by protection paths are satisfied.

5.1.3 Problem Formulation

We consider a network ($\mathcal{G}$) with bidirectional links, the set of simple rings[1] in $\mathcal{G}$ and the set of sessions $\mathcal{D}$ with demand vector γ are given. In addition to the set of variables defined in Section 3.4, we define the following variables: $w_\ell^{d_i}$ is used to determine the routing of the flows as well as the estimated flow on the links in working state; it is equal to the amount of flow ($\delta_i \times \gamma_i$) of session d_i which is routed through ℓ in working state. $w_{\ell'}^{\ell,d}$ is used to determine the routing as well as permissible flow in protection state: it is equal to the amount of flow ($\delta_i \times \gamma_i$) of session d_i which is routed through ℓ in case of failure of ℓ'.

The constraints of the MILP formulation are presented in different groups based on their purpose of usage. The first set of constraints as defined in (3.1) to (3.5) is reused in this model to design optimal ring hierarchies and RPL

[1] A simple ring is a ring without any straddling links within its perimeter.

placements. Other constraints for flow routing and rate allocation are defined as follows:

$$\sum_{\ell \in v^+} w_\ell^{d_i} - \sum_{\ell \in v^-} w_\ell^{d_i} = \begin{cases} \delta_i.\gamma_i & \text{if } v = s_i \\ -\delta_i.\gamma_i & \text{if } v = t_i \\ 0 & \text{Otherwise} \end{cases} \quad d_i \in \mathcal{D} \tag{5.1}$$

$$w_\ell^{d_i} \leq M(1 - \sum_{r \in R} \eta_r^\ell) \qquad d_i \in \mathcal{D}, \ell \in \mathcal{L} \tag{5.2}$$

$$w_\ell^{d_i} \leq \delta_i \times \gamma_i \qquad d_i \in \mathcal{D}, \ell \,\&\, \ell' \in \mathcal{L} \tag{5.3}$$

$$w_\ell^{d_i} \leq \sum_{r \in R} y_r^\ell \qquad d_i \in \mathcal{D}, \ell \in \mathcal{L} \tag{5.4}$$

Constraint (5.1) is the flow conservation for the demands of a session $d_i \in \mathcal{D}$ in working state. (5.2) states that a link ℓ can be used to carry traffic in working state only if it is not the RPL of any ring and (5.3) estimates the flow on ℓ in working state. M is a large integer. Similarly, (5.4) ensures that a session d_i can use a link ℓ only if ℓ belongs to an activated ring.

$$\sum_{\ell \in v^+} w_{\ell'}^{\ell,d_i} - \sum_{\ell \in v^-} w_{\ell'}^{\ell,d_i} = \begin{cases} \delta_i\gamma_i & \text{if } v = s_i \\ -\delta_i\gamma_i & \text{if } v = t_i \\ 0 & \text{Otherwise} \end{cases} \quad d_i \in \mathcal{D} \tag{5.5}$$

$$w_{\ell'}^{\ell,d_i} \leq M(2 - y_r^{\ell'} - \sum_{r' \in \mathcal{R} \setminus r} \eta_{r'}^\ell)$$

$$d_i \in \mathcal{D}, r \in \mathcal{R}, \ell \in \mathcal{L} \tag{5.6}$$

$$w_{\ell'}^{\ell,d_i} \leq \delta_i \times \gamma_i \qquad d_i \in \mathcal{D}, \ell \,\&\, \ell' \in \mathcal{L} \tag{5.7}$$

$$w_{\ell'}^{\ell,d_i} = 0 \qquad \ell = \ell', d_i \in \mathcal{D} \tag{5.8}$$

$$\max(\sum_{d_i \in \mathcal{D}} w_{\ell}^{d_i}, \max_{\forall \ell'} \sum_{d_i \in \mathcal{D}} w_{\ell'}^{\ell,d_i}) \leq c(\ell) \qquad \ell \in \mathcal{L} \tag{5.9}$$

Constraint (5.5) is the flow conservation in the protection state for sessions $d_i \in \mathcal{D}$ in case link ℓ' fails. (5.6) states that the flows that are affected by a link failure (ℓ') cannot be restored through link ℓ, if ℓ is the RPL of a ring other than the ring containing ℓ'. Constraint (5.7) estimates the flow on link ℓ in case of failure of link ℓ'. (5.8) ensures that a link cannot protect itself. (5.9) limits the admissible flow to the link capacity.

The **objective** of the optimization problem is to maximize the minimum δ for any session which is expressed as:

$$\max \{\min \delta_i \gamma_i\}$$

5.1.4 Numerical results

We evaluate the performance of our proposed design in terms of overall permissible network flows as well as fairness of resource allocation to incoming sessions. We compare the performance of our ILP-based design method with an arbitrary ERP design strategy (ARD) where the RPL placements and the ring hierarchies are selected randomly. In both design methods, we use two flow-maximization approaches. The first one is the max-min approach (ILP-MM, ARD-MM) as presented in this paper. The other approach maximizes the overall network flows with the objective of $\max \sum_i^K \delta_i \gamma_i$ and referred to as ILP-MF and ARD-MF. We present the numerical results for two well-known network topologies: COST239 (11 nodes, 15 links) and NSF (14 nodes, 18 links)

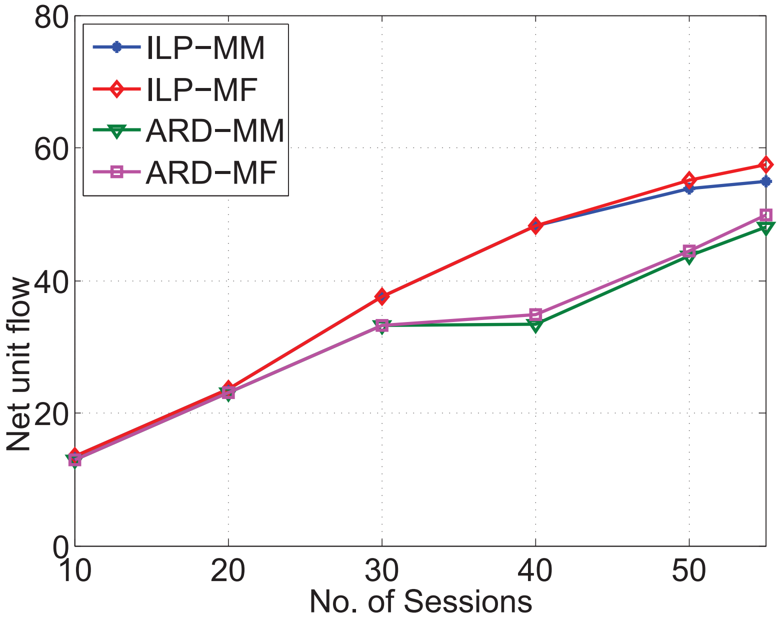

Figure 5.3: Net flow in COST239 network

networks [34]. The link capacities are randomly chosen from the range of 10 - 50 units. The comparisons are shown for various network loads by varying the number of sessions. The sources/destinations of the sessions are randomly selected and the demand vector γ for the incoming sessions is uniformly distributed over the range of 1 - 5 units for each session. In all cases, the results are averaged over multiple (5) runs.

Fig. 5.3 presents the permissible network flows in COST239 network as we vary the traffic load. Clearly both ILP-MM and ILP-MF outperform the arbitrary ERP design strategies (ARD cases). The overall network flow accommodated by ILP-MF is 38.5% greater than that of ARD-MF and is increased to 44.7% by ILP-MM than that of ARD-MM. The ILP-MF approach improves the overall network flow by (2.4-4.5)% in some cases comparing to ILP-MM which is somehow predictable, since ILP-MM rather focuses more on fair distribution of flows among the sessions than increasing the overall network flows. Similar results are observed for NSF network presented in Fig. 5.4 which shows that

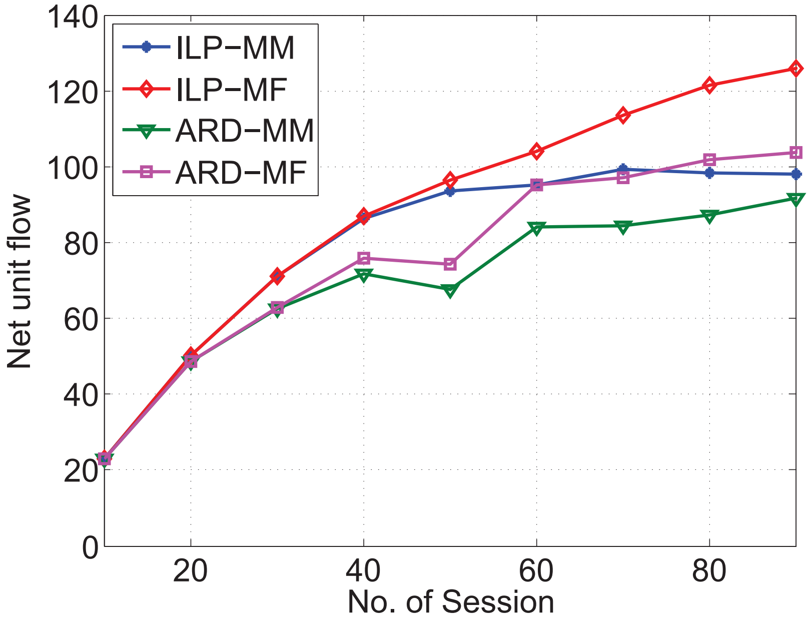

Figure 5.4: Net flow in NSF network

ILP-MF increases the network flow up to 30%-38.4% than the ARD-MF.

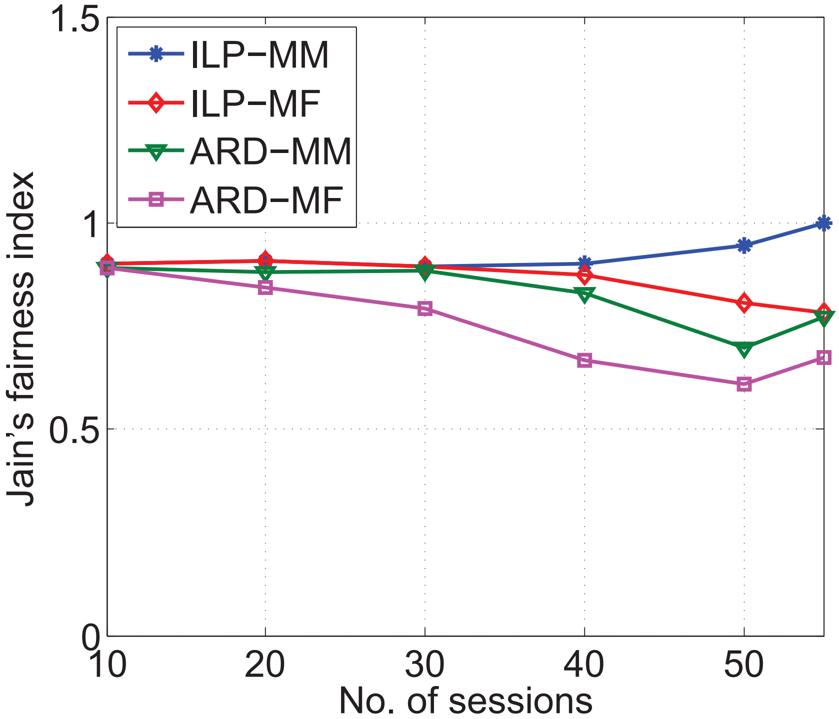

Figure 5.5: Fairness in COST239 network

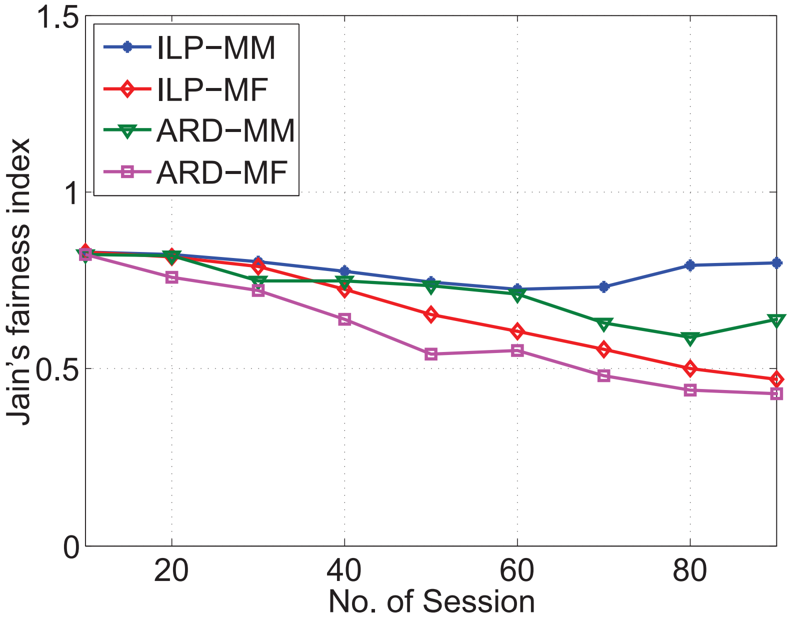

Figure 5.6: Fairness in NSF network

Fig. 5.5 compares the fairness (Jain's fairness index) in bandwidth allocation achieved by different strategies in COST239 network. Again, the proposed ILP-based design approaches (ILP-MM, ILP-MF) distribute the bandwidth more fairly than ARD-MM and ARD-MF. Unlike to the net flow comparison, ILP-MM outperforms ILP-MF and achieves better fairness. In some cases, ILP-MM achieves 27.7% and 48.8% better fairness in comparison to ILP-MF and ARD-MF respectively. Similar results are observed for NSF network in Fig. 5.6 where ILP-MM obtains significant improvement (0.8) in fairness over ILP-MF (0.47) and ARD-MF (0.43) respectively especially with larger number of sessions.

5.2 Traffic engineering over multiple ERP instances

Network operators are expected to be naturally interested to implement multiple ERP instances over a single underlying physical ring since multiple ERP instances can be utilized to reduce end-to-end service latency and to improve resource utilization. This can be achieved without any increase in capital expenditure (capEx) and with a little impact on operational expenses (opEx). The effect on opEx includes increased complexity in network design and in ERP configurations. Multiple ERP instances are managed and controlled by the use of VLAN identifiers (VIDs). Customer traffic from one VID or a group of VIDs are mapped to be protected by one of the ERP instances. The performances of network services that are protected by ERP, e.g. end-to-end service latency is directly related to such mapping. Hence, in addition to the typical ERP design issues (RPL placements and ring hierarchy selection), mapping customer traffic to protecting ERP instance requires careful consideration, in order to ensure optimized network performances, resulting in increased complexity in network design. In this section, we study this combinatorially complex design challenge of implementing multiple ERP instances in interconnected multi-ring mesh networks and develop an optimization model which provides necessary guideline to overcome this challenge.

5.2.1 Operation of multiple ERP instances

Since ERP is a logical entity, one can activate/implement multiple ERP instances over a single underlying physical ring or interconnected rings. Each ERP instance maintain its RPL, RPL owner node and RPL neighbor node. The

RPLs of different ring instances may be configured as different links or a single link. Each ERP instance activate its own R-APS channel for failure notification and protection switching procedures. The R-APS channel for different ERP instances are differentiated by the use of different VIDs. Delivering and protecting traffic channels by multiple ERP instances are also managed by the use of VIDs. Traffic channels are either identified by separate VLAN or grouped into different sets of VLANs. Each ERP instance is configured to protect a subset of those VLANs. When a failure is notified, each ERP instance act independently based on the received control messages of its own R-APS channel.

5.2.2 Design perspectives using multiple ERP instances

According to the ITU-T G.8032 recommendation, while implementing multiple ERP instances, each ERP instance may select its own RPL independently. One can take advantage of this feature to reduce the end-to-end service latency compared to implementing single ERP instance. Implementing multiple ERP instances can also be useful to avoid congestion in some parts of the network and to ensure fair utilization of network resources. Multiple ERP instances can be implemented without increasing capEx for network operators, though it requires a VID to be assigned to each R-APS channel of each ERP instance. Hence, a network operator might desire to implement as many ERP instances as required. Virtually, there is no limit on the number of ERP instances that could be implemented over a physical topology. However, it might not be advantageous to implement two or more ERP instances with the same link configured as their RPLs. Thus, the suitable number of ERP instances could be equal to the number of links where each link would be configured as the RPL of one ERP instance. Besides, some other factors may limit the number of ERP instances to be implemented. One of these factors is that Ethernet switches may pose a limit on the number of ERP instances to be configured. Indeed, given the recency of the ITU-T recommendation, only few vendors' equipment support the implementation of multiple ERP instances while limiting the maximum number of ERP instances to be implemented by two. However, the trend is growing. The requirement of VID for each ERP instance also somehow limit the implementable number of ERP instances. The number of VIDs that a service provider can use is limited (around 4000) and service providers may wish to use as many VIDs as possible to carry customer traffic. Hence, fewer number of VIDs would be reserved for implementing multiple ERP instances.

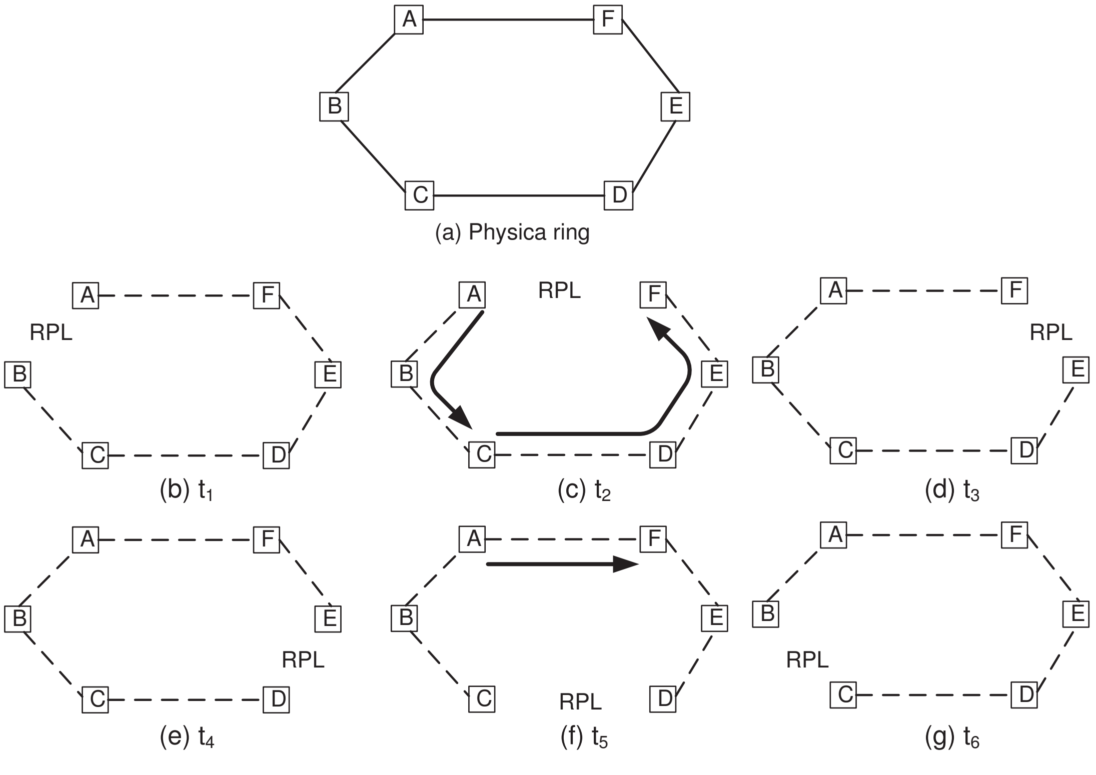

Figure 5.7: Logical ERP instances over a single physical ring

Once the number of multiple ERP instances to be implemented is chosen, one needs to map the subset of VIDs that are carrying customer traffic to suitable ERP instances. This adds another dimension of complexity to the network design consists of selection of RPL placements and the ring hierarchies. In the context of multiple ERP instances, the selection of RPL placements represent the selection of a subset of preferred ERP instances to be implemented among the set of all possible ERP instances. The subset of preferred ERP instances can be chosen based on the objective of network design. One of the important design objectives for network operators could be reducing end-to-end service latency. Such a network design should identify the best possible subset of ERP instances, i.e., the RPL placements for each ERP instance and the hierarchy among interconnected rings. However, one of our previous studies shows that the selection of RPL placements and ring hierarchies play important role in determining maximum admissible traffic flows in a network with fixed capacity. Thus, certainly there is a trade-off between reducing end-to-end service latency and allowable traffic flows while determining the subset of ERP instances to be implemented. Next, we present an illustrative example which visualizes this trade-off.

5.2.3 Problem Statement

Let $\mathcal{G}(\mathcal{V}, \mathcal{L})$ be a bidirectional graph with positive finite capacity $c(\ell)$, $\forall \ell \in \mathcal{L}$ and each link is assumed to have unit latency, i.e., the route with minimum hop count represents the route with minimum latency. Let k be the number of sessions indexed by $d_1, d_2, .., d_k$. Each of the sessions is specified by the triplet $d_i =< s_i, e_i, \gamma_i >$ where s_i, e_i denote the source and destination of session i respectively and γ_i denotes its demand. Given the capacity constraint on the links, satisfying all the incoming demands may not be always possible. We define a rate vector δ whose elements δ_i denote the rate allowed for the i-th session. A flow f^{s_i,e_i} is defined to be feasible if the network can allocate enough bandwidth in both the working and protection states to accommodate the allowable demand ($\delta_i \times \gamma_i$) of the session i. Note that the network is provisioned to survive against any single link failure in one ring. Therefore, the objective is to find the set of optimal virtual topologies, i.e., multiple ERP instances with their RPL placements and ring hierarchies, in order to either minimize the overall service latency or to maximize the minimum allowed rate δ_i of each session or to strike a balance between both.

5.2.4 Mapping Problem

As mentioned earlier, the number of implementable ERP instances is limited by either the number of reserved VIDs or by vendors' specifications. Regardless of the source of the imposed limitation, a network operator must select a subset of ERP instances to be implemented among all the possible instances in order to satisfy the imposed constraint. The preference may vary according to the network design objective. The selected ERP instances are then configured to provide protection to a group of traffic flows differentiated by their VIDs. We define the "mapping subproblem" as the mapping of a group of VLAN-IDs (traffic flows) to one of the selected ERP instances which will be responsible for providing protection to those mapped flows.

To illustrate, let us consider a simple ring topology with six links as shown in Fig. 5.7(a). Six virtual topologies ($t_1,\ t_2, \dots,\ t_6$) can be created over the given physical ring by implementing six ERP instances where six different links

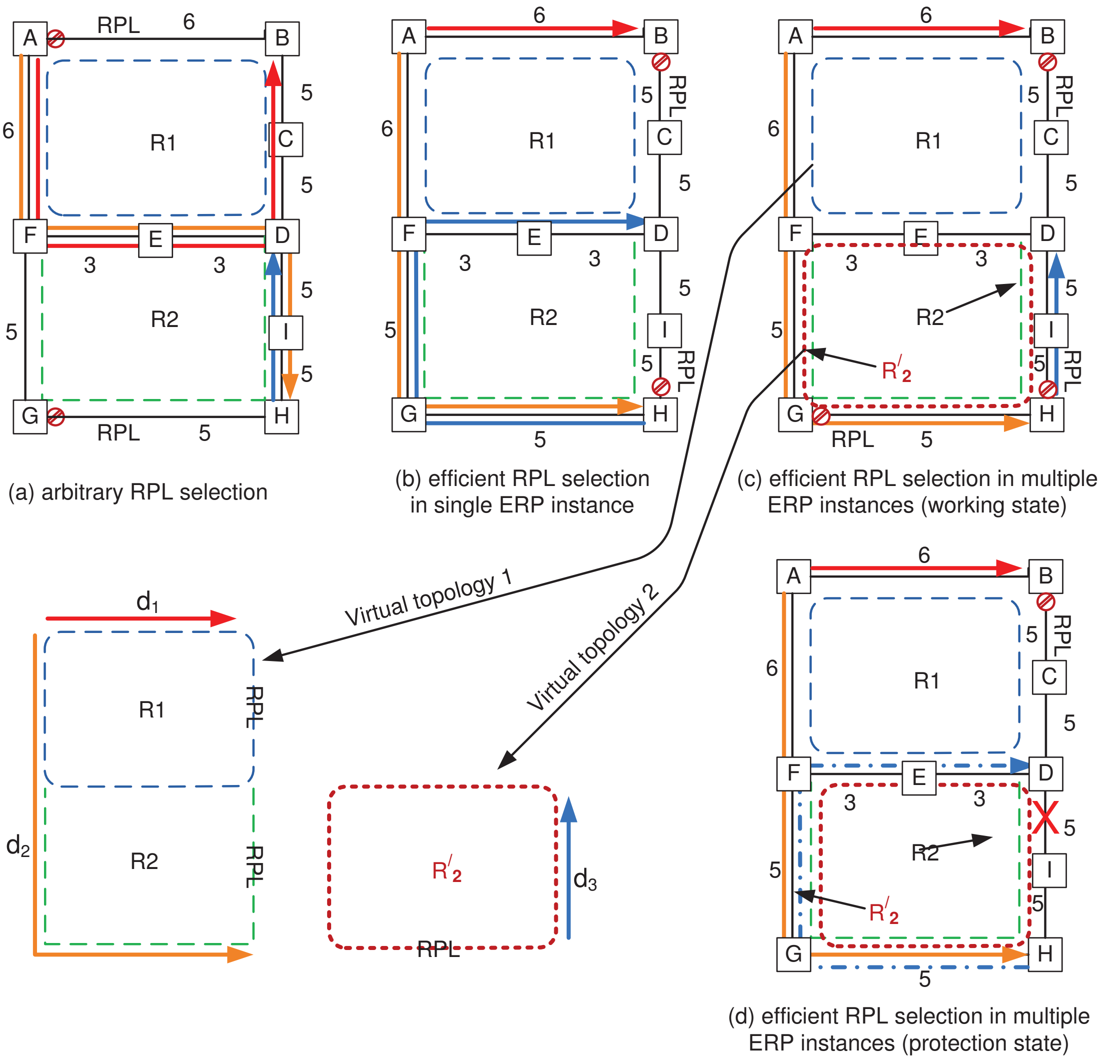
A
B
C
D
E
F
G
H
I
RPL
6
5
3
R1
R2
(a) arbitrary RPL selection
(b) efficient RPL selection in single ERP instance
(c) efficient RPL selection in multiple ERP instances (working state)
(d) efficient RPL selection in multiple ERP instances (protection state)
Virtual topology 1
Virtual topology 2
d_1
d_2
d_3
R'_2

Figure 5.8: Illustrative example

would be configured as their RPLs as shown in Fig. 5.7(b) to Fig. 5.7(g) respectively. The terminologies "ERP instance" and "virtual topology" are used interchangeably hereafter. We further assume that the traffic flows are grouped into three sessions ($d_1 =< C, F, 1 >$, $d_2 =< A, F, 1 >$, $d_3 =< A, C, 1 >$) and at most two virtual topologies are allowed to be implemented. Thus, one needs to select two among the six possible virtual topologies and must map all three sessions to any of the selected virtual topology. However, in order to select two virtual topologies that are best suited according to the network design objective, all six virtual topologies require to be evaluated and compared based on the measurement parameters. The number of comparisons can be represented by the sum of multinomial coefficient as $\sum_{t_1+t_2+...+t_6=3} \binom{3}{t_1,\ t_2,\ ...\ ,t_6}$ which is equivalent to 6^3. In general, if there is m number of possible virtual topologies in a given physical network and k number of sessions to be mapped, the total number of comparison would be $\sum_{t_1+t_2+...+t_m=k} \binom{k}{t_1,\ t_2,\ ...\ ,t_m} = m^k$. Hence, it is computationally inefficient to exhaustively enumerate all possible combinations to determine the best subset of virtual topologies in a larger network. In the context of this particular example, let us assume that the virtual topologies t_2 and t_5 are selected and t_2 is configured to protect sessions d_1 and d_3 while t_5 is configured to protect d_2 as shown in Fig. 5.7(c) and Fig. 5.7(f). Note that, the RPL port is blocked based on VIDs in the implementation of multiple ERP instances. Hence, when t_2 is configured to protect the sessions d_1 and d_3, the RPL of t_2 will block the traffic on its port only from those VIDs that are grouped to d_1 and d_3 while the traffic from VIDs that are associated with d_2 will be allowed to pass through.

5.2.5 Illustrative example

Figure 5.8 presents an illustrative example to demonstrate the impact of efficient ERP design on network performance for both single and multiple ERP instances implementations. Throughout this example, we consider a mesh network composed of two interconnected rings and three sessions each of which has a demand of 3 units, i.e., $d_1 =< A, B, 3 >$, $d_2 =< A, H, 3 >$ and $d_3 =< H, D, 3 >$. The capacity of the links are presented by the numbers placed beside each link.

Figure 5.8(a) shows an arbitrary selection of RPLs with an implementation of single ERP instance where R_1 is the major ring and R_2 is the sub ring. The hierarchy of the two rings are shown by the dotted lines and the connections between the s-d pairs are presented by the solid directed lines. Note that, the capacity on links $D-E$ and $E-F$ do not allow us to grant more than 50% of the demands for each δ_1 and δ_2 i.e., 1.5 unit demand for each session. Session d_3 can be granted 100% of its demand, however such amount of flow cannot be protected post failure of any of the two links $H-I$ and $I-D$. Since we consider, in our design approach, to guarantee 100% protection for allowed network flows, d_3 will also be granted 1.5 unit demand. On the other hand, service latency for the given sessions are 4, 5 and 2 units respectively. A network operator may however choose to design this network in a more efficient manner to achieve the objective of minimizing overall service latency. The placements of RPLs can be selected through an efficient network design as shown in Fig. 5.8(b) resulting in overall service latency for the given sessions of 1, 3 and 4 units respectively. However, the amount of flows to be granted remains 1.5 unit demand for each session due to the capacity constraints on links $D-E$ and $E-F$.

So far, the benefits of multiple ERP instances are not exploited in this example. Fig. 5.8(c) considers the same physical network topology and traffic of Fig. 5.8(b) while the network is allowed to implement multiple ERP instances. In addition to the ERP instance of Fig. 5.8(b) where R_1 is the major ring and R_2 is the sub ring, another major ring is implemented over the lower physical ring, referred to as $R_2^{'}$. The links $H-I$ and $G-H$ are configured as the RPLs of R_2 and $R_2^{'}$ respectively. The given session d_3 is configured to be protected by the ERP instance $R_2^{'}$. The ERP instance which is composed of the major ring

R_1 and the sub ring R_2 provides protection for the sessions d_1 and d_3. Figs. 5.8(c) and (d) show the working and protection states of the network with multiple ERP instances. Through the configuration of VIDs and mapping VID of d_2 to protecting ERP instance of R_1 and R_2, session d_2 is allowed to be routed through the RPL of $R_2^{'}$ in working state. In protection state of Fig. 5.8(d) where link $D-I$ fails, both R_2 and $R_2^{'}$ unblock their RPLs. In this design, the service latency for the sessions d_1, d_2 and d_3 is reduced to 1, 3 and 2 units respectively. In addition, the amount of flows to be granted for the given sessions is increased to 3, 2.5 and 2.5 unit demands respectively resulting in an increase of overall network flows comparing to previous designs implementing single ERP instance.

5.2.6 Problem Formulation

We assume that the physical topology $\mathcal{G}(\mathcal{V},\mathcal{L})$, where $\mathcal{V}$ is the set of nodes and $\mathcal{L}$ is the set of links, and the capacity on each link C_ℓ are given. We define the set of all possible hierarchies by $\mathcal{H}$ indexed by h and the set of all possible virtual topologies in h by $\mathcal{T}_h$, indexed by t. We further assume that the set of sessions $\mathcal{D}$, indexed by d_i, with demand vector γ and the maximum number (T_p) of virtual topology can be implemented are given. We use the parameter $\mathcal{L}_r$ as a set containing the links spanned by physical ring r. We define the following variables:

$Z_h :$ 1 if hierarchy h is chosen, 0 otherwise.

$K_t^h :$ 1 if virtual topology t of hierarchy h is chosen, 0 otherwise.

$\eta_{r,\ell}^{h,t} :$ 1 if link ℓ of ring r is RPL in virtual topology t of hierarchy h, 0 otherwise.

$y_{r,\ell}^h :$ 1 if link ℓ belongs to ring r in hierarchy h, 0 otherwise.

$\sigma_{d_i}^{h,t} :$ 1 if demand d_i is to be routed through virtual topology t of hierarchy h, 0 otherwise.

$w^{h,t}_{\ell,d_i}$: amount of flow of session d_i traversed through link ℓ in virtual topology t of hierarchy h in working state.

$P^{d_i}_{\ell}$: 1 if session d_i traversed through link ℓ in working state, 0 otherwise.

$w^{h,t}_{\ell,\ell',d_i}$: amount of flow of session $d_i$traversed through ℓ in virtual topology t of hierarchy h in case of link ℓ' fails and the network is in failure state.

The constraints of the MILP formulation are presented into different groups based on their functionalities. The first set of constraints 5.10 to 5.15 is used to build the logical relationship between the set of virtual topologies and the RPL positions of each hierarchy.

$$\sum_{h \in \mathcal{H}} Z_h = 1 \tag{5.10}$$

$$\sum_{t \in \mathcal{T}_h} k^h_t \leq T_p \qquad h \in \mathcal{H} \tag{5.11}$$

$$k^h_t \leq Z_h \qquad h \in \mathcal{H}, t \in \mathcal{T}_h \tag{5.12}$$

$$\sum_{\ell \in \mathcal{L}} \eta^{h,t}_{r,\ell} = 1 \qquad r \in \mathcal{R}, t \in \mathcal{T}, h \in \mathcal{H} \tag{5.13}$$

$$\sum_{r \in \mathcal{R}} y^h_{r,\ell} = 1 \qquad \ell \in \mathcal{L}, h \in \mathcal{H} \tag{5.14}$$

$$y^h_{r,\ell} = y^h_{r,\ell'} \qquad \ell, \ell' \in \mathcal{L}_r \cap \mathcal{L}_{r'}, r, r' \in \mathcal{R}, h \in \mathcal{H} \tag{5.15}$$

Constraints (5.10) and (5.11) limit the number of hierarchy to be selected and the number of implementable virtual topologies respectively. Constraint (5.12) states that a hierarchy has to be selected to implement one of its virtual topologies. Constraint (5.13) ensures that a ring can have at most one RPL for each virtual topology. In any given hierarchy, a link can belongs to only one ring which is enforce by Constraint (5.14). Constraint (5.15) states that any set of links that are shared by a pair of rings r and r' must logically belong to only one of those rings.

The other two sets of variables are defined for flow rate allocation and routing in both working ((5.16) to (5.23)) and protection ((5.24) to (5.28)) states as follows:

$$\sum_{t\in\mathcal{T}_h}\sum_{\ell\in v^+} w_{\ell,d_i}^{h,t} - \sum_{t\in\mathcal{T}_h}\sum_{\ell\in v^-} w_{\ell,d_i}^{h,t} = \begin{cases} \delta_i.\gamma_i & \text{if } v = s_i \\ -\delta_i.\gamma_i & \text{if } v = t_i \\ 0 & \text{Otherwise} \end{cases} \quad d_i \in \mathcal{D}, h \in \mathcal{H} \tag{5.16}$$

$$w_{\ell,d_i}^{h,t} \leq M(1 - \sum_{r\in R}\eta_{r,\ell}^{h,t}) \quad d_i \in \mathcal{D}, \ell \in \mathcal{L}, t \in \mathcal{T}, h \in \mathcal{H} \tag{5.17}$$

$$w_{\ell,d_i}^{h,t} \leq M\sum_{r\in R} y_{r,\ell}^{h} \quad d_i \in \mathcal{D}, \ell \in \mathcal{L}, t \in \mathcal{T}, h \in \mathcal{H} \tag{5.18}$$

$$w_{\ell,d_i}^{h,t} \leq \delta_i \times \gamma_i \quad d_i \in \mathcal{D}, \ell \in \mathcal{L}, t \in \mathcal{T}, h \in \mathcal{H} \tag{5.19}$$

$$w_{\ell,d_i}^{h,t} \leq M\ (\sigma_{d_i}^{h,t}) \quad d_i \in \mathcal{D}, \ell \in \mathcal{L}, t \in \mathcal{T}, h \in \mathcal{H} \tag{5.20}$$

$$p_\ell^{d_i} \geq \sum_{h\in\mathcal{H}}\sum_{t\in\mathcal{T}} w_{\ell,d_i}^{h,t}/C_\ell \quad d_i \in \mathcal{D}, \ell \in \mathcal{L}, \tag{5.21}$$

$$\sum_{h\in\mathcal{H}}\sum_{t\in\mathcal{T}}\sigma_{d_i}^{h,t}\leq 1 \qquad d_i\in\mathcal{D} \tag{5.22}$$

$$\sigma_{d_i}^{h,t}\leq k_t^h \qquad d_i\in\mathcal{D}, t\in\mathcal{T}, h\in\mathcal{H} \tag{5.23}$$

Constraints (5.16) and (5.19) are used for flow conservation and determining the amount of admissible flow in working state for each session. Constraints (5.17) and (5.18) enforce the blocking of flows on RPL. Constraints (5.20) and (5.23) ensures that a virtual topology of a hierarchy needs to be selected to route any flow. Constraint (5.22) imposes that a demand must be routed through only one virtual topology. Constraint (5.21) is used to compute the latency for each routed session.

$$\sum_{t\in\mathcal{T}_h}\sum_{\ell\in v^+} w_{\ell,\ell',d_i}^{h,t} - \sum_{t\in\mathcal{T}_h}\sum_{\ell\in v^-} w_{\ell,\ell',d_i}^{h,t} = \begin{cases} \delta_i\gamma_i & \text{if } v=s_i \\ -\delta_i\gamma_i & \text{if } v=t_i \\ 0 & \text{Otherwise} \end{cases} \qquad d_i\in\mathcal{D}, h\in\mathcal{H} \tag{5.24}$$

$$w_{\ell,\ell',d_i}^{h,t}\leq M(2-y_{r,\ell}^h-\sum_{r'\in\mathcal{R}\backslash r}\eta_{r,\ell}^{h,t}) \qquad d_i\in\mathcal{D}, r\in\mathcal{R}, \ell\in\mathcal{L}, t\in\mathcal{T}, h\in\mathcal{H} \tag{5.25}$$

$$w_{\ell,\ell',d_i}^{h,t}\leq \delta_i\times\gamma_i \qquad d_i\in\mathcal{D}, \ell \,\&\, \ell'\in\mathcal{L}, t\in\mathcal{T}, h\in\mathcal{H} \tag{5.26}$$

$$w^{h,t}_{\ell,\ell',d_i} = 0 \qquad \ell = \ell', d_i \in \mathcal{D}, t \in \mathcal{T}, h \in \mathcal{H} \tag{5.27}$$

$$w^{h,t}_{\ell,\ell',d_i} \leq M\ (\sigma^{h,t}_{d_i}) \\ d_i \in \mathcal{D}, \ell \ \&\ \ell' \in \mathcal{L}, t \in \mathcal{T}, h \in \mathcal{H} \tag{5.28}$$

$$\max(\sum_{t\in\mathcal{T}}\sum_{d_i\in\mathcal{D}} w^{h,t}_{\ell,d_i},\ \max_{\forall\ell'}\sum_{t\in\mathcal{T}}\sum_{d_i\in\mathcal{D}} w^{h,t}_{\ell,\ell',d_i}) \leq C_\ell \\ \ell \in \mathcal{L}, h \in \mathcal{H} \tag{5.29}$$

Similar to the constraints of working state, constraints (5.24) and (5.26) are used for flow conservation and to determine the amount of flow in failure state for each session. Constraint (5.25) enforces the rules of the RPL and constraint (5.27) states that a link cannot protect itself. Constraint (5.29) limits the admissible flow to link capacity.

We study the above optimization problem with multiple objectives. One of the objectives of the optimization problem is to maximize the minimum δ for any session which is expressed as:

$$\max\{\min \delta_i \gamma_i\}$$

Another objective is to minimize the maximum service latency $\sum\limits_{\ell\in\mathcal{L}} P^{d_i}_{\ell}$ for any session which is expressed as follows:

$$\min\left\{\max_{\forall d_i}\sum_{\ell\in\mathcal{L}} P^{d_i}_{\ell}\right\}$$

5.2.7 Numerical results

We evaluate the performance of our proposed design in terms of admissible network flows and end-to-end latencies. We compare the network performances over two alternatives of ERP deployment: one with single ERP instance and the other with multiple ERP instances to be implemented. Due to the large running time of the developed model we are unable to evaluate the performances in standard telecommunication networks and thus we present the numerical results for a small network with smaller amount of traffic. We use a network topology with 3 rings, 12 nodes and 14 links, very similar to the one presented in Fig. 5.2. The link capacities are randomly chosen from the range of 5 - 20 units. The comparisons are shown for various network loads by varying number of sessions. The sources/destinations of the sessions are randomly selected and the demand vector γ for the incoming sessions is uniformly distributed over the range of 1 - 5 units for each session. In all cases, the results are averaged over multiple (5) runs. The numerical results that are presented in this section are obtained by using the first objective function of the proposed model.

Figure 5.9 presents the total permissible network flows and the total latency with the both options of single and multiple implementable logical ERP instances. In this evaluation, we limit the maximum number of implementable ERP instances by two. The overall network flow accommodated by implementing multiple ERP instances is 15.4% to 31.2% higher than that of implementing single ERP instance. Since the objective function focuses on network flows only, the end-to-end service latency is not optimized. However, our results show that implementing multiple ERP instances can offer either same or reduced latency in most cases (2 out of 3) especially in higher loads comparing

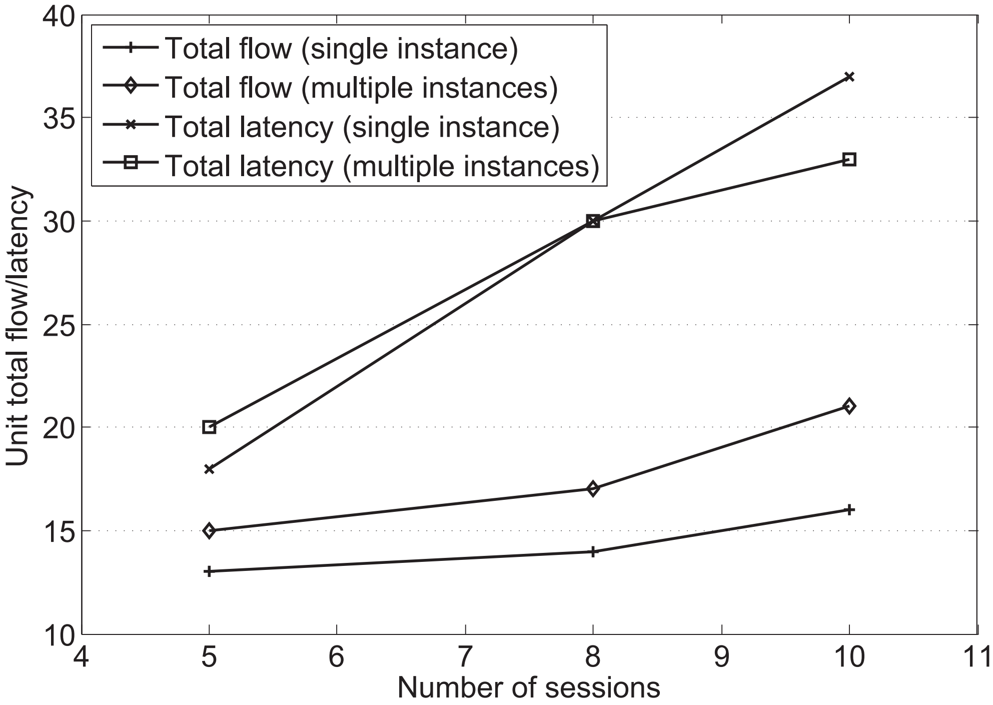

Figure 5.9: Comparison of total flow/latency

to implementing single ERP instance. The similar set of results are depicted in Fig. 5.10 where the average admissible flows and the average end-to-end service latencie are presented.

5.3 Chapter remark

In this chapter, we proposed efficient and traffic engineering-aware ERP network design strategies with the alternatives of implementing either single or multiple logical ERP instances over a physical underlying network while the network traffic flow is maximized subject to fixed link capacities. In section 5.1, we developed an ILP model which maximizes the network flow using max-min approach ensuring fairness in bandwidth allocation as well as guarantees survivability against single link failures. Numerical results indicate a substantial

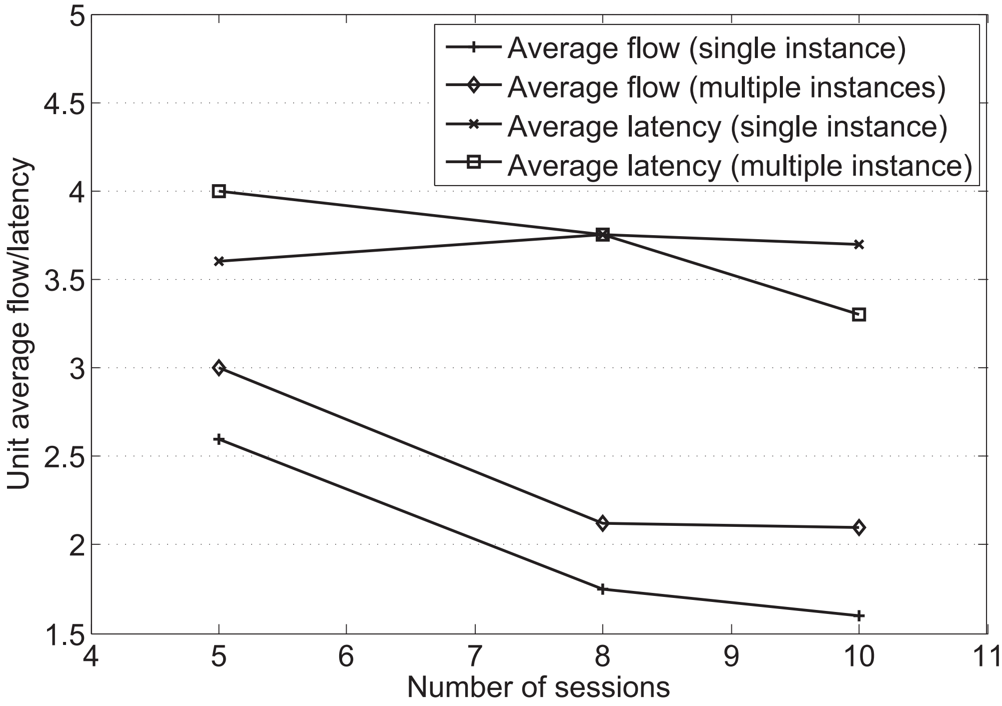

Figure 5.10: Comparison of average flow/latency

improvement in the overall network flow and better fairness in comparison to an arbitrary ERP design. In section 5.2, we extended the work of section 5.1 by exploiting the ability of implementing multiple logical ERP instances. Numerical results indicate a significant improvement in the overall network flow and better latency in comparison to implementing single ERP instance.

Chapter 6

Green Ethernet Transport Network

In this chapter, we focus on the latest carrier Ethernet technology called *Provider Backbone Bridge-Traffic Engineering (PBB-TE)*, which was ratified in IEEE standard 802.1Qay in June 2009. PBB-TE enhances carrier Ethernet networks with the support of deterministic Quality-of-Service (QoS), traffic engineered point-to-point and point-to-multipoint connections called Ethernet Switched Paths (ESPs). PBB-TE preserves the connectionless Ethernet behavior and adds a connection-oriented forwarding mode to current Ethernet networks by simply turning off traditional flooding and learning techniques. In doing so, the existing Ethernet control protocol (Spanning Tree Protocol [STP] and its derivatives) and all its associated constraints and problems, e.g., slow convergence time and lack of load balancing, disappear.

This chapter addresses open issues of PBB-TE networks and explores next-generation carrier Ethernet switch architectures with advanced packet switching capabilities, evolutionary migration from legacy SONET/SDH TDM, as well as their coexistence with IP/MPLS routers and backward compatibility with existent Ethernet switches. We propose two novel architectures of photonic PBB-TE (PPBB-TE) edge and core nodes, which enhance the usability of PBB-TE networks by reducing the power consumption in individual nodes in conjunction with the new standard IEEE 802.3az Energy Efficient Ethernet (EEE), which was recently approved on September 30, 2010, representing the first standard on energy efficiency in the history of IEEE 802.3. The proposed PPBB-TE core nodes are designed to use passive optical correlators to forward incoming flows all-optically, while the PPBB-TE edge nodes detect flows and transmit them through optical or Ethernet ports. Both core and edge nodes may integrate EEE enabled Ethernet ports. In addition, we formulate the problem of optimal energy-aware scheduling as a mixed integer linear program (MILP); our model provides optimal transmission schedules which guarantee the delay requirements of incoming frames while yielding the minimum energy consumption. A comparative performance analysis is presented between the optimal model and with a promising approach called packet coalescing [4]. To overcome the complexity and scalability issues of our model, we develop an efficient heuristic for solving the MILP by adopting a sequential fixing approach. We study the impact of our relaxed model on the objective function and show the accuracy of our heuristic. Finally, we study the impact of frame delay requirements and frame sizes on the overall energy consumption and discuss the findings.

To the best of our knowledge, no such architecture is proposed for carrier Ethernet networks before. In addition, no other formal model exists that minimize the energy consumption of EEE and the proposed optimal energy-aware scheduling is the unique of its kind. The success of the proposed architecture relies on the flow switching and the available number of OC labels that current optical technology permits. The remainder of the chapter is structured as follows. Section 6.1 describes the salient features of PBB-TE, reports on recent progress on GMPLS Ethernet Label Switching (GELS) as the control plane for PBB-TE networks, and outlines remaining open issues in PBB-TE networks and EEE standard. The proposed PPBB-TE switches are presented in Section 6.2. Section 6.3 consists of an illustrative example and an optimization model for energy-aware scheduling to minimize the EEE overhead. Numerical results are presented in Section 6.4. Section 6.5 includes chapter remarks.

6.1 GMPLS Ethernet Label Switching (GELS) and open issues

6.1.1 GMPLS Ethernet Label Switching (GELS)

PBB-TE introduces a connection-oriented forwarding mode to the data plane of traditional connection-less Ethernet networks assuming that the forwarding tables of PBB-TE switches are populated with ESP related table entries through an external control (or management) plane. The development of a control plane to set up, modify, and tear down ESPs is currently one of the key open issues in PBB-TE. There is a risk to be tempted to add too many replicated networking functions to Ethernet and thus lose its trademarks of low cost and simplicity. Instead, Ethernet should be viewed as a highly effective complement to IP/MPLS and should not attempt to replace it [40].

Given that GMPLS supports a wide range of interface switching capabilities and allows for explicit constraint-based routing, and the administrative benefits of using a single control plane are enormous, the GMPLS control plane is extended for PBB-TE networks at present named *GMPLS Ethernet Label Switching (GELS)*. To establish an ESP, only the GMPLS signaling protocol RSVP-TE requires extensions. The GMPLS routing protocols OSPF-TE and IS-IS-TE may be used unmodified, while the Link Management Protocol (LMP) may not be needed at all and may be replaced with IEEE Connectivity Fault Management (CFM) and Link Layer Discovery Protocol (LLDP) [41]. The use of GMPLS as a control plane for the set-up, teardown, protection, recovery of ESPs and the required RSVP-TE extensions are described in [42]. GMPLS established ESPs are referred to as Ethernet-LSPs (Eth-LSPs). When configuring an Eth-LSP with GMPLS, the Eth-LSP-MAC DA and Eth-LSP-VID are carried in a generalized label object and are assigned hop by hop but are invariant within the PBB-TE network. According to [42], to establish a bidirectional point-to-point Eth-LSP the initiator of the RSVP-TE PATH message, i.e., the ingress BEB, must set the encoding type to Ethernet and the LSP switching type to PBB-TE. Furthermore, the ingress BEB must set the upstream label to its own MAC address Eth-LSP-MAC1 and a locally administered Eth-LSP-VID1. The tuple <Eth-LSP-MAC1, Eth-LSP-VID1> contained in the upstream label is used to create a static entry in the forwarding table of each traversed BCB for the upstream direction. The egress BEB allocates a locally administered Eth-LSP-VID2 to its MAC address Eth-LSP-MAC2. The tuple <Eth-LSP-MAC2, Eth-LSP-VID2> is passed in the (downstream) label object of the RSVP-TE RESV message upstream to the ingress BEB and is installed as a static entry in the forwarding table of each traversed BCB. Upon arrival of the RSVP-TE RESV message at the ingress BEB, the bidirectional point-to-point Eth-LSP is established. In the case of a bidirectional point-to-multipoint Eth-LSP, the label consists of an Eth-LSP-VID and a group MAC address, whereby each branch of the point-to-multipoint Eth-LSP is associated with a reverse congruent point-to-point Eth-LSP. The RSVP-TE extensions for associating OAM attributes with an Eth-LSP are described in [43].

6.1.2 Open Issues

Despite recent progress, a number of open issues exist for PBB-TE switches and networks:

Energy Consumption

Power consumption represents one of the most serious obstacles of expanding the capacity of today's routers and switches due to their underlying optical-to-electrical-to-optical (OEO) conversion, which is a highly power-consuming process. In fact, almost 50% of power is consumed by OEO conversion and chip-to-chip communication [44]. More specifically, it was recently shown that the two by far most power-hungry components of a typical high-end electronic router are the forwarding engine (32% of total router energy consumption) and the power supplies for cooling fans/blowers (35% of total router energy consumption), while each of the remaining components represents 11% or even less of the total [45]. Clearly, to achieve major energy savings and energy efficiency gains, the forwarding engine and heat dissipation blocks are the two most important components that need to be replaced with less power hungry solutions.

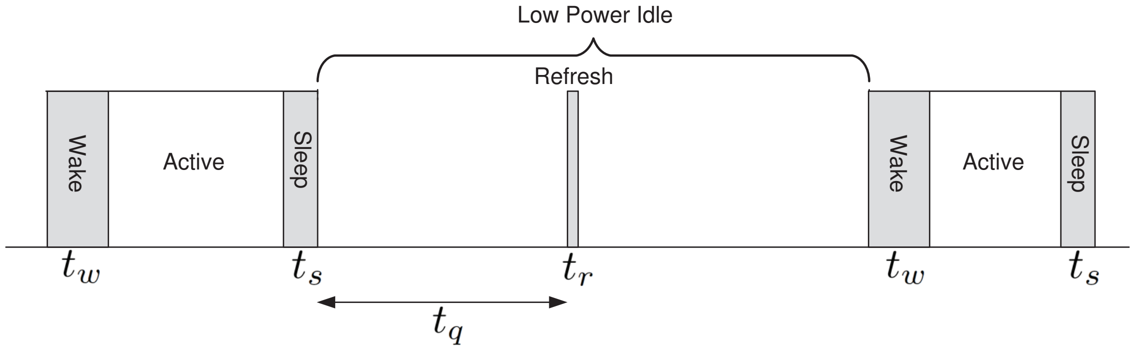

Figure 6.1: EEE 802.3az transition policy between Low Power Idle and active mode [4].

Energy Efficient Ethernet (EEE) Overhead

EEE uses the Low Power Idle (LPI) mode to reduce the energy consumption of a link. In the LPI mode, data is transmitted in the active state and the link enters the low power idle state when no data is being sent. In the idle state, short *refresh* signals are periodically sent to keep the link alive and to align the receivers with current link conditions. Fig. 6.1 illustrates the operation of EEE. Transition to the low power mode requires t_s seconds. While the device is in sleep mode, it only sends a signal for synchronization during refresh interval t_r and stays quiet during the interval t_q. When there is data available to send, the device takes t_w seconds to wake up and enter the active state again.

EEE may suffer from a significant overhead stemming from the wake time (t_w) and sleep time (t_s). For illustration, assume that a 10 Gb/s Ethernet link initially stays in sleep mode. Upon receiving an Ethernet frame of size 1500 bytes, the EEE port needs to wake up (requires t_w time), transmit the frame (requires t_{frame} time) and return to sleep mode again (requires t_s time). For 10 Gb/s Ethernet, transmission of the Ethernet frame takes 1.2 μs and the values for t_w and t_s in IEEE 802.3az standard are specified as 4.48 μs and 2.88 μs, respectively. Thus, the energy efficiency, defined as the transmission time over active time (transmission time + overhead), is about 14%. The situation is even worse in the case of TCP ACK packets (64 bytes) of duration 0.0512 μs, where the energy efficiency reduces to 0.69%. This clearly indicates the need for improvement. The challenge is to ensure the maximal use of sleep mode, thus minimizing the detrimental impact of EEE overheads.

Recently, packet coalescing has been proposed in [4] to mitigate the EEE overhead, whereby a number of packets are collected for a certain amount of time and transmitted as a burst of back-to-back packets. It improves the energy efficiency in some cases, but increases the latency in the network and degrades QoS in terms of end-to-end delays.

6.2 Photonic PBB-TE (PPBB-TE) Switches

Most of today's carriers recognize that the success of large packet networks is based on the operation and manageability of their underlying SONET/SDH transport networks. In their migration toward NGNs, carriers desire to integrate the latest packet networking technologies such as connection-oriented Ethernet and MPLS with installed optical network technologies such as WDM, reconfigurable optical add-drop multiplexer (ROADM), and optical cross-connect (OXC), giving rise to converged *Packet Optical Transport Networks (P-OTNs)* [46].

The granularity of circuit-switching ROADM and OXC at the wavelength level is too coarse to carry packet traffic efficiently. Despite different efforts such as Optical Code Division Multiple Access (OCDMA), photonic IP router, etc. it remains questionable whether integral functions of electronic IP/MPLS routers (e.g., packet header reading/writing, label swapping, or random access memory) can be done optically at comparable costs and complexity.

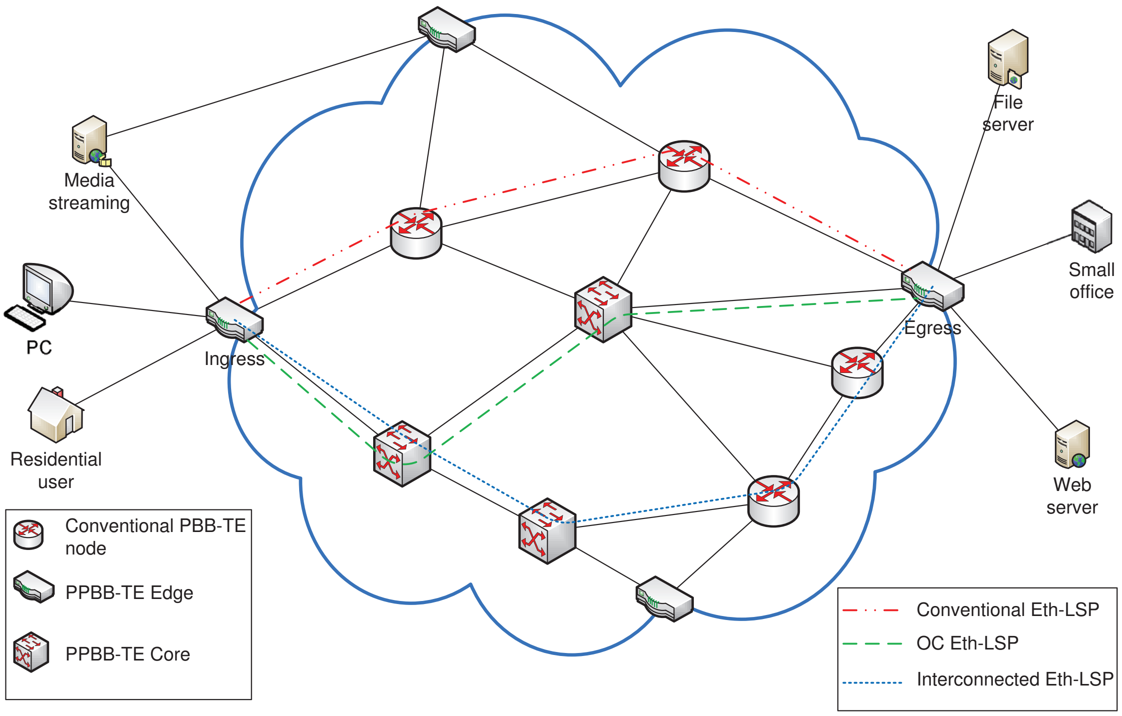

Figure 6.2: Proposed network architecture with Photonic PBB-TE (PPBB-TE) edge and core nodes supporting different types of Eth-LSP.

Carrier Ethernet switches differ from IP/MPLS routers significantly. Carrier Ethernet uses an end-to-end frame header whose fields are not changed as they pass through the switches. As opposed to IP/MPLS, PBB-TE does not deploy label swapping and Ethernet frame headers do not have a time-to-live (TTL) field that needs to be decremented at each intermediate node. At the downside, PBB-TE switches still require a forwarding table lookup for each Ethernet frame, which not only entails increased power consumption and cost but also forms a severe performance bottleneck which becomes increasingly critical for emerging Ethernet switches operating at 40 Gb/s, 100 Gb/s, or potentially even Tb/s in the future.

In this chapter, we propose a novel *Photonic PBB-TE (PPBB-TE)* switch that enhances PBB-TE switches with optical bypassing and ultra-fast label switching capabilities in conjunction with a new forwarding model that completely avoids table lookups. There are two types of PPBB-TE switches with different functionality: (*i*) edge PPBB-TE switches are located at the ingress/egress of a PBB-TE network, and (*ii*) core PPBB-TE switches are intermediate nodes within a PBB-TE network. An edge PPBB-TE switch attaches an *optical coding (OC) label* to the head of an Ethernet frame at the ingress (and removes it at the egress). The OC label consists of short optical pulses, called chips, which are generated by means of optical encoding/decoding techniques, e.g., phase and/or amplitude coding using coherent light sources [47].

A potential network scenario featuring PPBB-TE edge and core switches is illustrated in Fig. 6.2. A possibility of co-existence of PPBB-TE switches with conventional PBB-TE nodes is demonstrated in this evolutionary network architecture. It also exhibits the capability of step-by-step migration from PBB-TE to PPBB-TE networks. Three types of connections can be established between ingress and egress nodes, as demonstrated in Fig. 6.2: (*i*) connections through conventional PBB-TE switches only (conventional Eth-LSP) (*ii*) connections through PPBB-TE core switches only (OC Eth-LSP), and (*iii*) connections through both PPBB-TE core and conventional PBB-TE switches (interconnected Eth-LSP), whose control works as follows:

- **Conventional Eth-LSP:** PPBB-TE edge nodes establish this type of connection through their Ethernet ports along conventional PBB-TE core switches to reach destination egress nodes. A conventional Eth-LSP is denoted as dash-dotted line in Fig. 6.2. The establishment and control of conventional Eth-LSPs follow the extensions of GMPLS, described in Section 6.1.1.

- **OC Eth-LSP:** This type of connection is established through the optical data plane of PPBB-TE edge and core switches. PPBB-TE edge nodes (both ingress and egress) establish the connection through their associated optical ports and the connections are set up all-optically via PPBB-TE core nodes. An OC Eth-LSP is depicted as dashed line in Fig. 6.2. For the control of PPBB-TE switches and set-up of OC Eth-LSPs, we propose the following additional extensions to the GMPLS routing and signaling protocols. To advertise their capability of OC label switching, core PPBB-TE switches disseminate this information using the so-called Interface Switching Capability Descriptor available in the two GMPLS routing protocols OSPF-TE [48] and IS-IS-TE [49] and setting it to a pre-specified value that uniquely identifies the OC label switching capability of core PPBB-TE switches. Edge PPBB-TE switches may use this routing information sent by core PPBB-TE switches for explicit constraint-based routing of OC Eth-LSPs. Toward this end, we propose to extend the GMPLS signaling protocol RSVP-TE [50] as follows. To establish an OC Eth-LSP, an ingress PPBB-TE switch constructs the so-called Explicit Route Object that specifies the path across core PPBB-TE switches. Next, the ingress PPBB-TE sends an RSVP-TE Path message containing the so-called Generalized Label Request Object in which the LSP encoding type is set to value 8 to indicate photonic switching and the switching type is set to the aforementioned pre-specified value to indicate OC label switching. In addition, the RSVP-TE Path message includes the upstream OC label of the requested OC Eth-LSP in the so-called Generalized Label Object. After receiving the RSVP-TE Path message, the egress PPBB-TE switch sends an RSVP-TE Resv message containing the downstream OC label to the ingress PPBB-TE switch. The OC Eth-LSP is set up in both directions when the Resv message arrives at the ingress PPBB-TE switch. The ingress PPBB-TE switch may apply the same procedure to establish additional pre-provisioned OC Eth-LSPs to the same (for MPLS Fast Reroute (FRR) mesh restoration in the event of an OC Eth-LSP failure) or other intended egress PPBB-TE switches. Unlike the conventional Eth-LSPs, the OC Eth-LSPs are proposed to be processed all optically by fully passive devices, such as fiber Bragg gratings, and hence the label processing speed is only limited by the propagation speed of light. The number of OC Eth-LSPs is limited by the number of available OC labels. The recognition, processing and some other distinguished attributes of OC Eth-LSPs are discussed in greater detail in Section 6.2.1.

- **Interconnected Eth-LSP:** Interconnected Eth-LSPs are established from ingress to egress nodes through both PPBB-TE and conventional PBB-TE core switches. An interconnected Eth-LSP is demonstrated as dotted line in Fig. 6.2. The rationale for proposing this type of connection is to reduce any abrupt increase in CAPEX of service providers given the fact that CAPEX is one of the important factors considered by the service providers in acceptance of new technologies [45]. We propose the following extension to the GMPLS routing and signaling protocols to set up interconnected Eth-LSPs. The previously proposed GMPLS extension for OC Eth-LSPs includes the advertisement of OC label switching capability by PPBB-TE core nodes, thus edge nodes are aware of the placement of PPBB-TE core switches. Explicit constraint-based routing can be used in the set-up process of interconnected Eth-LSP with the intention that PPBB-TE core switches will be used up to their availability through the routes. Conventional PBB-TE core switches will be used in the event of unavailability of any PPBB-TE core nodes to reach the destination egress node. The set of PPBB-TE core switches and PBB-TE core switches that must be traversed along the path are considered as separate segments. Each segment can be distinguished as an abstract node [51] in the set-up process of interconnected Eth-LSP by the extended GMPLS protocol. To establish an interconnected Eth-LSP, the ingress node constructs the Explicit Route Object (ERO) comprising the abstract nodes along the path as sub-objects in ERO. The RSVP-TE Path message sent by the ingress node contains two levels of Generalized Label Request Object: one sets the encoding type to photonic (value 8) and the switching type to the pre-specified value for OC-label switching, the other one sets Ethernet (value 2) and PBB-TE as the encoding type and switching type, respectively. The RSVP-TE Path message also includes two levels of label in the Generalized Label Object: one is the upstream OC label and the other one is the tuple <Eth-LSP-MAC1, Eth-LSP-VID1>, as proposed in GELS. At the transition of an abstract node, one level of label is removed from the frames traveling along the interconnected Eth-LSP. Frames are forwarded from the optical to the Ethernet data plane and vice versa through the add/drop ports associated in the PPBB-TE core nodes. Upon receiving the Path message, the egress node will send the Resv message comprising similar labels: the downstream OC label and the tuple <Eth-LSP-MAC2, Eth-LSP-VID2>. The bi-directional interconnected Eth-LSP will be set up when the ingress node receives the Resv message from the egress node.

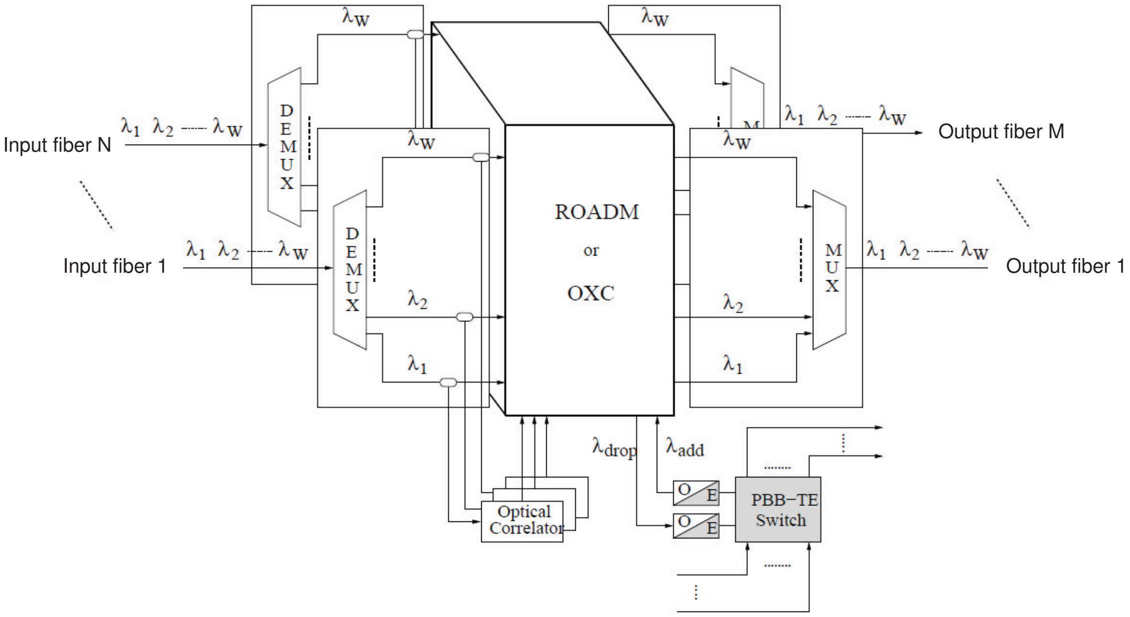

Figure 6.3: Architecture of PPBB-TE core switch.

6.2.1 PPBB-TE Core Switch

The architecture of an $N \times M$ core PPBB-TE switch is shown in Fig. 6.3. Each input/output fiber carries W wavelengths $\lambda_1, \ldots, \lambda_W$. It integrates a ROADM or OXC with a PBB-TE switch, which is able to add and drop one or more wavelengths λ_{add} and λ_{drop} by means of optical-electrical (OE) conversion, respectively. In addition, the PPBB-TE switch is equipped with an array of *optical correlators*, one for each wavelength on every input fiber of its co-located ROADM/OXC. The number of OC labels supported by each optical correlator depends on the number of desired all-optical OC Eth-LSPs per wavelength channel and constraints of current optical encoding technologies, whereby each OC label represents a different OC Eth-LSP exiting the traversed core PPBB-TE switch through a different output port. For OC label recognition, an incoming OC label is tapped off and optically replicated via optical amplification and power splitting into multiple copies. Subsequently, optical correlations between the replicated copies and each OC label is performed in parallel. The exact matching pair of copy and OC label generates an auto-correlation peak which is used to control the ROADM/OXC and switch the corresponding Ethernet frame to the appropriate output (or drop) port.

Note that the PPBB-TE core switch does not use any cumbersome optical logic operations due to the fact that PBB-TE does not require any header processing (e.g., label swapping). As a consequence, the PPBB-TE core switch requires only optical correlators which can be realized using simple, low-cost, and completely passive (i.e., unpowered) optical devices, e.g., fiber Bragg gratings [52]. More importantly, by using passive optical correlators the label processing speed is only limited by the propagation speed of light while completely avoiding costly forwarding table lookups and OEO conversions, resulting in reduced power consumption, cost, and complexity. PPBB-TE avoids the shortcomings of previously proposed solutions. Unlike [53], OC labels are attached to non-overlapping PPBB-TE Ethernet frames instead of encoding the entire frame, thus eliminating the major shortcoming (MAI) of OCDMA. PPBB-TE does not impose any constraints on the number of required OC labels, as opposed to optical correlator based photonic IP/MPLS routers [54] which require a huge number of OC labels to identify IP addresses, resulting in large splitting losses in optical correlators, and involve complex optical logic operations for rewriting TTL fields and swapping labels. Also note that PPBB-TE differs from the widely studied optical label switching (OLS) technique [55] in that PPBB-TE (i) completely eliminates costly OEO conversions of not only the payload but also the header and (ii) targets *flow switching* [56] rather than optical packet switching due to the slow switching time (microseconds to milliseconds) of current ROADM/OXCs.

6.2.2 PPBB-TE Edge Switch

PPBB-TE edge nodes are responsible for examining incoming traffic, detect and classify traffic flows, aggregate traffic if necessary and forward it to appropriate output ports. PPBB-TE edge nodes include two types of output ports: one (1 to m in Fig. 6.5) is associated with the optical domain and the other type ($m + 1$ to n in Fig. 6.5) is Ethernet ports, more precisely EEE ports which are connected to conventional PBB-TE nodes in the network. PPBB-TE edge nodes consist of the following four major components to perform the above mentioned functions as illustrated in Fig. 6.5.

- **Flow detection, classification, and aggregation:** To leverage the proposed network architecture with PPBB-TE nodes, we propose to use a flow switching model since flow switching relieves switching overheads in core nodes as opposed to packet switching [56]. Thus, each PPBB-TE edge node contains a flow detection module. The flow detection module determines whether the incoming traffic is a new flow or belongs to an existing flow. Each flow is characterized based on <B-SA, B-DA, I-SID> frame headers. Existing flow identifiers are stored in a hash table that may contain the hashed flow identifier, mapped OC label and the designated output port for the identified flow as depicted in Fig. 6.4. Once an OC Eth-LSP is established through the extended RSVP-TE of GMPLS, identified flows can be dispatched for transmission.

- **OC label mapper:** For identified flows that are transmitted through the optical data plane, an OC label is attached to the header of the Ethernet frames. The forwarding table of edge nodes needs to be populated by the

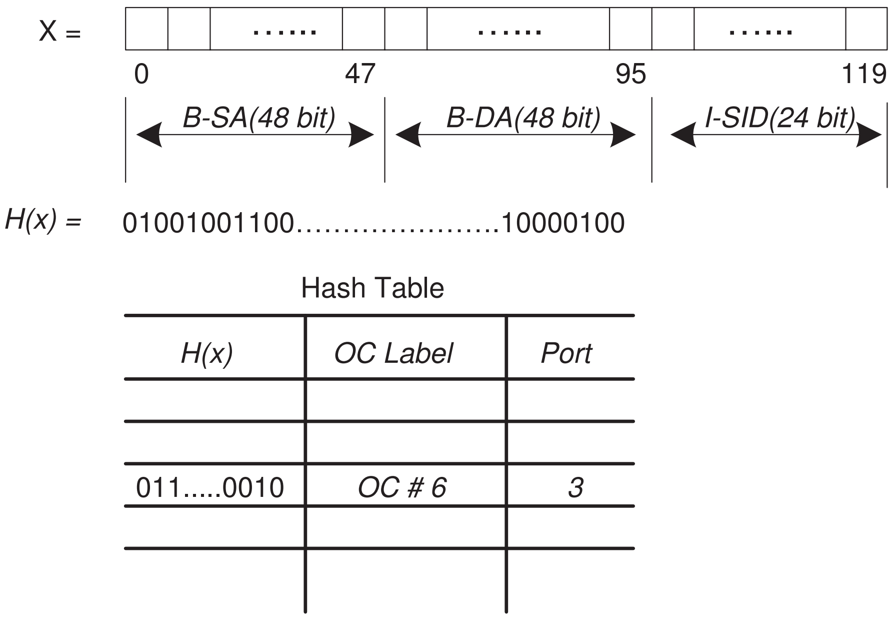

H(x)	OC Label	Port
011.....0010	OC # 6	3

Figure 6.4: Hash Table

flow identifiers and the assigned OC labels. The core PPBB-TE nodes will forward the flows according to the attached OC labels. The OC label mapper module is responsible for assigning an OC label to each aggregated flow. It also includes the E/O transponders. One of the challenges in mapping and generating OC labels is the number of available OC labels which are limited. The number of bits to be encoded in OC labels are limited. Also the signal power loss in the splitters that are used in PPBB-TE core nodes limits the number of OC labels. The scalability of OC labels can be partly reduced by multiplexed OC label processing [57] in point-to-multipoint transmission. Multicast video traffic, which is one of the dominant traffic types in current network, is one of the beneficiary of flow switching. In case of such multicast or point-to-multipoint transmission, the required number of OC labels can be reduced from 2^n to n by multiplexed label processing [57] where n in the number of nodes in the

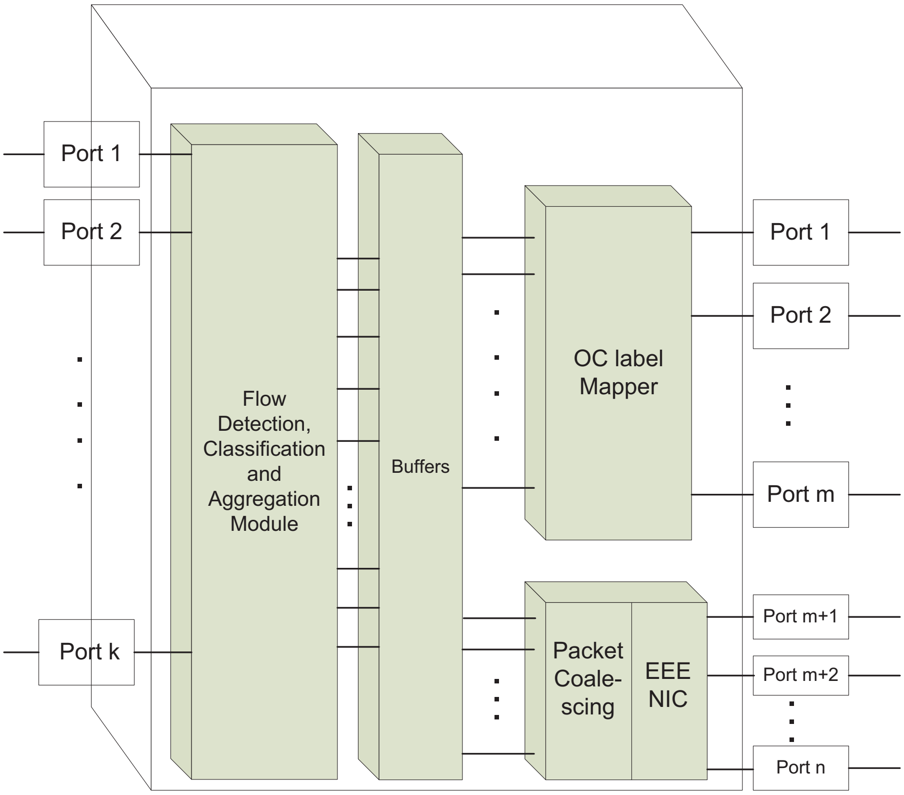

Figure 6.5: Architecture of PPBB-TE edge switch.

network.

- **EEE network interface card and packet coalescing:** This module is the interface to the Ethernet data and control plane. The Ethernet ports that are used in this module are EEE enabled. Packet coalescing, proposed in [4], is applied to improve the efficiency of EEE ports in terms of energy consumption and to reduce the impact of EEE overheads.

Since the PPBB-TE core nodes use fully passive components (optical correlators) to forward traffic, it is preferable to transmit as many flows through optical switches as possible. This approach leads to less overall power consumption in the network. The decision of how many traffic flows to transmit through the optical or electronic domain is an open issue and needs more elaboration. It may result in some Ethernet ports enter the sleep mode. Besides, the decision to put Ethernet ports into the sleep mode needs to be taken carefully due to the transition overhead associated with it. We address this problem of EEE transition overhead in Section 6.3.

6.3 Energy-Aware scheduling

The recent standard IEEE 802.3az EEE enhance the usability of Ethernet networks by being more energy efficient. However, EEE may suffer from a significant overhead stemming from the wake time (t_w) and sleep time (t_s) without a suitable scheduling of incoming frames which will impact on overall energy consumption (see Section 6.1.2 for further detail). Packet coalescing [4] as proposed lacks an efficient mechanism for scheduling the transmission times of Ethernet frames; that is, properly selecting the active intervals during which the frames will be transmitted on each port. Recall that in packet coalescing, a transmission timer is essentially set for each port; once this timer expires, all packets which have accumulated so far will be bursted out at line speed. Indeed, the selection of the timer plays a critical role in trading off the power consumption of the port and the delay experienced by the frames at each port. Hence, scheduling the activation events of the ports will be crucial in reducing power consumption as well as guaranteeing quality-of-service (QoS) in the network, in terms of end-to-end delay that frames will experience. Next, we present an illustrative example to explain the importance of scheduling in greater detail.

6.3.1 Illustrative Example

We consider a simple instance where five frames $f_1,\ f_2,\ f_3,\ f_4,$ and f_5 of different sizes with various delay thresholds arrive at times 3, 5, 8, 9, and 10 respectively (see Table 6.1). Table 6.1 presents other parameters used in this illustrative example, such as the size and delay requirement for each frame and transmission time of frames. The transmission time of a frame is computed under the assumption of a link rate of 10 Gb/s. For illustrative purpose, we assume two EEE ports (p_1 and p_2) are available to transmit these frames.

Frames	f_1	f_2	f_3	f_4	f_5
Arrival (unit time)	3	5	8	9	10
Size (Bytes)	1500	1500	1250	1250	750
Transmission time (μsec) assuming 10 Gb/s link	1.2	1.2	1	1	0.6
Delay (unit time)	7	6	6	3	3

Table 6.1: Parameter values

Fig. 6.6 demonstrates two different but possible scheduling alternatives that can be adopted, which work as follows. Fig. 6.6(a), referred to as Scheduling 1, assumes that the timer expires at time instant 9. At this time, frames $f_1,\ f_2,$ and f_3 are in the buffer and will start their transmission through port p_1. Thus, port p_1 will be in busy state from time 9 to 12.4 while transmitting frames $f_1,\ f_2,$ and f_3, as depicted in Fig. 6.6(a)-(ii). When frame f_4 arrives at time 9 with delay threshold 3, this frame (f_4) must be transmitted at time instant 12 the latest. Since p_1 is in busy state until time 12.4, the scheduler needs to activate port p_2 to transmit f_4 and satisfy its delay requirement. Next, frame f_5 arrives at time 10 and can be transmitted through either port p_1 or p_2. A possible scenario of transmission of frames f_4 and f_5 is presented in Fig. 6.6(a)-(iii). An alternative scenario for scheduler 1 is to transmit frame f_4 at time 9, subsequently followed by frame f_5 through port p_2, as shown in Fig.

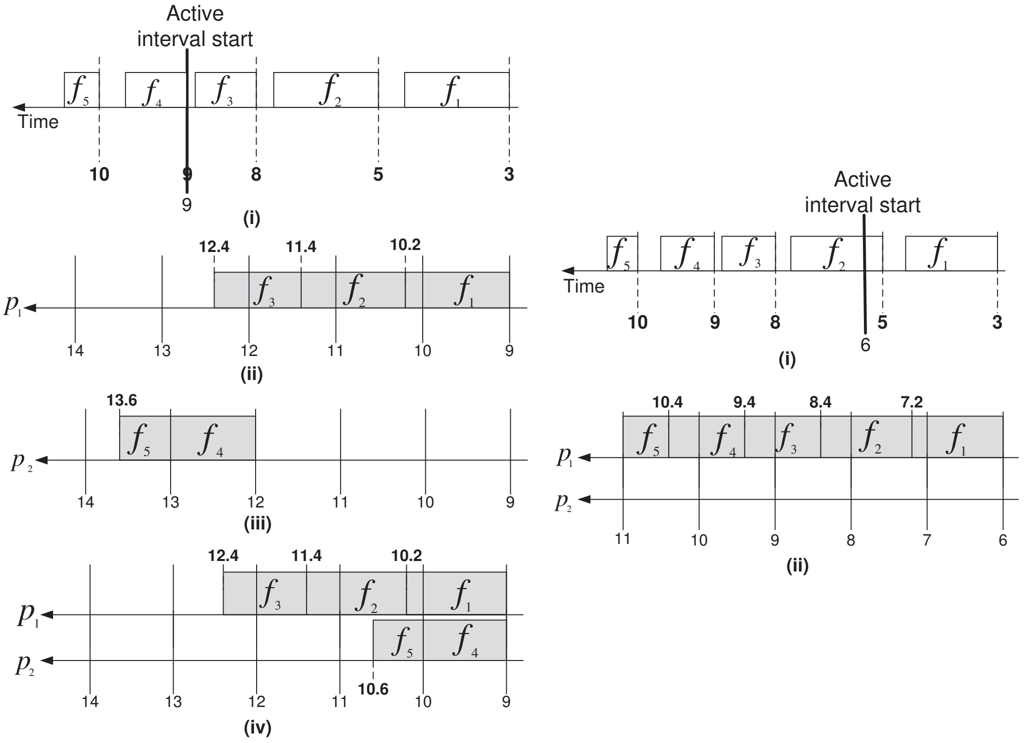

(a) Scheduling 1

(b) Scheduling 2

Figure 6.6: Scheduling options for a simple instance.

6.6(a)-(iv) to reduce the average delay of those frames. Notice that in both cases, scheduling 1 requires the activation of two ports. Fig. 6.6(b) illustrates an alternative schedule, referred to as Scheduling 2, where port p_1 is activated at time instance 6 to transmit frames f_1 and f_2. When frame f_3 arrives at time 8, it is scheduled at time 8.4 on the same port p_1. Similarly, frames f_4 and f_5 are scheduled for transmission on port p_1 at time instance 9.4 and 10.4 respectively, as depicted in Fig. 6.6(b)-(ii). Clearly, this transmission schedule is able to transmit all frames within their deadlines using only one port, while keeping the second port p_2 in LPI mode and thus conserving more energy. It is therefore clear that efficiently deciding the transmission schedules is key to reduce energy consumption while meeting the delay requirements of the traffic. Next, we present a mathematical model that achieves this objective.

6.3.2 Problem Formulation

In this section, we formulate the problem of energy-aware scheduling of Ethernet frames as a Mixed Integer Linear Program (MILP); the MILP determines the optimal transmission schedule at the ports, which both guarantees the delay requirement of the incoming frames and reduces the energy consumption by minimizing the period of active time of the ports. For the purpose of our model, we assume the knowledge of the traffic profile at each port; that is, the total number of frames F, the size of each frame z_f (bytes), and their arrival times are also assumed to be known in a window of time W. We further assume that the frames should be scheduled using a certain number of active intervals at each port and we let I be the maximum number of intervals required for completing the transmission of all the frames. Each frame has its own delay threshold parameter d_f and thus needs to be transmitted before d_f. Let us assume that the number of available EEE ports is P, each with the capacity of C_p (bps). Let $x_f^{p,i}$ be a binary variable, which denotes whether frame f is scheduled for transmission during an active interval i on port p ($x_f^{p,i} = 1$) or not ($x_f^{p,i} = 0$). Similarly, let y_p^i be a binary variable denoting whether port p is turned on during active interval i ($y_p^i = 1$) or not ($y_p^i = 0$). s_p^i and e_p^i are the start and end times of active interval i of port p, respectively. r_f is the release time of frame f. The other variables are defined as follows.

tr_p^i : Transmission time in active interval i on port p.

t_p^{active} : Total active duration of port p in time window W.

δ_{on} : Unit energy consumption of a port when it is on.

t_w : Wake-up time of a port. The value is 4.48μs for 10 Gb/s Ethernet in IEEE standard 802.3az [4].

δ_w : Unit energy consumption of a port while waking up.

t_s : Sleep transition time of a port. The value is 2.88μs for 10 Gb/s Ethernet in IEEE standard 802.3az [4].

δ_s : Unit energy consumption of a port while going to sleep.

t_p^{idle} : Total idle duration of port p in time window W.

δ_{idle} : Unit energy consumption of a port when idle. It can be as low as 10 percent of δ_{on} [4].

E_p : Total energy consumption of port p in time window W.

The objective of our model is to minimize the energy consumption when transmitting all the frames backlogged at each port p during a period of time W.

$$\mathit{\mathbf{Min}} \sum_{p=1}^{P} E_p \tag{6.1}$$

s.t.

$$E_p = t_p^{idle} \times \delta_{idle} + \sum_{i=1}^{I} [y_p^i \times (t_w \times \delta_w + t_s \times \delta_s) + tr_p^i \times \delta_{on}] \tag{6.2}$$

$$t_p^{idle} = W - t_p^{active} \tag{6.3}$$

$$t_p^{active} = \sum_{i=1}^{I} [y_p^i \times (t_w + t_s) + tr_p^i] \qquad \forall p \tag{6.4}$$

Constraint (6.2) represents the energy consumption per port p taking into account the total idle time and active period during the whole scheduling period consisting of all intervals I, where (6.3) and (6.4) determine the idle and active period at port p.

$$\sum_{p=1}^{P} \sum_{i=1}^{I} x_f^{p,i} = 1 \qquad \forall\, f \tag{6.5}$$

$$x_f^{p,i} \leq y_p^i \qquad \forall\, f, p, i \tag{6.6}$$

Constraints (6.5) and (6.6) ensure that each frame is transmitted at most once through an active port. More precisely, constraint (6.5) determines that a frame f must be scheduled on only one port during only one active interval. Constraint (6.6) will activate a port p if a frame is scheduled on that port.

$$r_f \geq a_f \quad \forall\, f \tag{6.7}$$

$$r_f - a_f \leq d_f \quad \forall\, f \tag{6.8}$$

$$r_f \leq s_p^i + M(1 - x_f^{p,i}) \quad \forall\, f, p, i \tag{6.9}$$

$$r_f \geq s_p^i - M(1 - x_f^{p,i}) \;\; \forall\, f, p, i \tag{6.10}$$

Constraints (6.7) to (6.10) define the boundary conditions of release time of a frame and the delay threshold of the frame is guaranteed by Equation (6.8). M is a large constant.

$$s_p^i \leq e_p^i \tag{6.11}$$

$$e_p^i - s_p^i = tr_p^i \tag{6.12}$$

$$tr_p^i \geq (\sum_{f=1}^{F} x_f^{p,i} \times z_f)/C_p \tag{6.13}$$

$$tr_p^i \leq M(y_p^i) \tag{6.14}$$

$$e_p^i \leq W \qquad\quad \forall p, i \tag{6.15}$$

Constraints (6.11) to (6.15) define the duration and bound of active intervals of each port. The duration of an active interval is estimated by the required transmission time of the frames that are scheduled for transmission during that interval. Constraint (6.16) imposes a minimum space between two consecutive active intervals of port p.

$$s_p^i - e_p^j \geq t_s + t_w - M(1 - y_p^i) - M(1 - y_p^j) \qquad \forall\, p \;\; and\; j < i \tag{6.16}$$

6.3.3 Sequential Fixing

The mathematical formulation of energy aware scheduling is clearly a combinatorially complex decision problem and does not scale for larger problem instances. To reduce the running time, we develop and implement a heuristic based on Sequential Fixing approach (SF). In our model, the binary variable $x_f^{p,i}$ indicates whether the port p is used by the frame f in time interval i. In our sequential fixing method, we relax the integrality of $x_f^{p,i}$ ($x_f^{p,i} \in [0,1]$) and solve the corresponding modified MILP model. For each frame f, we find the maximum value of $x_f^{p,i}$ and identify the value of corresponding p and i, which indicates the port and interval number, respectively. We fix the value of that particular $x_f^{p,i}$ to 1 and solve the modified model. If a feasible solution can be reached by this modification, the heuristic moves forward to the next frame. Otherwise, the value of $x_f^{p,i}$ is set to 0 and the model is solved. This process continues as long as the heuristic finds a feasible solution for current frame. The heuristic iterates until the values of $x_f^{p,i}$ turn into binaries.

6.4 Numerical Results

The authors of [58] and [4] evaluated the performance of EEE and packet coalescing on EEE ports. They showed that EEE can significantly reduce the

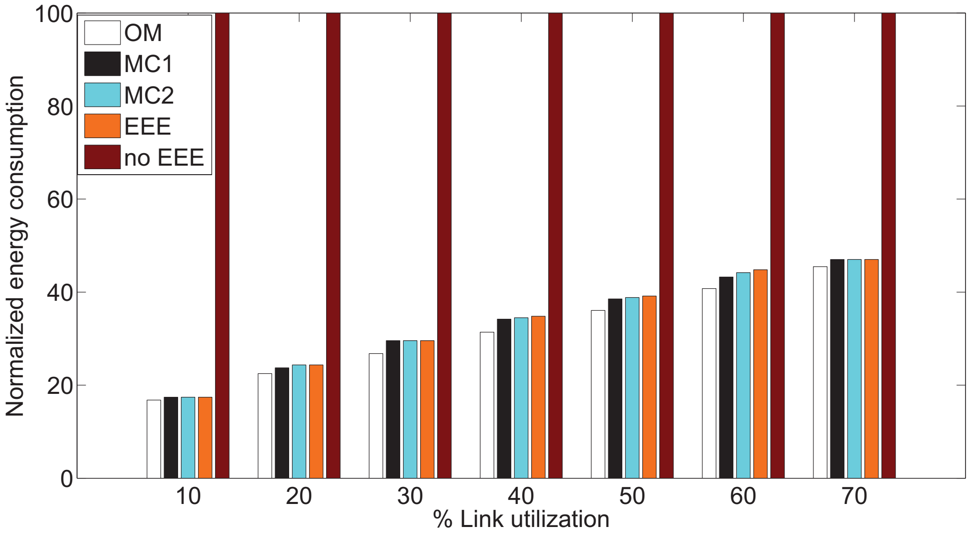

Figure 6.7: Energy consumption vs. link utilization

energy consumption of conventional Ethernet links and packet coalescing decreases the EEE overhead and thus reduces the energy consumption further. However, the energy efficiency is achieved in packet coalescing at the expense of an increased end-to-end delay. In this section, we evaluate the performance of our energy-aware optimal scheduling model. The objective is to compare the optimal results to the results achieved in [58] and [4]. The proposed energy-aware scheduling model is implemented in C++ and solved using CPLEX Concert Technology.

6.4.1 Comparison of MILP with existing approaches

Conventional Ethernet referred to as "no EEE" operates at maximum power all the time and thus consumes 100% of energy, regardless of the link utilization. In EEE, a link becomes active upon the arrival of a frame and enters the LPI mode when there is no frame to transmit. For fair comparison, the heuristic of packet coalescing [4] is modified to incorporate delay thresholds of the frames, referred to as “MC”. In addition to the timer and frame counter, MC activates the link as soon as the delay threshold of a frame is about to expire and transmits the accumulated frames. The energy-aware optimal scheduling model is referred to as “OM”. The heuristic with relaxed model is referred to as “SF”. γ represents the link utilization in percentage. All the experiments are performed on a 1 Gb/s Ethernet link and frames are assumed to arrive at the incoming link according to a Poisson process. We assume that the power consumption of EEE in LPI mode be 10 percent of that in the active mode specified in IEEE standard 802.3az. We further assume that EEE consume 90 percent of the active energy during its transition from active to LPI or LPI to active mode.

Fig. 6.7 demonstrates the normalized energy consumption of EEE over a range of link utilization. Two blocks labeled as MC1 and MC2 show the results for MC with timer set to 3 μs and frame counter set to 2 frames, and with timer set to 5 μs and frame counter set to 4 frames, respectively. The delay thresholds and size of the frames are generated randomly with mean value of 115 μs and 1250 bytes, respectively. The figure clearly shows that the model yields minimum energy consumption comparing to MC1, MC2 and EEE all achieving close performance. This indeed shows that the proposed concepts (Packet coalescing and EEE) are promising approaches for deployment in backbone switches to reduce energy consumption. It is to be mentioned that these performances are obtained for fewer number of frames; this is due to the prohibitively large running time of the optimization model with larger number of frames. However, we expect that performance will change as we increase the load.

Table 6.2 presents the average delay(μs) of the transmitted frames versus

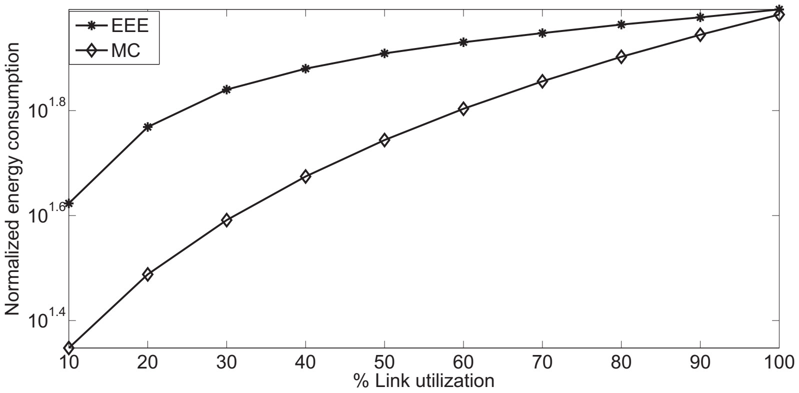

Figure 6.8: Energy consumption vs. link utilization

link utilization. In terms of delay performance, we note that all frames are scheduled within their delay requirements in all methods. The model however resulted in larger delays since our objective is simply to minimize energy consumption. EEE, as opposed to MC, results in better delay performance in both (fewer and larger number of frames) cases. Please note, however, that the frame delays are measured in micro-seconds and hence these increases remain acceptable and comparable.

γ	Average Delay (μs)					
	OM	SF	MC1	MC2	EEE	No EEE
10	63.25	37.62	15.38	9.080	4.88	0.0
20	51.93	29.75	16.02	9.274	5.85	0.97
30	55.29	44.54	15.76	9.418	4.82	0.42
40	64.95	62.84	16.18	9.720	6.04	1.71

Table 6.2: Avg. delay vs. link utilization

Fig. 6.8 presents the performance evaluation of EEE and MC with larger amount of frames which exhibits that MC yields substantial performance improvement (reduction in energy up to 47.6% in some cases) over EEE. This is consistent with the findings of [58] and provides the reasoning of our expectations. However, both of their performance traces predictably converge at excessive link utilization (100%). This is because, in high utilization, frames arrive very near to each other and mostly merge to the transmission time of each other, thus, reduces the number of EEE transition from one mode to other.

6.4.2 Optimization model and sequential fixing

To overcome the limitations of expensive running time of the model, we develop a heuristic as explained in Section 6.3.3. Fig. 6.10 compares the energy consumption achieved by OM and the heuristic SF. Fig. 6.9 presents the CPU time required to execute OM and SF with various link utilizations. The results show a substantial decrease in running time by the SF especially after 40% of link utilizations. However, the results of the objective function, i.e., energy consumption achieved by the SF is very near to the optimal values achieved by the OM. More precisely, 7 out of 10 instances achieved the optimal results by SF as presented in Fig. 6.10. The rest of the three instances are 0.6% to 1% apart from the optimal results. Thus SF can be a legitimate alternative of OM which can provide the opportunity to evaluate the performance in larger instances.

6.4.3 Impact of frame delay and sizes on the energy consumption

We further study the impact of delay and frame size in energy consumption and thus execute the experiments with SF by varying the delays and frame sizes as presented in Figs 6.11, 6.12, and 6.13. Four different delay ranges (50-70)μs, (70-90)μs, (90-110)μs, and (110-130)μs are examined in various link utilizations. Frame sizes are varied between (500-1000)bytes, (1000-1500)bytes, and (1500-2000)bytes in various link utilizations. Please note that, though the maximum size of Ethernet frames are 1500 bytes, we intentionally increase

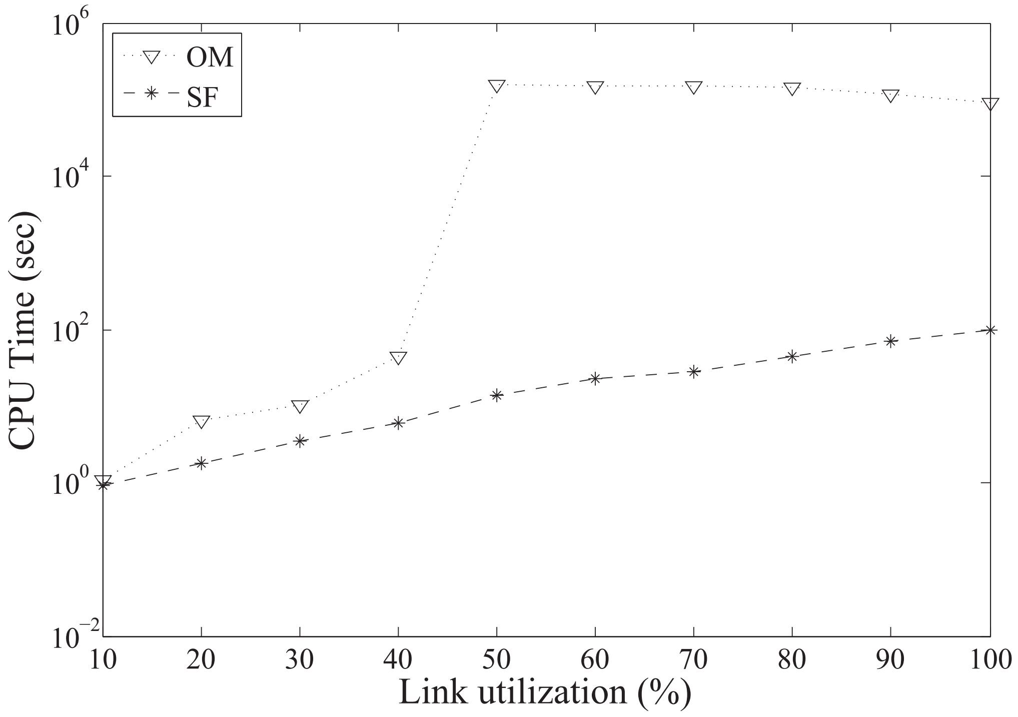

Figure 6.9: CPU time of OM vs. SF

the size of the frames over 1500 bytes[1] to observe the effect on energy consumption. It is trivial to predict that the energy consumption will be higher for larger frame sizes because of the longer transmission times. However, this should not be considered as a downside and more importantly energy efficiency need to be observed in this case. Energy efficiency (η) can be defined as the transmission time over total active time, i.e., (transmission time + EEE transition overhead). The higher value for energy efficiency indicates more energy is used in actual data transmission and less energy is consumed during EEE mode transition.

Fig. 6.11 presents the unit energy consumption of four delay variations. Since the tighter delay bound may force the scheduler to activate more ports,

[1] Although this exceeds the maximum size of Ethernet frames.

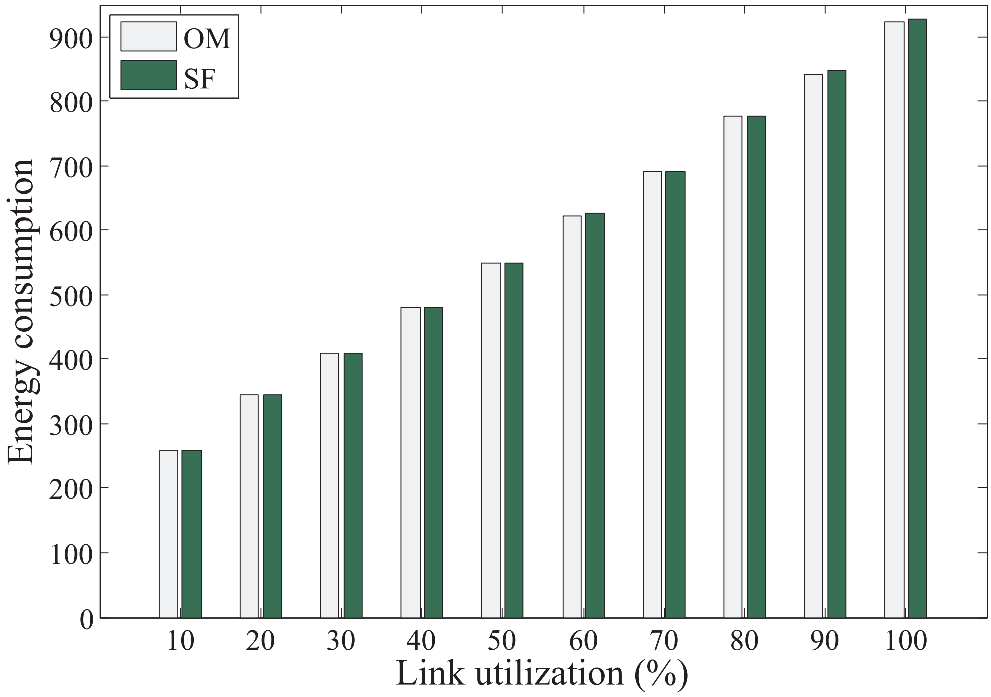

Figure 6.10: Energy consumption of OM vs. SF

understandably the results in Fig. 6.11 show that an increase in delay requirements can reduce energy consumption. Fig. 6.12 and 6.13 illustrates the comparisons of unit energy consumption and energy efficiency of three variations of frame sizes in different link utilizations. Predictably increase in frame size results in more energy consumption as presented in Fig. 6.12. However, the more interesting observation is that higher energy efficiency is achieved by increasing frame sizes as presented in Fig. 6.13, which states that energy is consumed more efficiently in larger frame sizes and desirably more energy is consumed in active data transmission over EEE overhead with larger frame sizes.

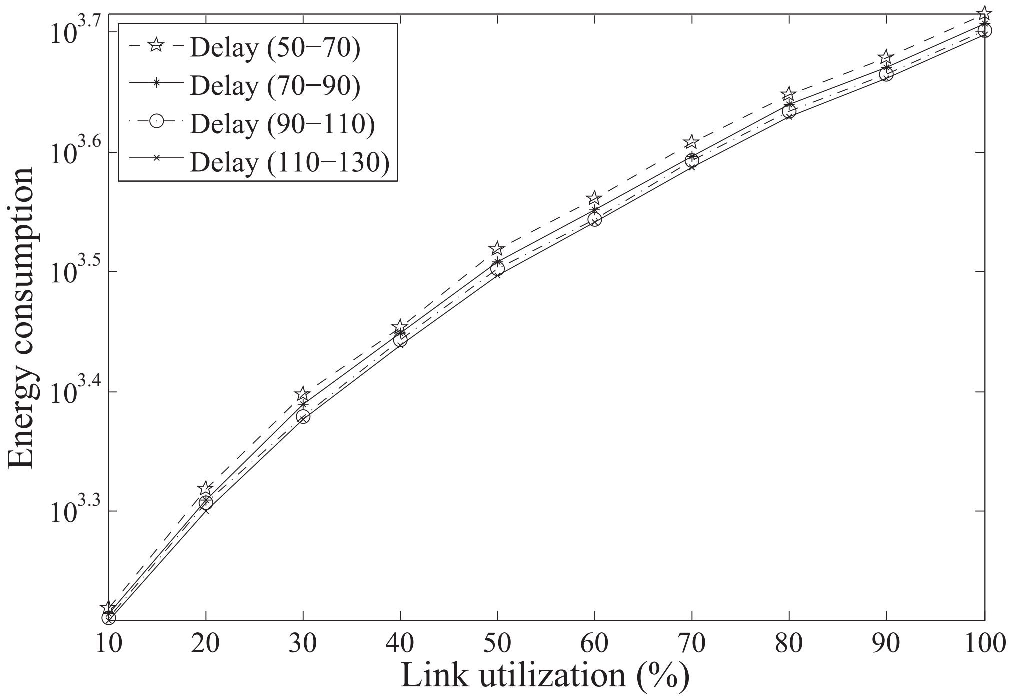

Figure 6.11: Energy consumption with varying delay range

6.5 Chapter remark

The ratification of the IEEE 802.1Qay PBB-TE increases the suitability of Ethernet in carrier transport networks. The new IEEE 802.3az Energy Efficient Ethernet will certainly help the service providers to proceed towards green transport networks. Photonic PBB-TE switches can increase the usability of PBB-TE networks further and can reduce power consumption by leveraging EEE. The proposed energy-aware scheduling optimization model provides a benchmark of energy efficiency and the heuristic with relaxed model can be greatly helpful to analyze the trade-offs between energy efficiency and latency in the networks. In this chapter, we studied the trade-off with guaranteed frame transmission within its delay requirement and the effect of various parameters such as delay range and frame sizes on energy consumption. It is evidenced from experimental results that lower delay tolerant traffic consume

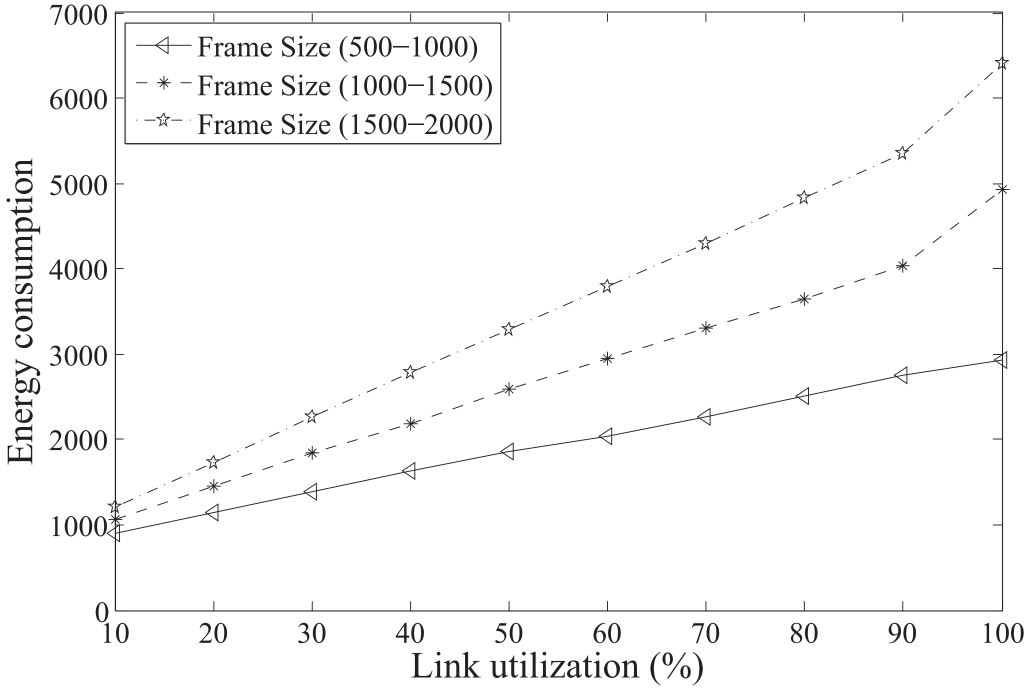

Figure 6.12: Energy consumption with varying frame size

up to 5% more energy than that of flexible traffic and the larger frames consume energy up to 31% more efficiently.

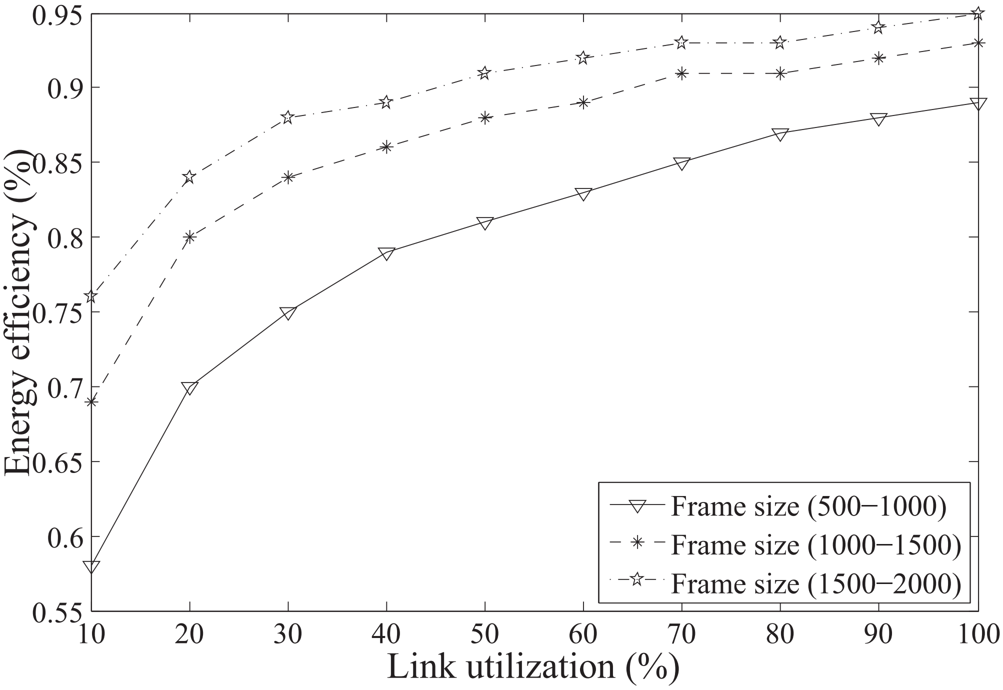

Figure 6.13: Energy efficiency with varying frame size

Chapter 7

Conclusion and Future Directions

7.1 Conclusions

This thesis addressed two important design aspects of carrier Ethernet networks, namely, (i) survivable Ethernet transport networks design using a fast restorable protection mechanism and (ii) design of a green Ethernet transport network using Energy Efficient Ethernet (EEE).

We first presented a survivable network design approach for Ethernet transport networks using Ethernet Ring Protection (ERP) protocol. We identified some subtle limitations of prior work which used a computationally expensive exhaustive enumeration approach for determining the best RPL locations and the best ring hierarchies. We then developed a modified routine to overcome those limitations. We developed an ILP model for optimal resource allocation in single ring networks as well as in multi-ring mesh networks by properly selecting the RPL placements and ring hierarchies. Unlike that prior work which sequentially selects the ring hierarchy and the RPL location one after another, our model jointly determine the RPL placements and the ring hierarchies while minimizing the capacity requirements. In this work, the network is designed to survive against any single link failure only.

We then extended our ERP-based network design approach by considering concurrent dual link failures scenarios. We showed that network services may suffer two types of service outages due to concurrent dual link failures in an Ethernet network which is protected by ERP protocol. One is for network partitioning (physical/logical) which we referred to as category-1 outages and category-2 outages are referred to as the service outages that are suffered from lack of capacity. First, we developed an optimization model to minimize the category-1 service outages by efficient selection of the RPL placements and ring hierarchies. We also developed a routine to estimate the additional capacity requirement to eliminate category-2 outages. This two-step approach cannot guarantee optimal capacity allocation. We formally proved that a network designed with the objective of maximizing network flows ultimately minimizes both categories of service outages caused by dual link failures. Then we developed another optimization model which jointly minimizes both categories of service outages by maximizing network flows while minimizing capacity requirements.

We then presented the ERP-based mesh networks design from a different perspective which is more practical from network operators point of view, i.e. traffic engineering approach. We mathematically formulated the ERP design problem for a network with fixed capacity with the objective of fair distribution of network resources among the given traffic sessions, hence avoiding congestion in some parts of the network while other parts remained under-utilized. Then, we exploited one of the advantageous features of ERP protocol which is the ability to deploy multiple logical ERP instances over a single physical ring. We developed a design model which provides the best possible set of ERP instances to be implemented with their RPLs and ring hierarchies.

Finally, we presented a carrier Ethernet network architecture which is expected to be energy efficient. We designed the architectures of two novel Ethernet switches: the core switch is equipped with passive optical correlators for optical packet bypassing and the edge switch is equipped with newly standardized Energy Efficient Ethernet (EEE) ports. We then developed an optimization model to minimize energy consumption in EEE ports by efficient scheduling of Ethernet frames. The scheduling problem turned out to be a combinatorially complex problem and thus unsolvable for large number of frames. Thus, we developed a heuristic based on sequential fixing technique and obtained very near to optimal solutions in faster time.

7.2 Future Work

The work presented in this thesis provided considerable amount of insight for survivable Ethernet transport network design using the promising ERP protocol. However, there remain several future research works of immense interest, especially in the context of newly emerging data-center networks.

The design strategies of ERP-based mesh networks that are presented in this thesis considered only E-line services or point-to-point Ethernet virtual connections. However, E-tree services and point-to-multipoint virtual connections are more suitable for providing emerging data-center services. Hence, in order to provision protection plans using ERP for data-center based networks require particular attention and further research.

The design strategies of this thesis, in particular the design model for multiple ERP instances requires further research to improve its scalability. Large scale optimization methods or efficient meta-heuristic methods might be helpful to make the model more scalable.

In this thesis, we only considered simple physical rings of mesh networks to configure single or multiple ERP instances. However, further research could be performed to investigate the benefit of considering all possible physical rings and then select the best set of physical rings to implement ERP. This research direction has immense potential to improve the performance of ERP dramatically.

Bibliography

[1] MEF, “Carrier Ethernet Services Overview.” [Online]. Available: http://www.metroethernetforum.org/PPT_Documents/Reference-Presentation%s/Nov-2011/Carrier-Ethernet-Services-Overview-Reference-Presentation-R03-2011-11-15.ppt%x

[2] D. Allan, N. Bragg, A. Mcguire, and A. Reid, “Ethernet as carrier transport infrastructure,” *IEEE Communications Magazine*, vol. 44, no. 2, pp. 95 – 101, feb. 2006.

[3] ITU-T Rec. G.8032/Y.1344, “Ethernet ring protection switching,” 2012.

[4] K. Christensen *et al.*, “IEEE 802.3az: The Road to Energy Efficient Ethernet,” *IEEE Communications Magazine*, vol. 48, no. 11, pp. 50 –56, Nov. 2010.

[5] Infonetics Research, “Service providers capitalize on Ethernet and IP MPLS VPN services,” Jul 2011.

[6] ——, “Service Provider Plans for Metro Optical and Ethernet: North America, Europe, and Asia Pacific 2007,” Sep 2007.

[7] IEEE, “IEEE Standard for Local and metropolitan area networks: Media Access Control (MAC) Bridges,” *IEEE Std 802.1D-2004 (Revision of IEEE Std 802.1D-1998)*, pp. 1–277, 9 2004.

[8] ——, “IEEE Standards for Local and Metropolitan Area Networks— Virtual Bridged Local Area Networks— Amendment 3: Multiple Spanning Trees,” *IEEE Std 802.1s-2002 (Amendment to IEEE Std 802.1Q, 1998 Edition)*, pp. 1–211, 2002.

[9] ——, “IEEE Standard for Local and Metropolitan Area Networks - Common Specification. Part 3: Media Access Control (MAC) Bridges - Amendment 2: Rapid Reconfiguration,” *IEEE Std 802.1w-2001*, 2001.

[10] K. Fouli and M. Maier, “The Road to Carrier-Grade Ethernet,” *IEEE Communications Magazine*, vol. 47, no. 3, pp. S30–S39, Mar 2009.

[11] A. KIRSTÄDTER, C. GRUBER, J. RIEDL, and T. BAUSCHERT, “Carrier-grade ethernet for packet core networks,” in *Proceedings of SPIE, the International Society for Optical Engineering*. Society of Photo-Optical Instrumentation Engineers, 2006.

[12] MEF, “service provider study: Operating expenditures”.” [Online]. Available: ”http://metroethernetforum.org/PDF_Documents/Provider-Business-Case-OpEx-Study-Summary_old.pdf”

[13] M. Huynh and P. Mohapatra, “Metropolitan ethernet network: A move from lan to man,” *Computer Networks*, vol. 51, no. 17, pp. 4867 – 4894, 2007.

[14] A. Kern, I. Moldovan, and T. Cinkler, “Bandwidth guarantees for resilient ethernet networks through rstp port cost optimization,” in *International Conference on Access Networks Workshops*, Aug. 2007, pp. 1 –8.

[15] M. Marchese, M. Mongelli, and G. Portomauro, “Simple protocol enhancements of rapid spanning tree protocol over ring topologies,” in *IEEE GLOBECOM*, Dec. 2010, pp. 1–5.

[16] E. Bonada and D. Sala, “Rstp-sp: Shortest path extensions to rstp,” in *International Conference on High Performance Switching and Routing*, Jun 2012, pp. 223 –228.

[17] G. Ibanez, A. Garcia, and A. Azcorra, “Alternative multiple spanning tree protocol (amstp) for optical ethernet backbones,” in *IEEE International Conference on Local Computer Networks*, nov. 2004, pp. 744 – 751.

[18] A. De Sousa, “Improving load balance and resilience of ethernet carrier networks with ieee 802.1s multiple spanning tree protocol,” in *International Conference on Systems and Networking*, Apr. 2006, p. 95.

[19] A. Meddeb, “Multiple spanning tree generation and mapping algorithms for carrier class ethernets,” in *IEEE GLOBECOM*, Dec. 2006, pp. 1 –5.

[20] H. T. Viet, Y. Deville, O. Bonaventure, and P. Francois, “Traffic engineering for multiple spanning tree protocol in large data centers,” in *International Teletraffic Congress (ITC)*, Sept. 2011, pp. 23–30.

[21] M. Fine, S. Gai, and K. McCloghrie, “Shared spanning tree protocol,” Feb 2001, uS Patent 6,188,694.

[22] J. Im, J. Ryoo, and J. Rhee, “Managed FDB algorithm and protection in ethernet ring topology,” in *Joint International Conference on Optical Internet and Australian Conference on Optical Fibre Technology*, June 2007, pp. 1 –3.

[23] K. Lee, J.-K. Rhee, S. Yoo, and P. Cho, “Flush optimization in ethernet ring protection network,” in *International Conference on ICT Convergence*, Sept. 2011, pp. 513 –514.

[24] K. Lee, J. Ryoo, and S. Min, “An Ethernet ring protection method to minimize transient traffic by selective FDB advertisement,” *ETRI journal*, vol. 31, no. 5, pp. 631–633, 2009.

[25] J. Rhee, J. Im, and J. Ryoo, “Ethernet ring protection using filtering database flip scheme for minimum capacity requirement,” *Etri Journal*, vol. 30, no. 6, pp. 874–876, 2008.

[26] K. Lee, C. Lee, and J. Ryoo, “Enhanced protection schemes to guarantee consistent filtering database in Ethernet rings,” in *IEEE GLOBECOM*, Dec. 2010, pp. 1 –6.

[27] D. Lee, J.-K. Rhee, K. Lee, and P. Cho, “Efficient Ethernet multi-ring protection system,” in *International Workshop on Design of Reliable Communication Networks*, Oct. 2009, pp. 305 –311.

[28] D. Lee, K. Lee, S. Yoo, and J.-K. Rhee, “Efficient ethernet ring mesh network design,” *Journal of Lightwave Technology*, vol. 29, no. 18, pp. 2677 –2683, Sept. 15 2011.

[29] K.-k. Lee, J.-d. Ryoo, S. H. Kim, and D. Kim, “An optimal Ring-Protection-Link positioning algorithm in carrier Ethernet ring networks,” *IEEE Communications Letters*, vol. 16, no. 8, pp. 1332 –1335, Aug 2012.

[30] K. Lee, D. Lee, H.-w. Lee, N.-g. Myoung, Y. Kim, and J.-K. Rhee, “Reliable network design for ethernet ring mesh networks,” *Journal of Lightwave Technology*, vol. 31, no. 1, pp. 1 –9, Jan. 2013.

[31] L. K.-k, J.-d. Ryoo, S. Kim, and J. Lee, “Effective load balancing in ethernet rings,” in *IEEE Network Operations and Management Symposium*, April 2012, pp. 482 –485.

[32] S. Taniguchi, K. Kitayama, Y. Baba, and H. Yamanaka, “Detection and recovery of the blocked ports defect for the reliable ethernet ring protection switching,” in *15th OptoeElectronics and Communications Conference*, Jul 2010, pp. 572 –573.

[33] K.-K. Lee and J.-D. Ryoo, “Flush optimizations to guarantee less transient traffic in ethernet ring protection,” *ETRI Journal*, vol. 32, pp. 184–194, Apr. 2010.

[34] R. Ramaswami, K. Sivarajan, and G. Sasaki, *Optical Networks: A Practical Perspective, 3rd Edition*, 3rd ed. San Francisco, CA, USA: Morgan Kaufmann Publishers Inc., 2009.

[35] M. Nurujjaman, S. Sebbah, C. Assi, and M. Maier, “Optimal capacity planning and RPL placement in carrier ethernet mesh network design,” in *IEEE International Conference on Communications*, Jun. 2012.

[36] M. Clouqueur and W. Grover, “Availability analysis of span-restorable mesh networks,” *IEEE JSAC*, vol. 20, no. 4, pp. 810–821, May 2002.

[37] T. Leighton and S. Rao, "Multicommodity max-flow min-cut theorems and their use in designing approximation algorithms," *Journal of the ACM (JACM)*, vol. 46, no. 6, pp. 787–832, Nov. 1999.

[38] M. Allalouf and Y. Shavitt, "Centralized and distributed algorithms for routing and weighted max-min fair bandwidth allocation," *IEEE/ACM Transactions on Networking*, vol. 16, no. 5, pp. 1015 –1024, oct. 2008.

[39] L. Tan, X. Zhang, L. Andrew, S. Chan, and M. Zukerman, "Price-based max-min fair rate allocation in wireless multi-hop networks," *IEEE Communications Letters*, vol. 10, no. 1, pp. 31 – 33, jan 2006.

[40] A. Reid *et al.*, "Carrier Ethernet," *IEEE Communications Magazine*, vol. 46, no. 9, pp. 96–103, Sep. 2008.

[41] A. Takács, H. Green, and B. Tremblay, "GMPLS Controlled Ethernet: An Emerging Packet-Oriented Transport Technology," *IEEE Communications Magazine*, vol. 46, no. 9, pp. 118–124, Sep. 2008.

[42] D. Fedyk, H. Shah, N. Bitar, and A. Takacs, "Generalized Multiprotocol Label Switching (GMPLS) control of Ethernet PBB-TE," *IETF Internet Draft*, Oct. 2009, work in progress.

[43] A. Takacs, B. Gero, D. Fedyk, D. Mohan, and H. Long, "GMPLS RSVP-TE Extensions for Ethernet OAM Configuration," *IETF Internet Draft*, Oct. 2009, work in progress.

[44] F. Farnoud, M. Ibrahimi, and J. A. Salehi, "A Packet-Based Photonic Label Switching Router for a Multirate All-Optical CDMA-Based GMPLS Switch," *IEEE Journal of Selected Topics in Quantum Electronics*, vol. 13, no. 5, pp. 1522–1530, Sept./Oct. 2007.

[45] R. Tucker, R. Parthiban, J. Baliga, K. Hinton, R. Ayre, and W. Sorin, “Evolution of WDM optical ip networks: A cost and energy perspective,” *Journal of Lightwave Technology*, vol. 27, no. 3, pp. 243 –252, 2009.

[46] TPACK, “P-OTN: Packet Optical Network Transformation,” 2008.

[47] K. Kitayama and N. Wada, “Photonic IP Routing,” *IEEE Photonics Technology Letters*, vol. 11, no. 12, pp. 1689–1691, Dec. 1999.

[48] IETF, “OSPF Extensions in support of Generalized Multi-Protocol Label Switching (GMPLS),” *IETF RFC 4203*, Oct. 2005.

[49] ——, “Routing Extensions in Support of Generalized Multi-Protocol Label Switching (GMPLS),” *IETF RFC 4202*, Oct. 2005.

[50] ——, “Generalized Multi-Protocol Label Switching (GMPLS) Signaling Resource ReserVation Protocol-Traffic Engineering (RSVP-TE) Extensions,” *IETF RFC 3473*, Jan. 2003.

[51] D. Awduche, L. Berger, D. Gan, T. Li, V. Srinivasan, and G. Swallow, “RSVP-TE: Extensions to RSVP for LSP Tunnels,” *IETF RFC 3209*, Dec. 2001.

[52] K. Fouli and M. Maier, “OCDMA and Optical Coding: Principles, Applications, and Challenges,” *IEEE Communications Magazine*, vol. 45, no. 8, pp. 27–34, Aug. 2007.

[53] T. Khattab and H. Alnuweiri, “Optical CDMA for All-Optical Sub-Wavelength Switching in Core GMPLS Networks,” *IEEE Journal on Selected Areas in Communications*, vol. 25, no. 5, pp. 905–921, 2007.

[54] M. Murata and K. Kitayama, “A Perspective on Photonic Multiprotocol Label Switching,” *IEEE Network*, vol. 15, no. 4, pp. 56–63, 2001.

[55] G.-K. Chang *et al.*, “Enabling Technologies for Next-Generation Optical Packet-Switching Networks,” *Proceedings of the IEEE*, vol. 94, no. 5, pp. 892–910, May 2006.

[56] L. G. Roberts, “A Radical New Router,” *IEEE Spectrum*, vol. 46, no. 7, pp. 34–39, Jul. 2009.

[57] N. Kataoka, N. Wada, G. Cincotti, K. Kitayama, and T. Miyazaki, “A novel multiplexed optical code label processing with huge number of address entry for scalable optical packet switched network,” *33rd European Conference and Ehxibition of Optical Communication (ECOC)*, pp. 1–2, Sept. 2007.

[58] P. Reviriego *et al.*, “Performance Evaluation of Energy Efficient Ethernet,” *IEEE Communication Letters*, vol. 13, pp. 697–699, Sept. 2009.